Design Guide: TIDA-010932

High-Efficiency 24 VAC to 5 V, 3.3 V Reference Design With Battery Backup and Charging

Description

This reference design provides a low BOM cost, high-efficiency power stage solution for smart thermostats, and other gateway building automation end equipment using an 24-VAC power source. This power stage takes a 24-VAC input and produces a 5-V and 3.3-V output rail, which can power additional point-of-load converters, if added. The design provides lithium polymer (LiPo) battery charging and seamless switching to battery power during a 24-VAC brownout. The BoosterPack™ Plug-in Module form factor allows the designer to evaluate this power architecture with other LaunchPad™ Development Kits and includes an LED driver and current-sensing capabilities.

Features

- 24-VAC or USB to 3.3-V power rail
- Battery backup
- Independent battery charging and load path
- Dynamic power path and battery power assist
- High efficiency over entire load current range
- USB overcurrent compliant
- Power rail current monitoring

Applications

- Thermostat
- Video doorbell
- HVAC gateway
- HVAC controller
- Heat pump

Resources

TIDA-010932	Design Folder
LMR36520, TPS2116	Product Folder
TLV62568, INA2180	Product Folder
TPS92360, TPS2640, BQ24072	Product Folder

Ask our TI E2E™ support experts

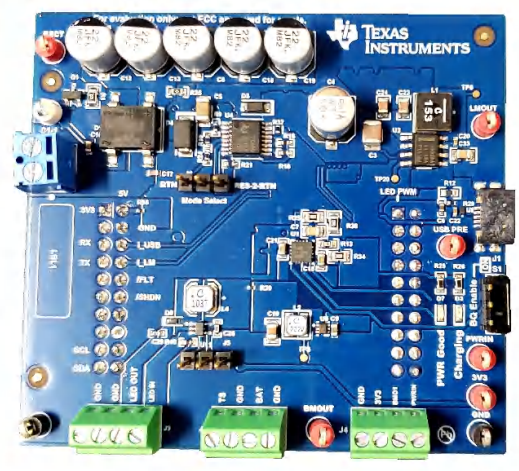

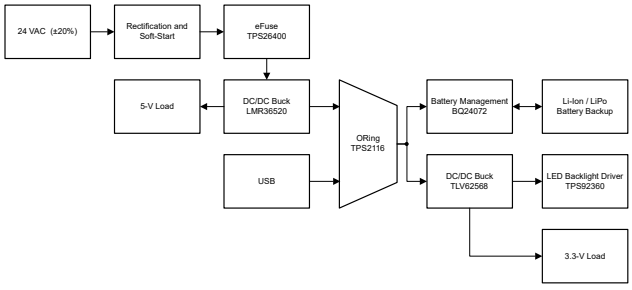

1 System Description

A standard home typically uses a 24-VAC power supply to the HVAC system controls. Thermostats, as well as many other home automation equipment, use this 24-VAC for power. Therefore, a power stage is needed to rectify the 24-V AC and supply a DC voltage at the levels required by the internal components of the thermostat. Low cost is typically a priority for thermostat designs because board space is often plentiful enough to avoid small-footprint, high-cost parts. For thermostats implementing a chargeable battery backup system, high efficiency also becomes a priority to allow a smaller, and therefore lower cost, battery to be used. The TIDA-010932 focuses on these priorities and can be easily adjusted to meet specific needs.

In addition to the 24-V AC and battery backup, this reference design allows a USB power supply to be used for charging and powering the system. Having two supply options, 24-V AC and USB, requires an ORing device. This reference design provides a TI-based ORing strategy based on the TPS2116. If a USB is not desired, the ORing device can be removed with very minimal changes to the design.

The 24-V AC is rectified and stepped down to a 5-V rail using an ultra-low I_Q, wide V_{IN}, 2-A buck converter. The wide V_{IN} of the buck converter helps handle transients, thus eliminating the need for a TVS diode and other protection circuitry. Smaller capacitors can be used as the input voltage ripple can be higher when using a wide V_{IN} buck.

The TIDA-010932 uses a battery-management device that allows independent current paths and monitoring for system power and battery charging. This device increases the cycle life of the battery. This reference design features a seamless transition to battery power in case the main supply fails, as well as battery power assist should the load requirement surpass the rating of the main supply. A very efficient, low cost, and low BOM count buck converter is used to step down the battery management voltage to 3.3 V for use by the general system. Both DC-DC buck converters in this design feature a low-load power saving feature to provide high efficiency even at light loads.

1.1 Key System Specifications

PARAMETER	SPECIFICATIONS	NOTES
Main Input Power Source	24 VAC ±20%	
Secondary Input Power Source	USB	
LM36520 Peak Efficiency	84.5%	I_{OUT} = 150 mA
TLV62568 Peak Efficiency	97.2%	I_{OUT} = 150 mA
LM36520 Maximum Output Current	2 A	
TLV62568 Maximum Output Current	1 A	
Battery Chemistry	Li-Po, Li-Ion	
Battery Charge Current	300 mA	
Input Protection Voltage Range	Minimum = 10 V Maximum = 36 V	

2 System Overview

2.1 Block Diagram

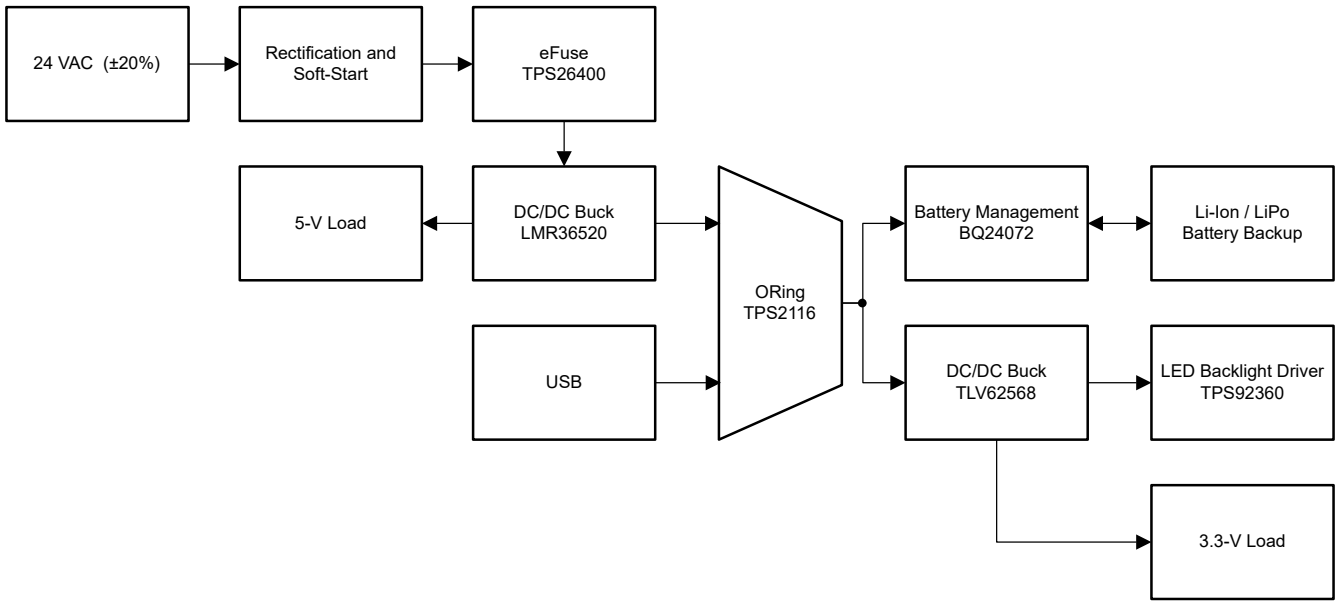

Figure 2-1. TIDA-010932 Block Diagram

2.2 Design Considerations

The TIDA-010932 provides the main power stages needed for building automation electronics that are primarily powered from the 24-VAC system used in typical homes. This reference design presents a system that is modular in design, allowing system designers to easily modify the design, if necessary, to more closely match the specifications of products.

Efficiency, particularly when using the battery backup, and heat loss are taken into consideration in this design. To keep costs low, avoiding an over-engineered system is required. The discrete nature of the TIDA-010932 allows designers to easily remove unnecessary features, or easily add features and power rails that are required for their specific application.

This section outlines the theory and design considerations used to develop and design the TIDA-010932.

2.2.1 24 VAC to DC Rectification

In this design a full-bridge rectifier is used for DC rectification. To prevent a significantly large inrush current during initial connection of 24 VAC, a soft-start circuit is implemented.

The schematic shown in Figure 2-2 shows the rectification and soft-start process. C1, C2, and C3 function as high-frequency bypass capacitors. R1, R2, C4, and C5 provide the soft-start time constant for the gate of the N-channel MOSFET (T1). Q1 has a gate threshold voltage range of 1.0 V to 2.5 V and a 92-mΩ $R_{DS(on)max}$ at V_{GS} = 10 V. The values of R2 and R3 are chosen to voltage divide a maximum of 42 V (the peak of the 24 VAC at the high end of the tolerance) down to approximately 10 V once steady state has been reached. Calculating R2 and R3 is shown in Equation 1.

$$42\ \text{V}\left(\frac{\text{R}_2}{\text{R}_2+\text{R}_3}\right) = 42\left(\frac{150\ \text{k}\Omega}{150\ \text{k}\Omega+453\ \text{k}\Omega}\right) = 10.4\ \text{V} \quad (1)$$

The Zener diode (D2) is used as a protective device for the MOSFET gate. R4 is used to provide an initial current path while T1 is still open. The use of R4 prevents significantly differing soft-start times due to variances in the 24-VAC transformer and the gate threshold voltage of Q1. The resulting circuit provides a relatively consistent soft-start time regardless of the 24-VAC source variances.

C6 and C7 function as the smoothing capacitors of the rectifier. The TIDA-010932 has a maximum power output of 10 W. The output ripple is a function of the load current. TINA-TI™ simulation shows a maximum worst-case ripple of 11.7 V. That worst-case condition is typically unlikely to occur depending on application; a more reasonable use case of a 100-mA output from the 3.3- V rail and a nominal 24-VAC transformer provides a rectification ripple of approximately 1.4 V. These ripple voltages must be checked in each application. Even at the worse-case scenario as previously outlined, the LMR36520 buck converter is capable of handling those ripple voltages and voltage ranges.

Figure 2-3 shows a simulation example of the schematic detailed in Figure 2-2 under an input power of approximately 750 mW. The time from applied input power to the output of the rectifier reaching steady-state is approximately 300 ms.

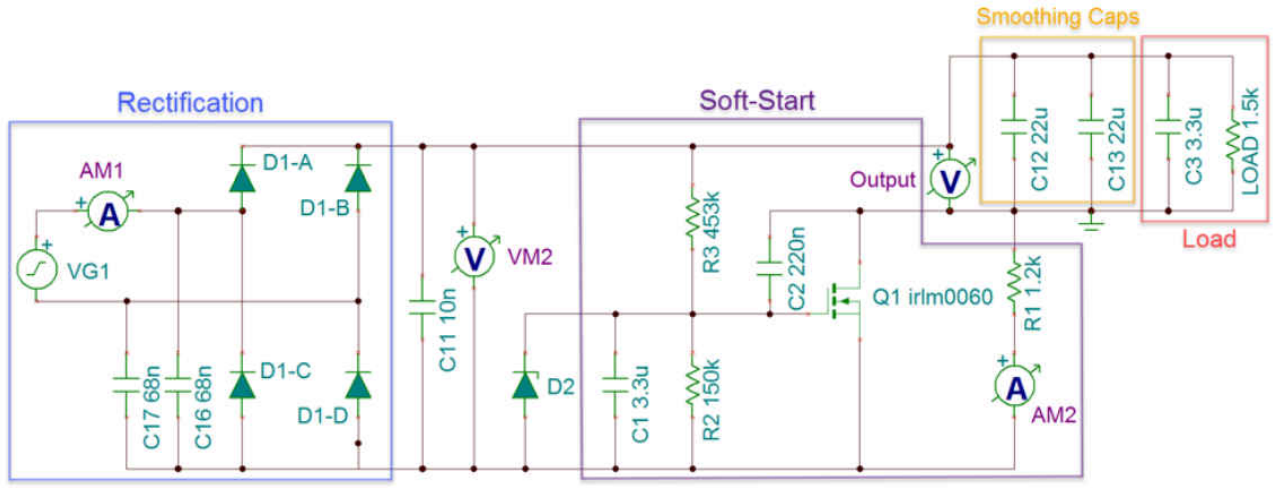

Figure 2-2. Soft-Start Schematic

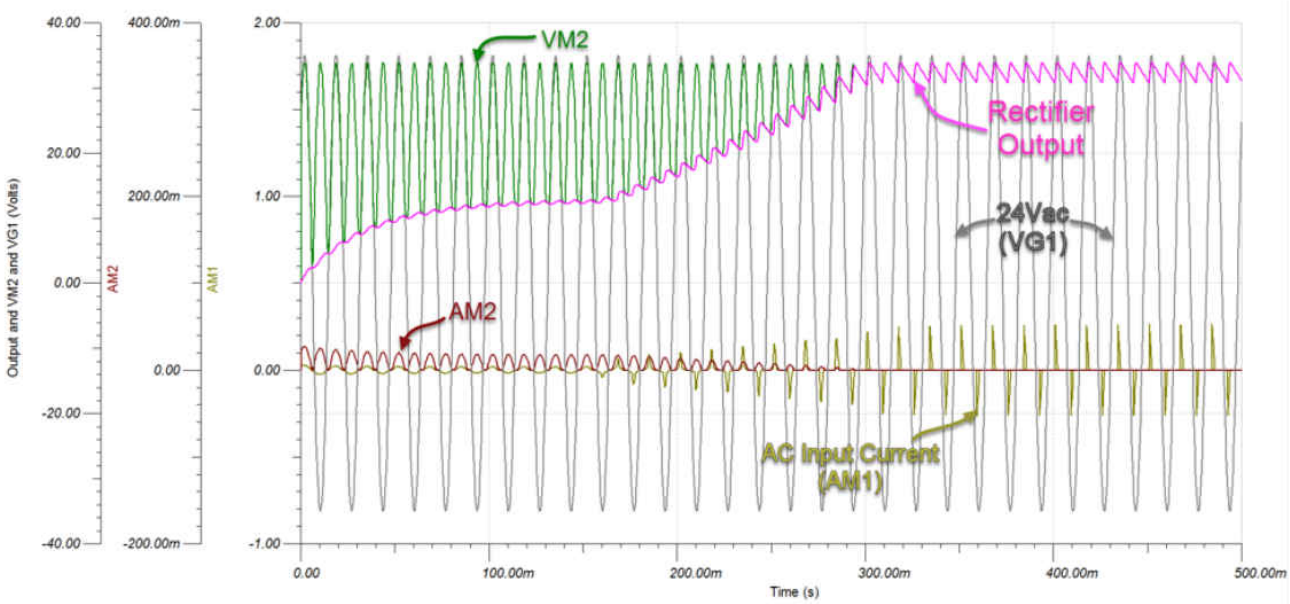

Figure 2-3. Soft-Start TINA-TI Simulation Example

2.2.2 eFuse Protection

The TIDA-010932 reference design leverages a TPS26400 eFuse to protect the ICs in the event of an overvoltage or overcurrent event. The load, source, and device protection are provided with many adjustable features including overcurrent, output slew rate, and overvoltage, undervoltage thresholds. The internal robust protection control blocks along with the high voltage rating of the TPS26400 helps to simplify the system designs for protection. Figure 2-4 shows the implementation of the TPS26400 in this reference design.

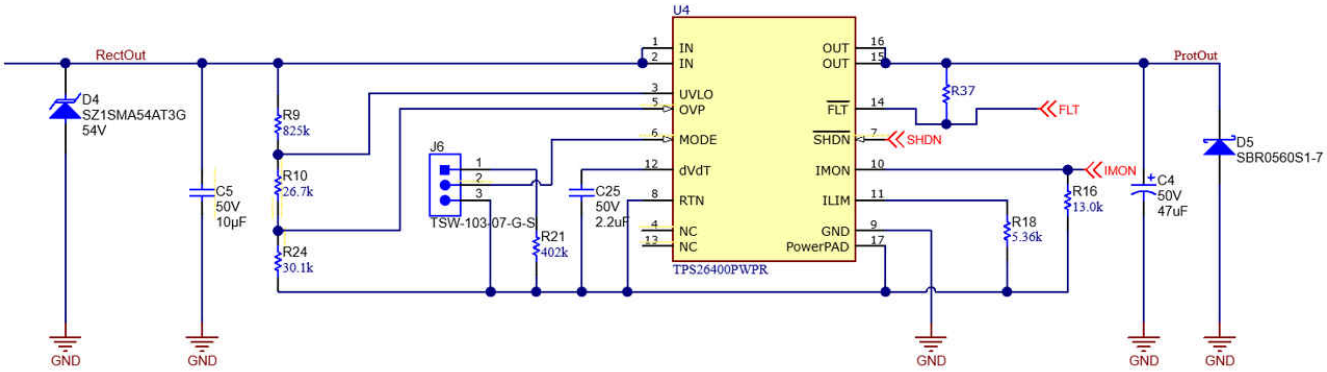

Figure 2-4. TPS2660 E-Fuse Implementation

To program the current limit threshold for the board, use Equation 2 to calculate the required resistance.

$$R_{(ILIM)} = \frac{12}{I_{LIM}} \quad (2)$$

Using the 2 A as the current limit, a resistance of 6 kΩ is calculated. Rounding to the nearest 1% resistor value results with a resistance of 5.36 kΩ.

For the UVLO and OVLO set points, Equation 3 and Equation 4 are used to calculate the required resistance values. For minimizing the input current drawn from the power supply {$I_{(R9,10,24)} = V_{(IN)} / (R9 + R10 + R24)$}, use higher value resistance for R9, R10, and R24 . However, the leakage current due to external active components connected at resistor string can add error to these calculations. So, the resistor string current, $I_{(R9,10,24)}$ must be chosen to be 20 × greater than the leakage current of the UVLO and OVP pins.

From the device electrical specifications, $V_{(OVPR)}$ = 1.19 V and $V_{(UVLOR)}$ = 1.19 V. From the design requirements, $V_{(OV)}$ is 36 V and $V_{(UV)}$ is 10 V. To solve the equation, first choose the value of R24 = 30.1 kΩ and use Equation 3 to solve for (R9 + R10) = 880.5 kΩ. Use Equation 4 and a value of (R9 + R10) to solve for R10 = 80 kΩ and finally R9 = 825 kΩ. Choose the closest standard 1% resistor values: R9 = 825 kΩ, R10 = 80 kΩ, and R24 = 30.1 kΩ.

$$V_{OVPR} = \frac{R_3}{R_1 + R_2 + R_3} \times V_{OV} \quad (3)$$

$$V_{UVLOR} = \frac{R_2 + R_3}{R_1 + R_2 + R_3} \times V_{UV} \quad (4)$$

J6 provides the option to change the mode for the eFuse based on the needs of the designer. The mode can be switched from current limiting with auto-retry, current limiting with latch off, and circuit breaker with auto-retry, and is based on whether the mode pin is connected to RTN, connected to the 402-kΩ resistor to RTN, or left open respectively.

2.2.3 5-V Rails

This section provides detail on both the LM5166 wide VIN buck that converts the rectified 24 VAC to 5 V as well as the USB 5-V rail.

2.2.3.1 LMR36520 Voltage Rail

The LMR36520 device is the best choice for this design. The device has a very wide input voltage range (4.2 V to 65 V), and has a 2-A load capacity. The LMR36520 also has low no-load quiescent current and high efficiency at light loads.

The LMR36520 is used to convert the rectified 24-VAC source to 5 VDC and is used as the primary source of power in the TIDA-010932.

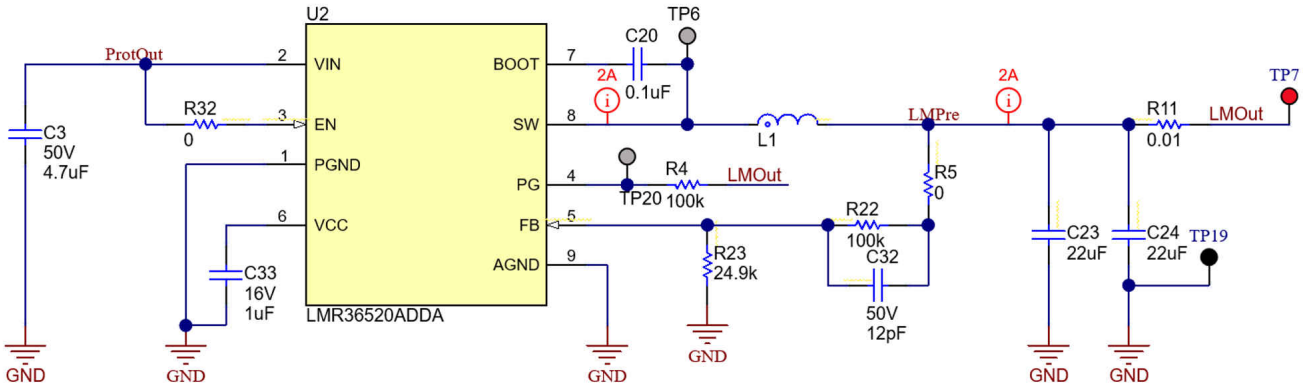

Figure 2-5. LMR36520 Implementation

The output voltage of LMR36520 is externally adjustable using a resistor divider network. The range of recommended output voltage is found in the *Recommended Operating Conditions* of the data sheet. The divider network is comprised of R_{FBT} and R_{FBB}, and closes the loop between the output voltage and the converter. The converter regulates the output voltage by holding the voltage on the FB pin equal to the internal reference voltage, V_{REF}. The resistance of the divider is a compromise between excessive noise pickup and excessive loading of the output. Smaller values of resistance reduce noise sensitivity but also reduce the light-load efficiency. The recommended value for R_{FBT} is 100 kΩ with a maximum value of 1 MΩ. If a 1 MΩ is selected for R_{FBT}, then a feedforward capacitor must be used across this resistor to provide adequate loop phase margin.

$$R_{FBB} = \frac{R_{FBT}}{\left[\frac{V_{Out}}{V_{Ref}} - 1\right]} = \frac{100\ k\Omega}{\left[\frac{5\ V}{1\ V} - 1\right]} = 25\ k\Omega \quad (5)$$

For this design, R_{FBB} = 25 kΩ and R_{FBT} = 100 kΩ.

The parameters for selecting the inductor are the inductance and saturation current. The inductance is based on the desired peak-to-peak ripple current and is normally chosen to be in the range of 20% to 40% of the maximum output current. Experience shows that the best value for inductor ripple current is 30% of the maximum load current. Note that when selecting the ripple current for applications with much smaller maximum load than the maximum available from the device, use the maximum device current. Equation 6 can be used to determine the value of inductance. The constant K is the percentage of inductor current ripple. This design uses K = 0.37 and with input voltage of 42 V, an inductance of L ≅ 15 µH can be calculated.

$$L = \frac{(V_{IN} - V_{OUT})}{f_{SW} \times K \times I_{OUT\ max}} \times \frac{V_{OUT}}{V_{IN}} = \frac{(42\ V - 5\ V)}{400\ kHz \times 0.37 \times 2\ A} \times \frac{5\ V}{42\ V} = 15\ \mu H \quad (6)$$

Inductors with a ferrite core material have very hard saturation characteristics, but usually have lower core losses than powdered iron cores. Powered iron cores exhibit a soft saturation, allowing some relaxation in the current rating of the inductor. However, powered iron cores have more core losses at frequencies above about 1 MHz. In any case, the inductor saturation current must not be less than the device low-side current limit, I_{LIMIT}. To avoid subharmonic oscillation, the inductance value must not be less than that given in Equation 7:

$$L_{MIN} \geq M \times \frac{V_{OUT}}{f_{SW}} = 0.42 \times \frac{5\ V}{400\ kHz} = 5.25\ \mu H \quad (7)$$

where

- L_{MIN} = minimum inductance (H)
- M = 0.42
- f_{SW} = switching frequency (Hz)

The value of the output capacitor and the respective ESR determine the output voltage ripple and load transient performance. The output capacitor bank is usually limited by the load transient requirements rather than the

output voltage ripple. Equation 8 can be used to estimate a lower bound on the total output capacitance, and an upper bound on the ESR that is required to meet a specified load transient.

$$C_{OUT} \geq \frac{\Delta I_{OUT}}{f_{SW} \times \Delta V_{OUT} \times K} \times \left[(1 - D) \times (1 + K) + \frac{K^2}{12} \times \left(2 - D\right)\right] \quad (8)$$

$$ESR \leq \frac{(2 + K) \times \Delta V_{OUT}}{2 \times \left[1 + K + \frac{K^2}{12} \times \left(1 + \frac{1}{(1 - D)}\right)\right]} \quad (9)$$

$$D = \frac{V_{OUT}}{V_{IN}} \quad (10)$$

where

- ΔV_{OUT} = output voltage transient
- ΔI_{OUT} = output current transient
- K = ripple factor from Inductor Selection

Once the output capacitor and ESR have been calculated, use Equation 11 to check the output voltage ripple.

$$V_r \cong \Delta I_L \times \sqrt{ESR^2 + \frac{1}{(8 \times f_{SW} \times C_{OUT})^2}} \quad (11)$$

The ceramic input capacitors provide a low impedance source to the regulator in addition to supplying the ripple current and isolating switching noise from other circuits. A minimum ceramic capacitance of 4.7 µF is required on the input of the LMR36520. This must be rated for at least the maximum input voltage that the application requires; preferably twice the maximum input voltage. This capacitance can be increased to help reduce input voltage ripple and maintain the input voltage during load transients. Most of the input switching current passes through the ceramic input capacitors. The approximate RMS value of this current can be calculated from Equation 12 and must be checked against the maximum ratings of the manufacturer.

$$I_{RMS} \cong \frac{I_{OUT}}{2} \quad (12)$$

In some cases, a feedforward capacitor can be used across R_{FBT} to improve the load transient response or improve the loop-phase margin. This is especially true when values of R_{FBT} > 100 kΩ are used. Large values of R_{FBT}, in combination with the parasitic capacitance at the FB pin, can create a small signal pole that interferes with the loop stability. A C_{FF} can help mitigate this effect. Use Equation 13 to estimate the value of C_{FF}.

$$C_{FF} < \frac{V_{OUT} \times C_{OUT}}{120 \times R_{FBT} \times \sqrt{\frac{V_{REF}}{V_{OUT}}}} \quad (13)$$

2.2.3.2 USB Power Input

Like the LMR36520 device, the USB power input is capable of powering the entire system. The USB can serve as a backup power source, be used for debugging other aspects of the systems in the product, or be used to charge the battery in case the main 24 VAC is not available. The TIDA-010932 does not supply power to USB; it only sinks power from a USB host. ESD and overvoltage protection are included as shown in Figure 2-6.

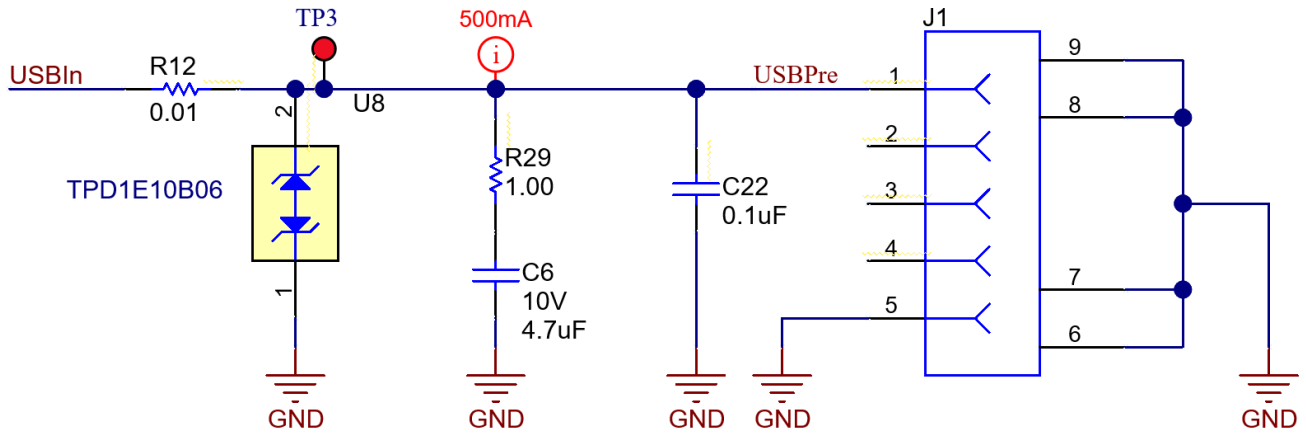

Figure 2-6. USB Implementation

This reference design uses USB 2.0, and therefore assumes the maximum current that can be pulled from a USB host is 500 mA. USB 2.0 specification allows a tolerance of 5% from the nominal 5 V, thereby giving a host voltage range of 4.75 V to 5.25 V. Furthermore, USB 2.0 specification also allows the worst case voltage drop across all cables and connectors to bring the total voltage at load to 4.35 V. The TIDA-010932 is designed to accommodate USB 2.0 at the worst-case specification.

R29 and C6 provide a snubber circuit to the USB Vbus, reducing the overshoot and ringing caused by the cable inductance and capacitive load resonance. The snubber circuit must be tuned for each system design; therefore, the snubber component values used in the TIDA-010932 must be tested when designed into a new system and the values must be changed appropriately.

2.2.4 Power Source ORing

TIDA-010932 leverages a TPS2116 ORing IC to switch between power sources. The device is set to automatic priority mode via R6 and R8, which autonomously switches depending on whether LMOut is available. The ST pin is tied to a pullup resistor to LMOut and can be used to relay power status to an MCU. In this design, the status pin is not used but the board can be easily modified to leverage this feature.

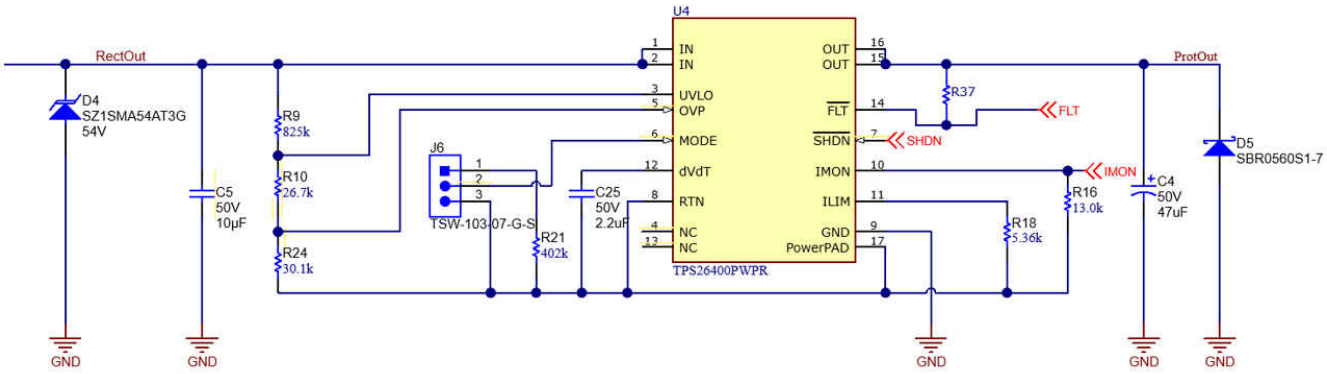

Figure 2-7. TIDA-010932 Power Source ORing Circuit

Figure 2-8 shows the truth table for the TPS2116, which can be used to determine the functionality based on various power modes.

MODE	VIN1	VIN2	PR1	ST	VOUT
VIN1 (Priority mode)	High ($V_{PR1} > V_{REF}$)	X	VIN1 through resistor divider	High	VIN1
	Low ($V_{PR1} < V_{REF}$)	≥ 1.6 V		Low	VIN2
External Bias ≥ 1 V (Manual mode)	≥ 1.6 V	X	High	High	VIN1
	X	≥ 1.6 V	Low	Low	VIN2
External Bias ≤ 0.35 V (Manual mode)	X	X	High	Low	Hi-Z
	> V_{IN2}	X	Low	High	VIN1
	X	> V_{IN1}	Low	Low	VIN2

Figure 2-8. TPS2116 Truth Table

2.2.5 Battery Management

Battery charging and power path management are performed by the bq24072 in the TIDA-010932. The bq24072 provides a low-cost system that features independent battery charging and load paths through the power path capability without the need for any external FETs. The device can monitor battery temperature through a dedicated pin, provides USB-compliant inrush current and current limits, and provides P_{GOOD} and charge signals.

The bq24072 is a single-power input device and was specifically chosen over dual-input devices due to cost. The bq24072 and ORing detailed in Section 2.2.4 provide the same functionality as a fully integrated dual-input device but at a lower cost. TIDA-010932 is designed with an understanding that end products can have different requirements and that ease of design changes to fit individual systems is necessary. If the end product does not use USB (or a secondary power source in general), the ORing remedy and the USB related components detailed in Section 2.2.2 can be eliminated and the single input of the bq24072 can be used for an even lower cost design. In such a scenario, a dual-input battery management IC is over-engineered for the application and incurs unnecessary costs or significant design changes. For those reasons, the bq24072 was chosen as the best low-cost design.

The bq24072 features power path capability, allowing the battery to supplement the main power source to meet high load demands. This feature allows the use of a smaller main power source, thus reducing costs further.

Figure 2-9 displays the setup and components chosen for the TIDA-010932. The bq24072 has a minimum recommended input voltage of 4.35 V, V_{OVP} of 6.6 V, and a maximum absolute input voltage of 28 V. The device charges the battery up to 4.2 V $_{(VBAT(REG))}$. The output is regulated to 200 mV above $V_{BAT(REG)}$.

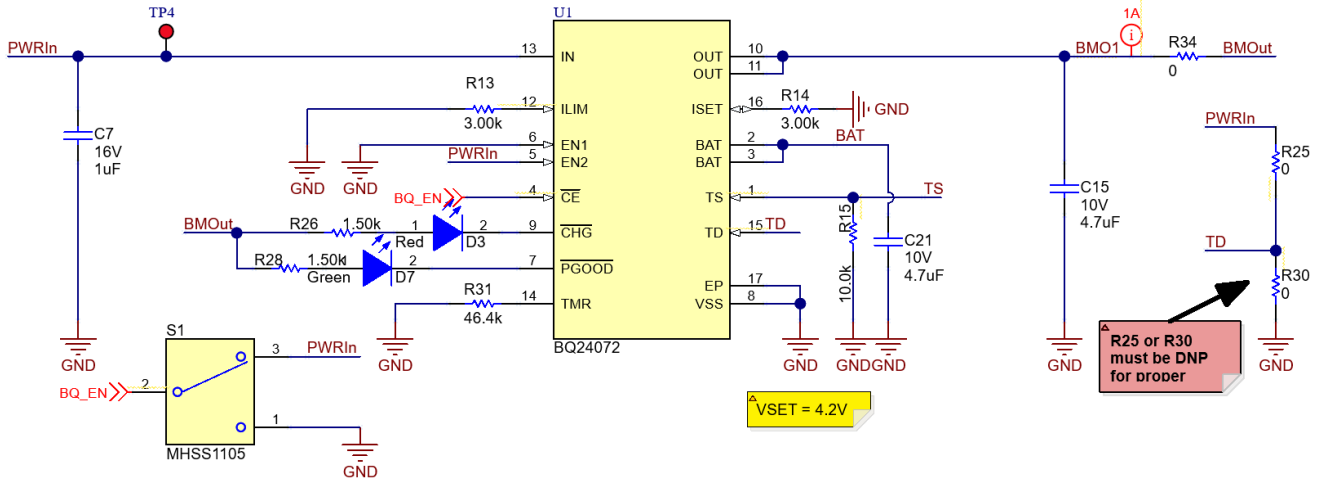

Figure 2-9. BQ24072 Circuit

A small input capacitor (C7) is chosen as USB 2.0 specifications require less than 10 µF to be hard started.

The bq24072 data sheet recommends between 1 µF and 10 µF of the input capacitance. A 4.7-µF battery input capacitor (C10) was chosen per data sheet recommendation. The output capacitor (C15) of 4.7 µF is the minimum recommended value per the data sheet.

To comply with USB 2.0 specifications, the input current must be limited to 500 mA. The EN1, EN2, and I_{LIM} pins of the bq24072 allow a programmable current limit. As per the data sheet, EN1 is set HIGH and EN2 is set LOW to program a 500-mA current limit. I_{LIM} must not be left floating, because doing so disables charging, so the I_{LIM} is set to provide a higher current limit (536 mA) than the EN1 and EN2 pins, which allows the EN1 and EN2 current limit to be the dominant, more conservative limit. Equation 14 shows the calculation used in the TIDA-010932 for R13.

$$R_{13} = R_{ILIM} = \frac{K_{ILIM}}{I_{IN-MAX}} = \frac{1610\ A\Omega}{536\ mA} = 3\ k\Omega \quad (14)$$

R14 is connected to the ISET pin and determines the fast charge current level of the battery ($I_{O(CHG)}$) shown in Figure 2-9. The calculation for R14 in this reference design is shown in Equation 15. However, the fast charge current must be chosen depending on the battery specifications used in the end product.

$$R_{14} = \frac{K_{ISET}}{I_{O(CHG)}} = \frac{890\ A\Omega}{300\ mA} = 3\ k\Omega \quad (15)$$

Net *TS* is used to monitor the battery temperature on battery packs that have a built-in thermistor. If using TS, R15 must be not populated. Use R15 if leaving TS floating and not using temperature sensing. The value of 10k is per the data sheet recommendation.

Pin *TD* is tied to GND to enable charger termination, with the option to depopulate the path to ground and instead connect to PWRIn. Pin $\overline{CE}$ goes to a dip switch which allows the user to determine if the battery charging is active. P_{GOOD} is pulled to BM_{Out} when a valid input source is detected and is high impedance when the input power is not within specified limits. P_{GOOD} can sink a maximum of 15 mA so R28 must be chosen appropriately to make sure P_{GOOD} does not sink more than 15 mA. The TIDA-010932 uses an indication LED (D7) on the $\overline{PGOOD}$ pin.

Pin $\overline{CHG}$ is pulled to BM_{OUT} when the battery is charging and is high impedance when the charging is complete or when the charger is disabled. R26 must be chosen to make sure $\overline{CHG}$ does not sink more than 15 mA. The TIDA-010932 uses an indication LED (D3) on the charge pin.

2.2.6 3.3-V Power Rail

The 3.3-V rail serves as the main power output that directly supplies power to the various system components in the end product. The input of the TLV62568 is connected to the output of the bq24072.

The 3.3-V rail ultimately receives power from either the 24-VAC line, USB, or the battery, depending on which source is available. Devices powered from this rail are battery backup protected and benefit from the power assistance features of the bq24072.

The TLV62568 is a very lost cost, low BOM count, high-efficient step-down converter. The device has a 100% duty cycle capability, which is particularly useful in battery-powered applications such as the TIDA-010932 to achieve the longest operation time by taking full advantage of the whole battery voltage range. The TLV62568 has an output current maximum of 1 A. In case more than a 1-A output is required, the TLV62569 offers pin-to-pin compatibility (though the input and output capacitors as well as inductor may need to be changed appropriately) with the TLV62568 but features a 2-A output current. Figure 2-10 shows the specific system implementation in the TIDA-010932 and highlights the simplicity of the part and the low external BOM count.

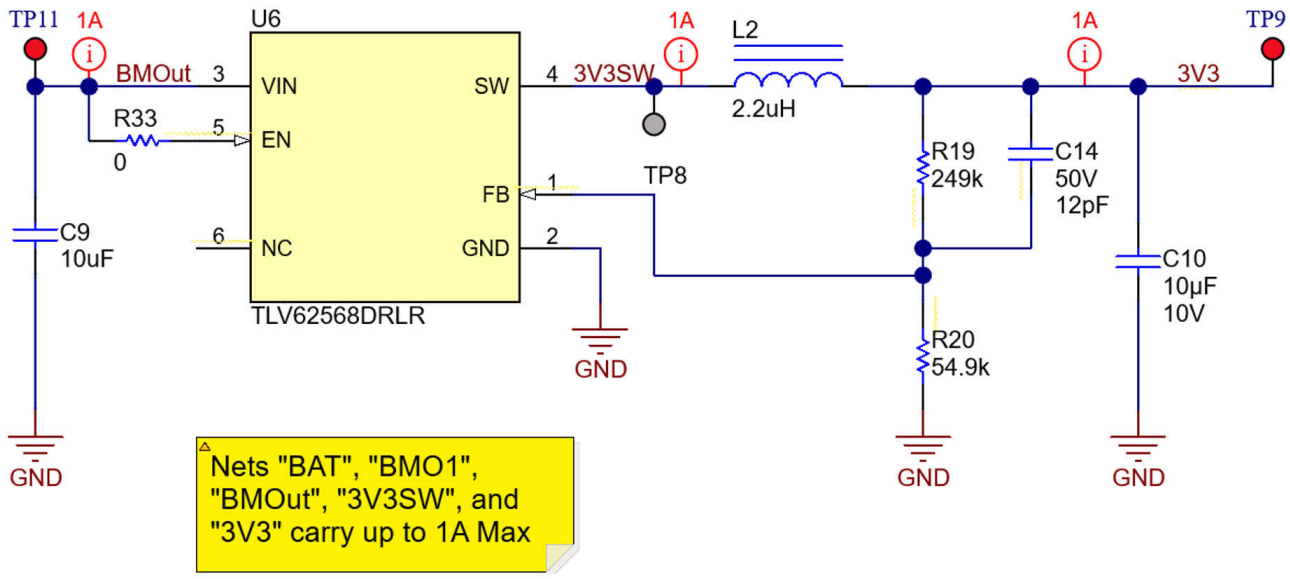

Figure 2-10. TIDA-010932 3.3V Rail Circuit

To set the output voltage of the TLV62568 to 3.3 V, Equation 16 is used to calculate the values of R19 and R20. When sizing R20, to achieve low current consumption and acceptable noise sensitivity, use a maximum of 200 kΩ. Larger currents through R20 improve noise sensitivity and output voltage accuracy but increase current consumption. A feed forward capacitor (C14) is added to the circuit, which improves the loop bandwidth to make a fast transient response.

$$V_{OUT} = V_{FB} \times \left[1 + \frac{R_{19}}{R_{20}}\right] = 0.6 \times \left[1 + \frac{R_{19}}{R_{20}}\right] \quad (16)$$

The main parameters for inductor selection is inductor value and then saturation current of the inductor. To calculate the maximum inductor current under static load conditions, Equation 17 and Equation 18 are given:

$$I_{LMAX} = I_{OUTMAX} + \frac{\Delta I_L}{2} \quad (17)$$

$$\Delta I_L = V_{OUT} \times \frac{1 - \frac{V_{OUT}}{V_{IN}}}{L \times f_{SW}} \quad (18)$$

where:

- $I_{OUT,MAX}$ is the maximum output current
- ΔI_L is the inductor current ripple
- f_{SW} is the switching frequency
- L is the inductor value

For this design, a 2.2-µH inductor is chosen.

2.2.7 Power Rail Current Sensing

TIDA-010932 also integrates an INA2180 (Figure 2-11) for current sensing of the two power rails (5 V from LMR36520 and 5 V from USB). The output of this device is also tied to the BoosterPack™ header for easier data collection as well as the ability to monitor system power if an MCU LaunchPad™ is connected.

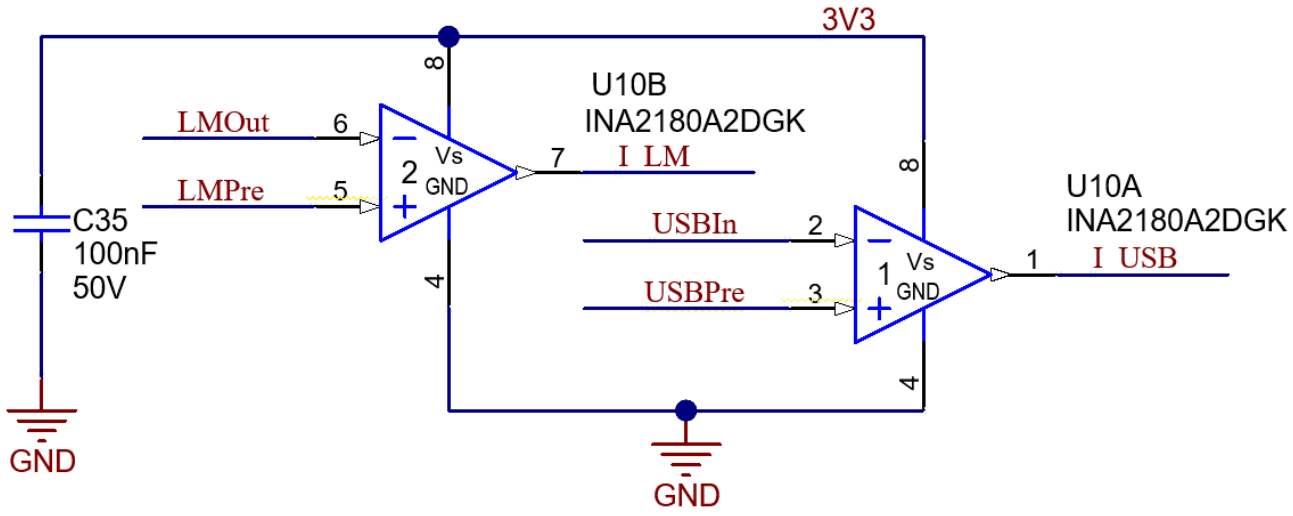

Figure 2-11. INA2180 Power Rail Current Sensing Circuit

The accuracy of the INAx180 is maximized by choosing the current-sense resistor to be as large as possible. A large sense resistor maximizes the differential input signal for a given amount of current flow and reduces the error contribution of the offset voltage. However, there are practical limits as to how large the current-sense resistor can be in a given application. Equation 19 gives the maximum value for the current sense resistor for a given power dissipation budget:

$$R_{SENSE} < \frac{PD_{MAX}}{I_{MAX}^2} \tag{19}$$

where

- PD_{MAX} is the maximum allowable power dissipation in R_{SENSE}
- I_{MAX} is the maximum current that flows through R_{SENSE}

To make sure that the current-sense signal is properly passed to the output, both positive and negative output swing limitations must be examined. Equation 20 provides the maximum values of R_{SENSE} and GAIN to keep the device from hitting the positive swing limitation.

$$I_{MAX} \times R_{SENSE} \times Gain < V_{SP} \tag{20}$$

where

- I_{MAX} is the maximum current that flows through R_{SENSE}
- GAIN is the gain of the current sense amplifier
- V_{SP} is the positive output swing as specified in the data sheet

The negative swing limitation places a limit on how small of a sense resistor can be used in a given application. Equation 21 provides the limit on the minimum size of the sense resistor.

$$I_{MIN} \times R_{SENSE} \times Gain > V_{SN} \tag{21}$$

where

- I_{MIN} is the minimum current that flows through R_{SENSE}
- GAIN is the gain of the current sense amplifier
- V_{SN} is the negative output swing of the device

2.2.8 Backlight LED Driver

TIDA-010932 also features a backlight LED driver (Figure 2-12) which can be used to drive backlight LEDs on displays for thermostats, and so forth. If not needed, this device can be disabled by depopulating R39.

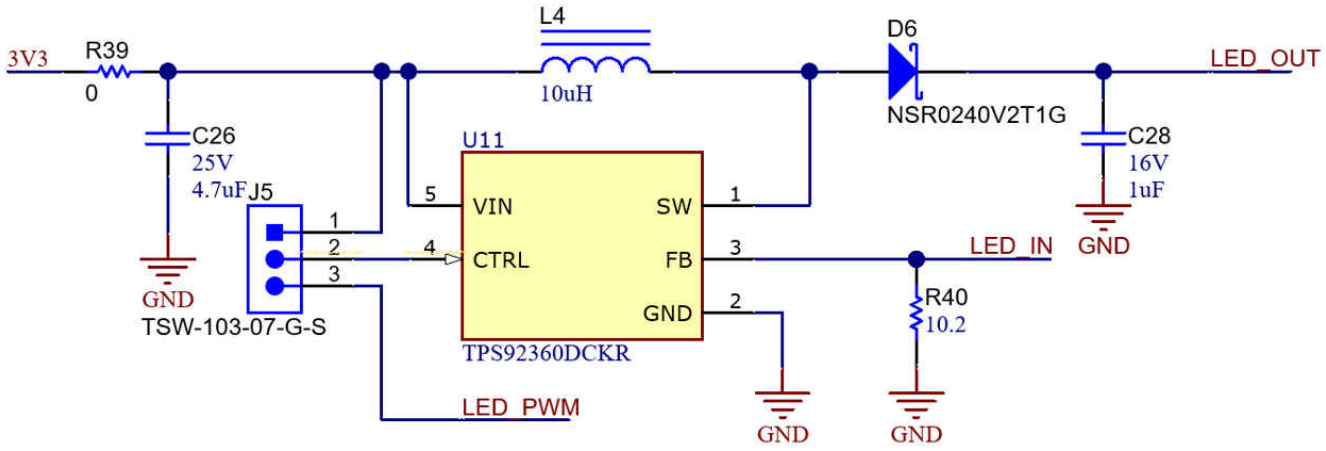

Figure 2-12. TIDA-010932 String LED Driver Circuit

For the inductor selection, there are three important inductor specifications, inductor value, DC resistance, and saturation current. Considering inductor value alone is not enough. The inductor value determines the inductor ripple current. Choose an inductor that can handle the necessary peak current without saturating. Follow Equation 23 and Equation 24 to calculate the peak current of the inductor. To calculate the current in the worst case, use the minimum input voltage, maximum output voltage, and maximum load current of the application. In a boost regulator, the input DC current can be calculated as Equation 22:

$$I_{L(DC)} = \frac{V_{OUT} \times I_{OUT}}{V_{IN} \times \eta} \quad (22)$$

where

- V_{OUT} = boost output voltage
- I_{OUT} = boost output current
- V_{IN} = boost input voltage
- η = power conversion efficiency

The inductor current peak to peak ripple can be calculated as Equation 23.

$$\Delta I_{L(P-P)} = \frac{1}{L \times \left(\frac{1}{V_{OUT} - V_{IN}} + \frac{1}{V_{IN}}\right) \times F_S} \quad (23)$$

where

- $\Delta I_{L(PP)}$ = inductor peak-to-peak ripple
- L = inductor value
- F_S = boost switching frequency
- V_{OUT} = boost output voltage
- V_{IN} = boost input voltage

Therefore, the peak current $I_{L(P)}$ seen by the inductor is calculated with Equation 24.

$$I_{L(P)} = I_{L(DC)} + \frac{\Delta I_{L(P-P)}}{2} \quad (24)$$

For output capacitor selection, the voltage ripple is related to capacitor capacitance and the equivalent series resistance (ESR). The additional part of the ripple caused by ESR is calculated using: $V_{ripple\_ESR} = I_{OUT} \times$

R_{ESR}. Due to the low ESR, V_{ripple_ESR} can be neglected for ceramic capacitors, a 1-µF to 4.7-µF capacitor is recommended for typical applications, in this design a 1-µF output capacitor is chosen.

2.2.9 BoosterPack Overview

This reference design also integrates BoosterPack™ headers which offer several advantages to designers. By mounting an MCU LaunchPad to the TIDA-010932 board, several important device outputs can be monitored by the host MCU, and in the case of a wireless MCU, can also relay this data to a gateway device.

Pins 6 and 8 on J7 in Figure 2-13 are tied to the output of the INA2180, which with an MCU attached and powered via the TIDA-010932 board, can characterize a more complete system current consumption. More BoosterPack™ Plug-in Modules can be added as well to allow for a complete systems estimate for power consumption.

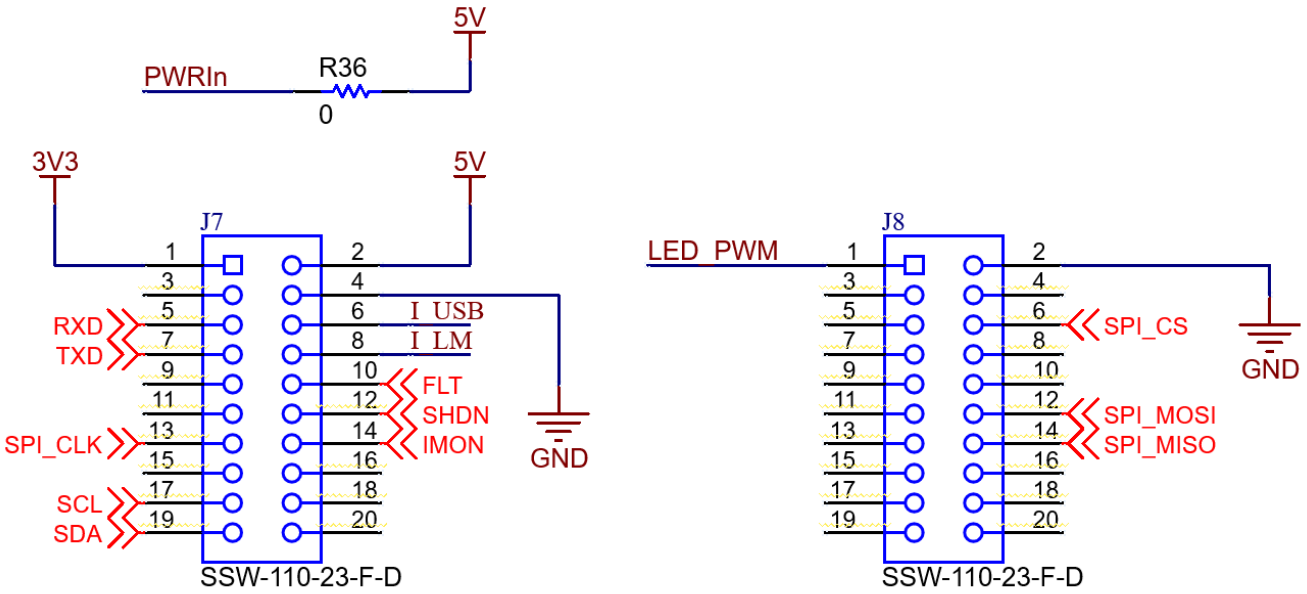

Figure 2-13. TIDA-010932 BoosterPack Pinout

2.3 Highlighted Products

2.3.1 LMR36520

The LMR36520 is a synchronous peak-current mode buck regulator designed for a wide variety of industrial applications. The regulator automatically switches modes between PFM and PWM, depending on load. At heavy loads, the device operates in PWM at a constant switching frequency. At light loads, the mode changes to PFM with diode emulation, allowing DCM. This reduces the input supply current and keeps efficiency high. The device features internal loop compensation, which reduces design time and requires fewer external components than externally compensated regulators.

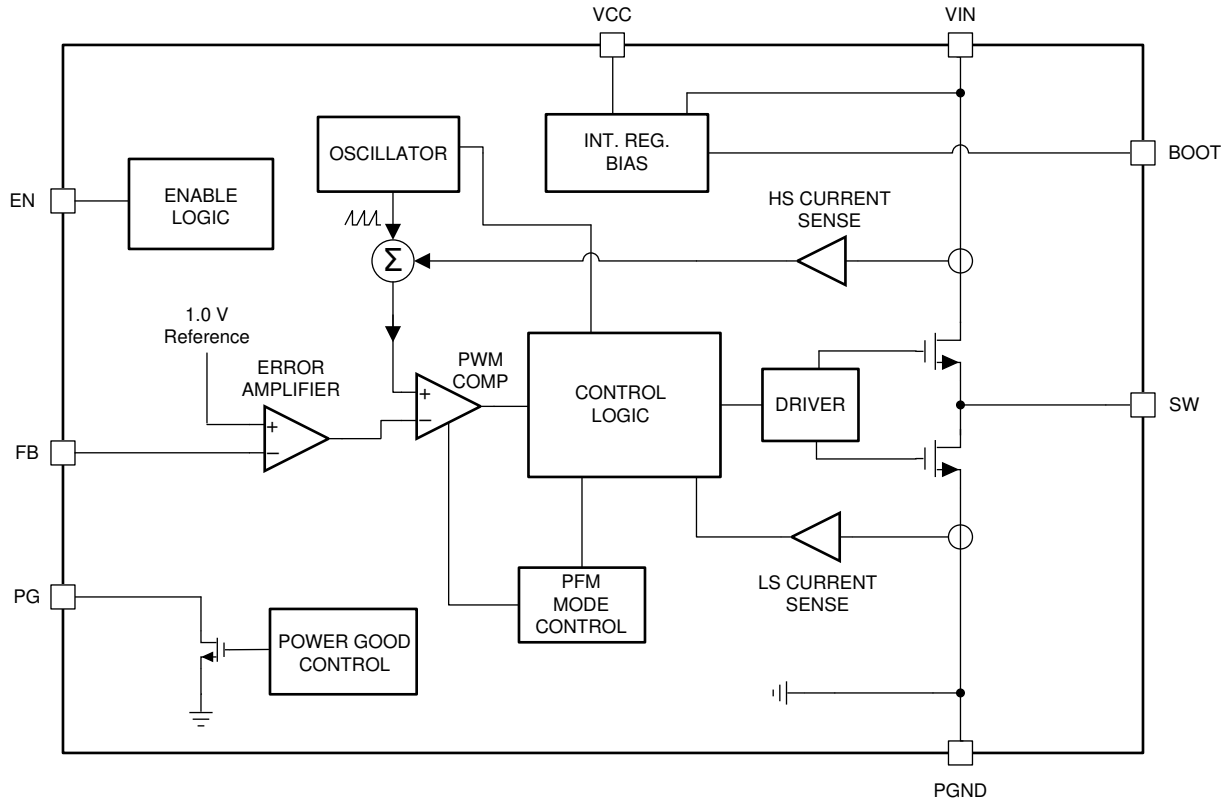

Figure 2-14. LMR36520 Functional Block Diagram

2.3.2 TPS2116

The TPS2116 is a power MUX device with a voltage rating of 1.6 V to 5.5 V and a maximum current rating of 2.5 A. The device uses N-channel MOSFETs to switch between supplies while providing a controlled slew rate when voltage is first applied. The TPS2116 can be configured for two different switchover behaviors depending on the application. Automatic priority mode prioritizes the supply connected to VIN1 and switches over to the secondary supply (VIN2) whenVIN1 drops. Manual mode allows the user to toggle a GPIO or enable signal to switch between channels. Due to the low quiescent of 1.32 µA (typical) and standby current of 50 nA (typical), the TPS2116 is an excellent choice for systems where a battery is connected to one of the inputs. These low currents extend the life and operation of the battery when in use.

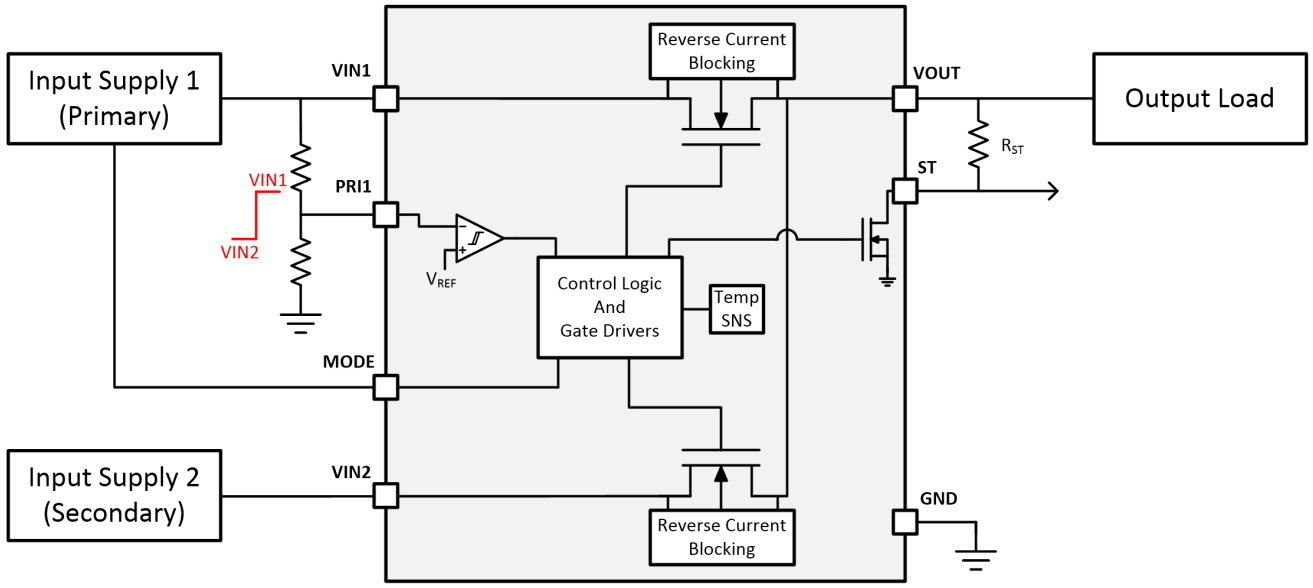

Figure 2-15. TPS2116 Functional Block Diagram

2.3.3 TLV62568

The TLV62568 is a high-efficiency synchronous step-down converter. The device operates with an adaptive off-time with peak current control scheme. The device operates at typically 1.5-MHz frequency pulse width modulation (PWM) at moderate to heavy load currents. Based on the V_{IN} / V_{OUT} ratio, a simple circuit sets the required off time for the low-side MOSFET. It makes the switching frequency relatively constant regardless of the variation of input voltage, output voltage, and load current.

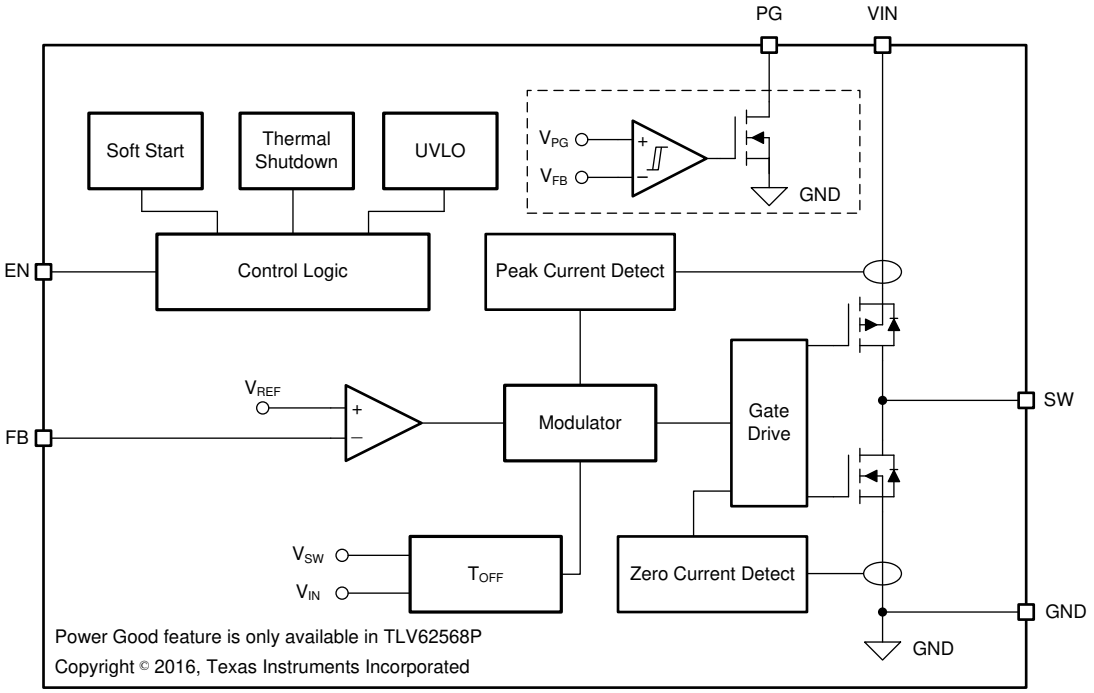

Figure 2-16. TLV62568 Functional Block Diagram

2.3.4 INA2180

The INA180, INA2180, and INA4180 (INAx180) are 26-V, common-mode, current-sensing amplifiers used in both low-side and high-side configurations. These specially-designed, current-sensing amplifiers accurately

measures voltages developed across current-sensing resistors on common-mode voltages that far exceed the supply voltage powering the device. Current can be measured on input voltage rails as high as 26 V, and the devices can be powered from supply voltages as low as 2.7 V

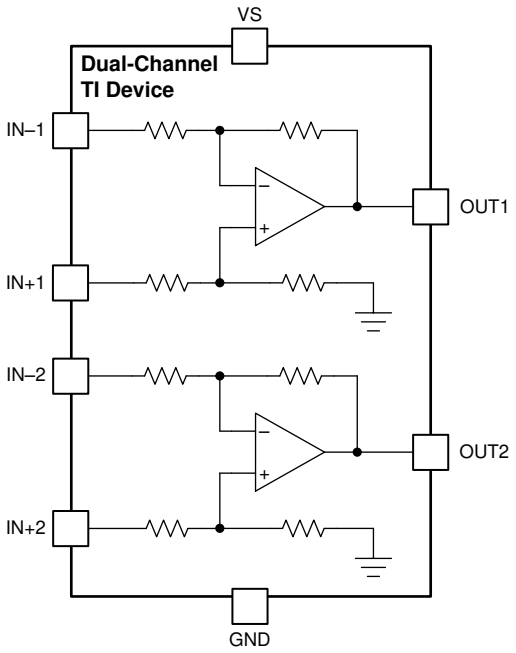

Figure 2-17. INA2180 Functional Block Diagram

2.3.5 TPS92360

The TPS92360 is a high-efficiency, high-output voltage boost converter in small package size. The device integrates 40-V, 1.8-A switch FET and is designed for output voltage up to 39 V with a switch peak current limit of 1.2-A minimum. The large driving capability can drive single or parallel LED strings for small to large size panel backlighting. The TPS92360 operates in a current mode scheme with quasi-constant frequency. It is internally compensated for maximum flexibility and stability. The switching frequency is 1.2 MHz, and the minimum input voltage is 2.7 V. During the on-time, the current rises into the inductor. When the current reaches a threshold value set by the internal GM amplifier, the power switch MOSFET is turned off. The polarity of the inductor changes and forward biases the schottky diode which lets the current flow towards the output of the boost converter. The off-time is fixed for a certain V_{IN} and V_{OUT}, and therefore maintains the same frequency when varying these parameters. However, for different output loads, the frequency slightly changes due to the voltage drop across the $R_{DS(on)}$of the power switch MOSFET, this has an effect on the voltage across the inductor and thus on t_{ON} (t_{OFF} remains fixed). The fixed off-time maintains a quasi-fixed frequency that provides better stability for the system over a wider range of input and output voltages than conventional boost converters. The TPS92360 topology has also the benefits of providing very good load and line regulations, and excellent line and load transient responses. The feedback loop regulates the FB pin to a low reference voltage (204-mV typical), reducing the power dissipation in the current sense resistor.

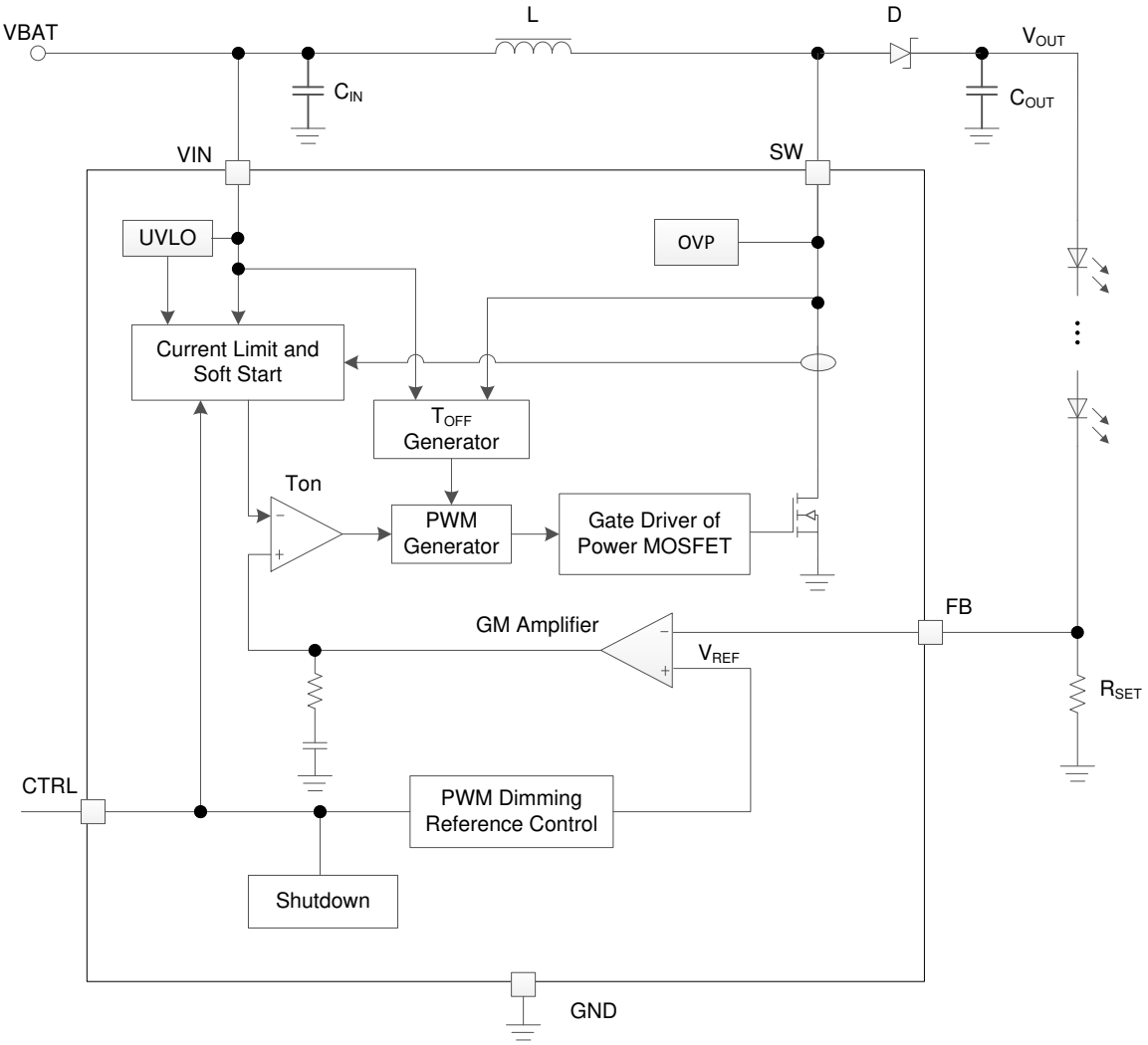

Figure 2-18. SNVSBZ5 Functional Block Diagram

2.3.6 TPS2640

The TPS26400 is a high-voltage industrial eFuse with integrated back-to-back MOSFETs and enhanced built-in protection circuitry. It provides robust protection for all systems and applications powered from 4.2 V to 42 V. The device can withstand ±42-V positive and negative supply voltages without damage. For hot pluggable boards, the device provides hot-swap power management with in-rush current control and programmable output voltage slew rate features. Load, source and device protections are provided with many programmable features including overcurrent, overvoltage, undervoltage. The precision overcurrent limit (±5% at 1 A) helps to minimize over design of the input power supply, while the fast response short circuit protection 250 ns (typical) immediately isolates the faulty load from the input supply when a short circuit is detected. The internal robust protection control blocks of the TPS26400 along with the ±42-V rating helps to simplify the system designs for the surge compliance ensuring complete protection of the load and the device. The device provides precise monitoring of voltage bus for brown-out and overvoltage conditions and asserts fault signal for the downstream system. The TPS26400 monitor functions threshold accuracy of ±3% ensures tight supervision of the supply bus, eliminating the need for a separate supply voltage supervisor chip. The device monitors $V_{(IN)}$ and $V_{(OUT)}$ to provide true reverse current blocking when a reverse condition or input power failure condition is detected. The TPS26400 is also designed to control redundant power supply systems. A pair of TPS26400 devices can be configured for active ORing between the main power supply and the auxiliary power supply .

Additional features of the TPS26400 include:

- Current monitor output for health monitoring of the system
- Electronic circuit breaker operation with overload timeout using MODE pin

- A choice of latch off or automatic restart mode response during current limit fault using MODE pin
- Overtemperature protection to safely shutdown in the event of an overcurrent event
- De-glitched fault reporting for brown-out and overvoltage faults
- Look ahead overload current fault indication

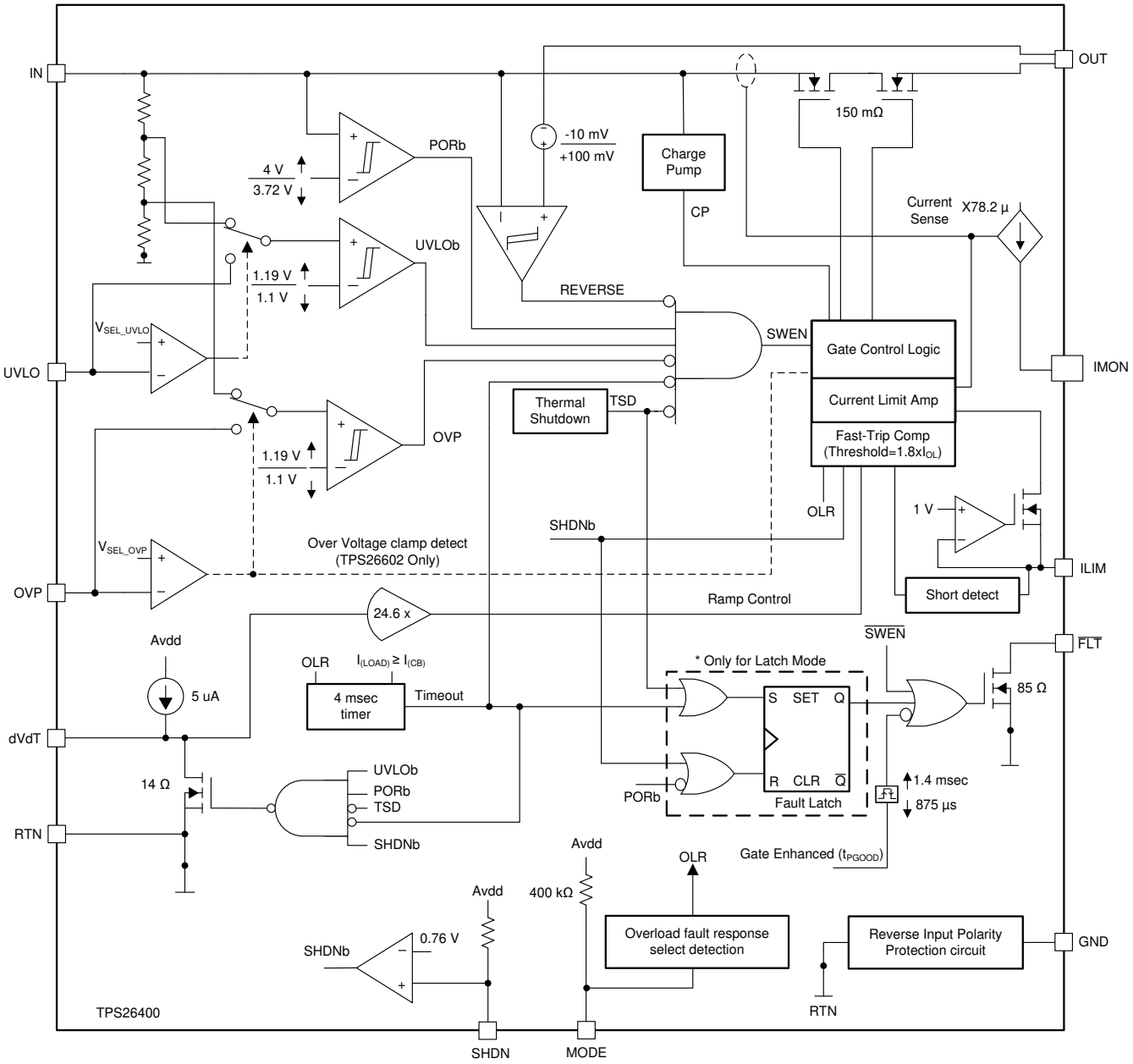

Figure 2-19. TPS2640 Functional Block Diagram

2.3.7 BQ24072

The BQ2407x devices are integrated Li-Ion linear chargers and system power path management devices targeted at space-limited portable applications. The device powers the system while simultaneously and independently charging the battery. This feature reduces the number of charge and discharge cycles on the battery, allows for proper charge termination and enables the system to run with a defective or absent battery pack. This feature also allows instant system turn-on even with a totally discharged battery. The input power source for charging the battery and running the system can be an AC adapter or a USB port. The devices feature Dynamic Power Path Management (DPPM), which shares the source current between the system and battery charging, and automatically reduces the charging current if the system load increases. When charging from a USB port, the input dynamic power management (V_{IN}-DPM) circuit reduces the input current if the input

voltage falls below a threshold, thus preventing the USB port from crashing. The power-path architecture also permits the battery to supplement the system current requirements when the adapter cannot deliver the peak system currents.

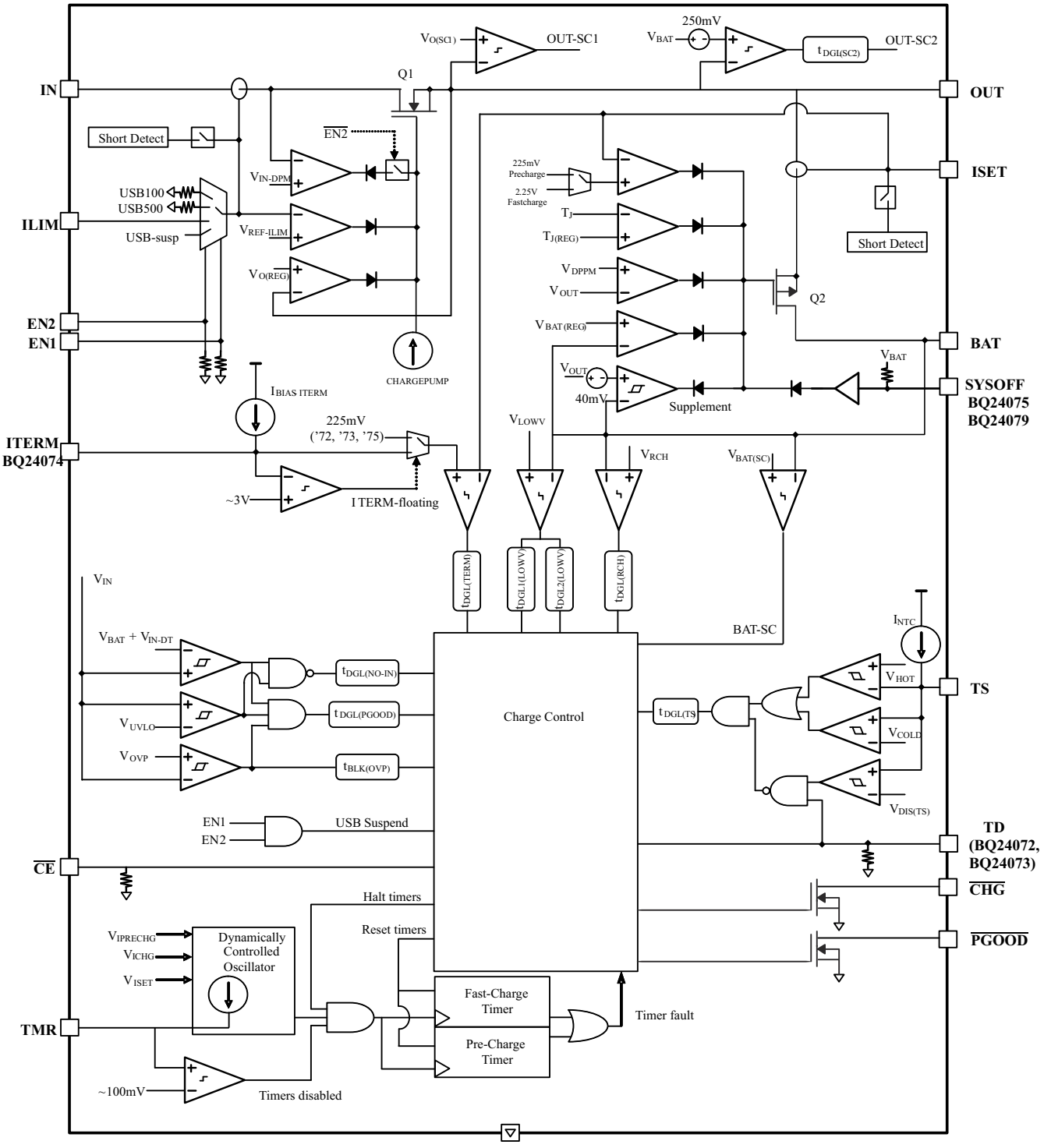

Figure 2-20. BQ24072 Functional Block Diagram

3 Hardware, Software, Testing Requirements, and Test Results

3.1 Hardware Requirements

3.2 Test Setup

Several test points are made available for each process on the PCB. However, when performing ripple, transient, and efficiency tests, do not use the break out test points due to parasitic noise. Instead, measure the output, input, or other point of interest as close to the IC pins as possible. An example of a transient test setup is shown in Figure 3-1 that uses a barrel wire to GND technique and the current-carrying wires are soldered directly onto the output capacitor of the DC-DC being tested. These current-carrying wires are connected directly to a programmable electronic load and the current is measured through a current probe as shown in Figure 3-2. When performing efficiency plots, separate wires from the current-carrying wires must be used, as shown in Figure 3-3 to avoid inaccurate measurements due to line voltage drops.

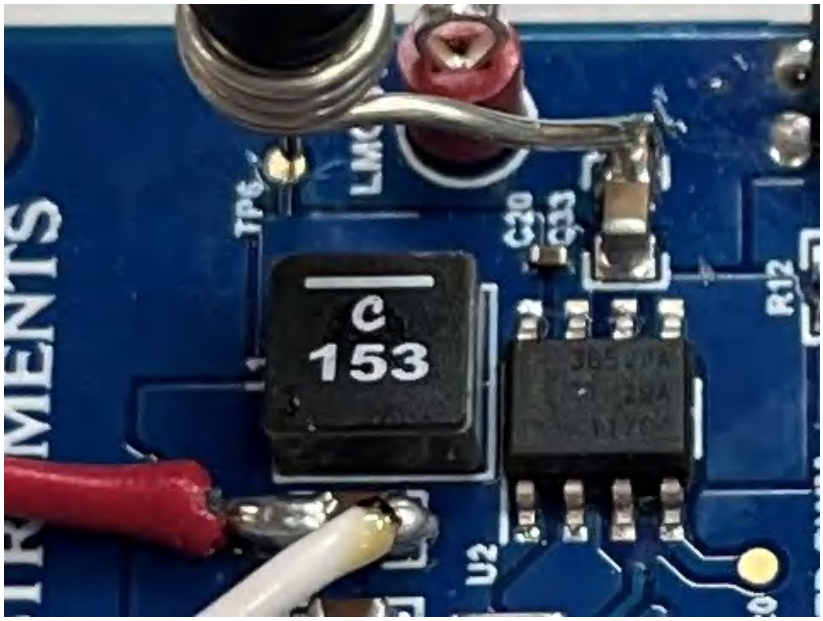

Figure 3-1. Soldered Output Wires and Scope Probe and Barrel Test Setup

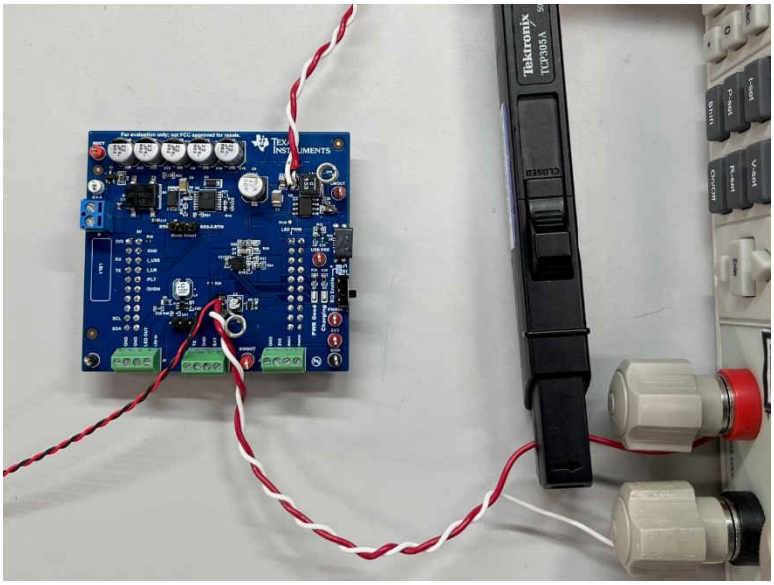

Figure 3-2. Current Probe and Electronic Load Test Setup

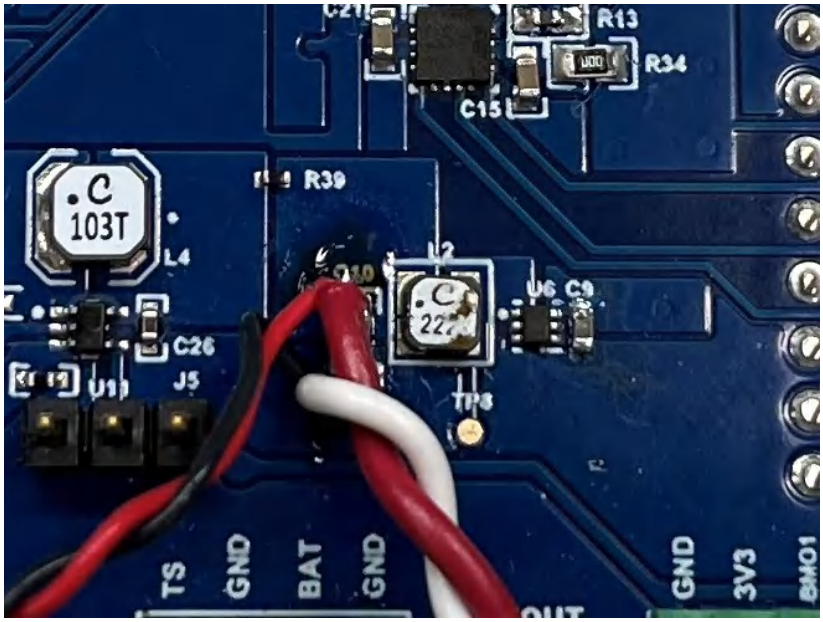

Figure 3-3. Separate Sensing and Current Carrying Wires Test Setup

3.3 Test Results

3.3.1 24-VAC Start-Up and Shutdown

Figure 3-4 shows the sequence of power up when a 24-VAC system is plugged in. The battery was already connected and powering the 3V3 rail before 24 VAC was plugged in. Upon plugging in the 24-VAC, the system begins charging the battery and takes over powering the system load. RectOut reaches steady state in approximately 240 ms from the initial 24-VAC plugin. Variances in the 24-VAC transformer cause variances in the steady-state rise time as can be observed by comparing Figure 3-4, Figure 3-8, and Figure 3-10. Note that the LMR36520 rail is tested at node PWRIn, which is directly on the output of the ORing solution. The 3V3 rail exhibits no distinguishable transient response during the transition from battery power to 24-VAC power. Figure 3-8 and Figure 3-10 provide start-up tests to account for tolerances present in 24-VAC transformers and show comparable results to Figure 3-4. Immediate loss of 24-VAC power is tested in Figure 3-5, Figure 3-9, and Figure 3-11. As is evident by the smooth nature of RectOut in these tests, the battery was fully charged and no significant load current was being supplied. Upon a 24-VAC power loss, RectOut discharges most of the rectification caps energy in 1 second for a nominal 24 VAC. Figure 3-6 and Figure 3-7 show a 24-VAC loss while a load on the 3V3 bus is demanding current. The rectification caps discharge considerably faster than no load conditions. The BMOut rail drops in voltage as the BM24072 transitions to battery power. The 3V3 rail exhibits no significant transient response to the loss of 24 VAC and remains regulated and supplying to output load.

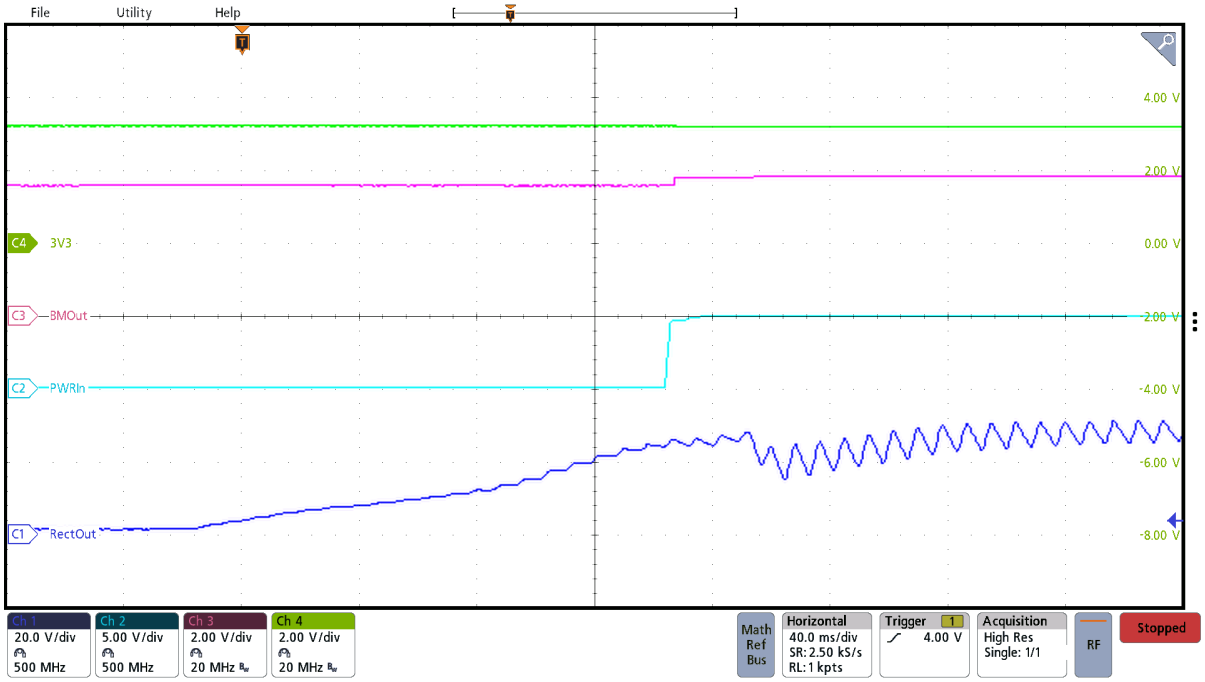

Figure 3-4. 24-VAC Start-Up

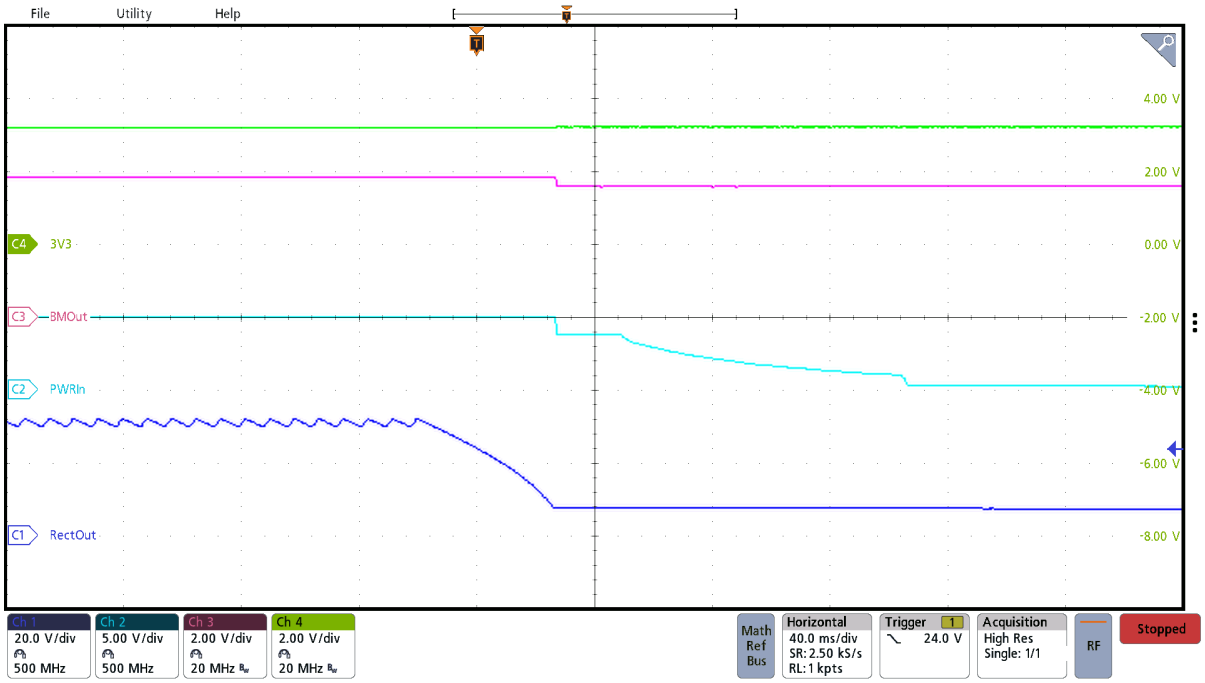

Figure 3-5. 24-VAC Shutdown

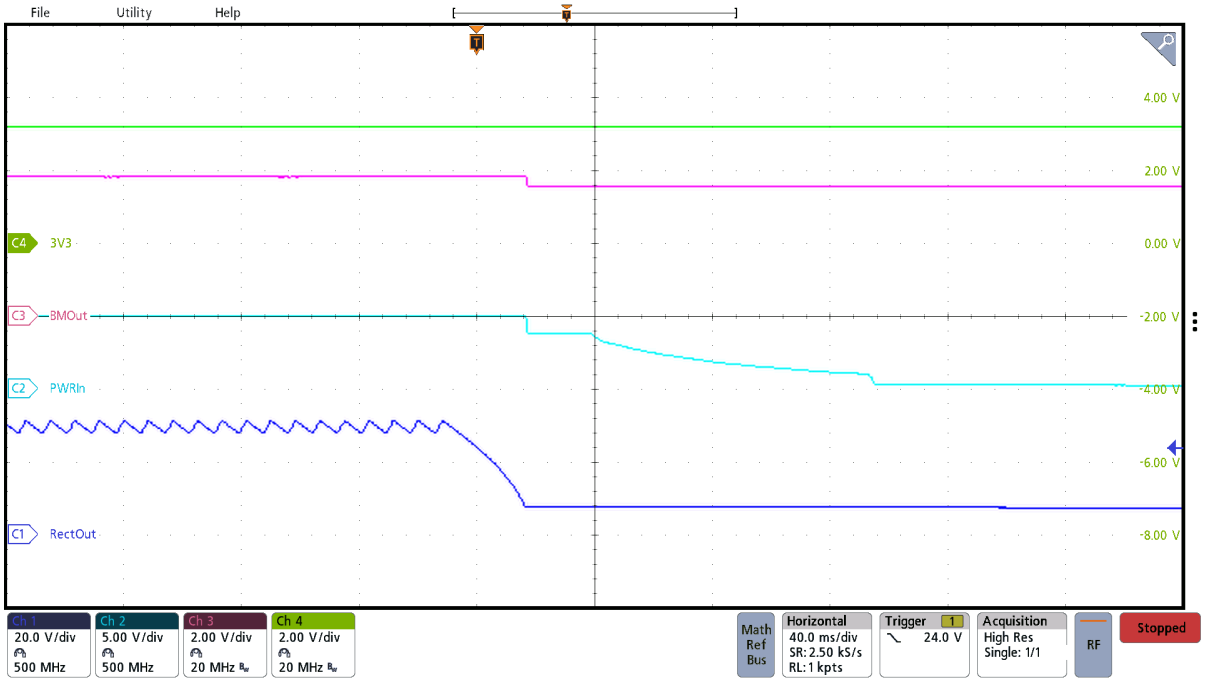

Figure 3-6. 24-VAC Shutdown (3V3 Load = 200 mA)

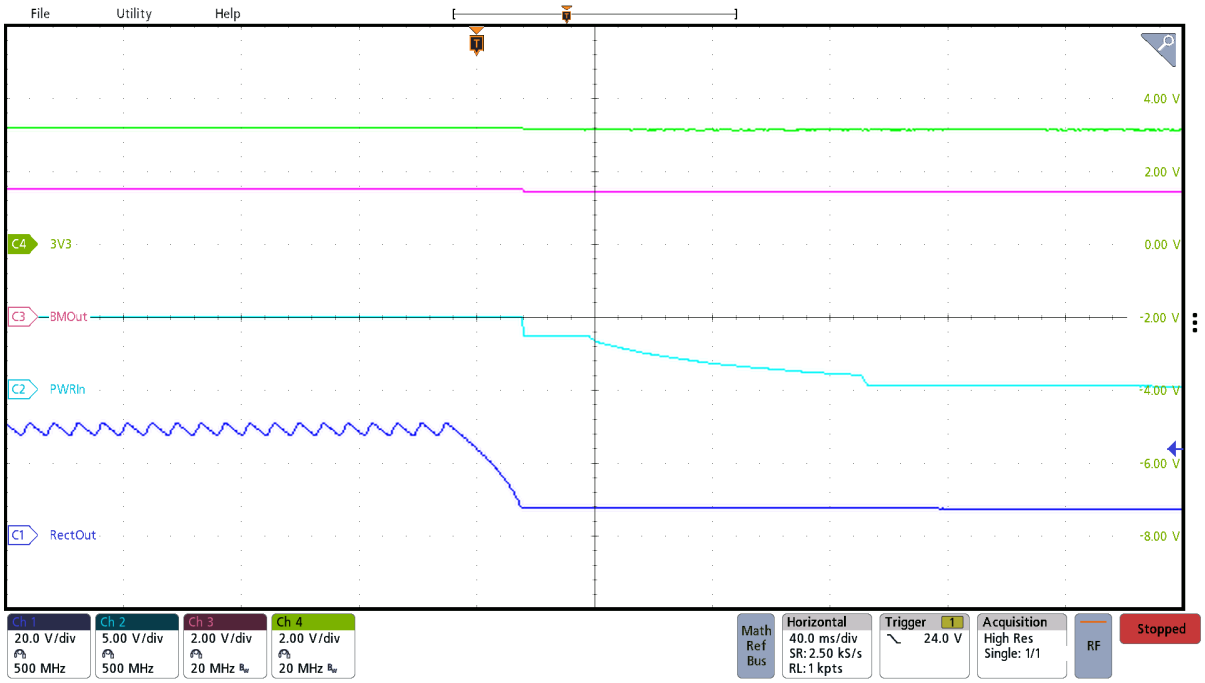

Figure 3-7. 24-VAC Shutdown (3V3 Load = 750 mA)

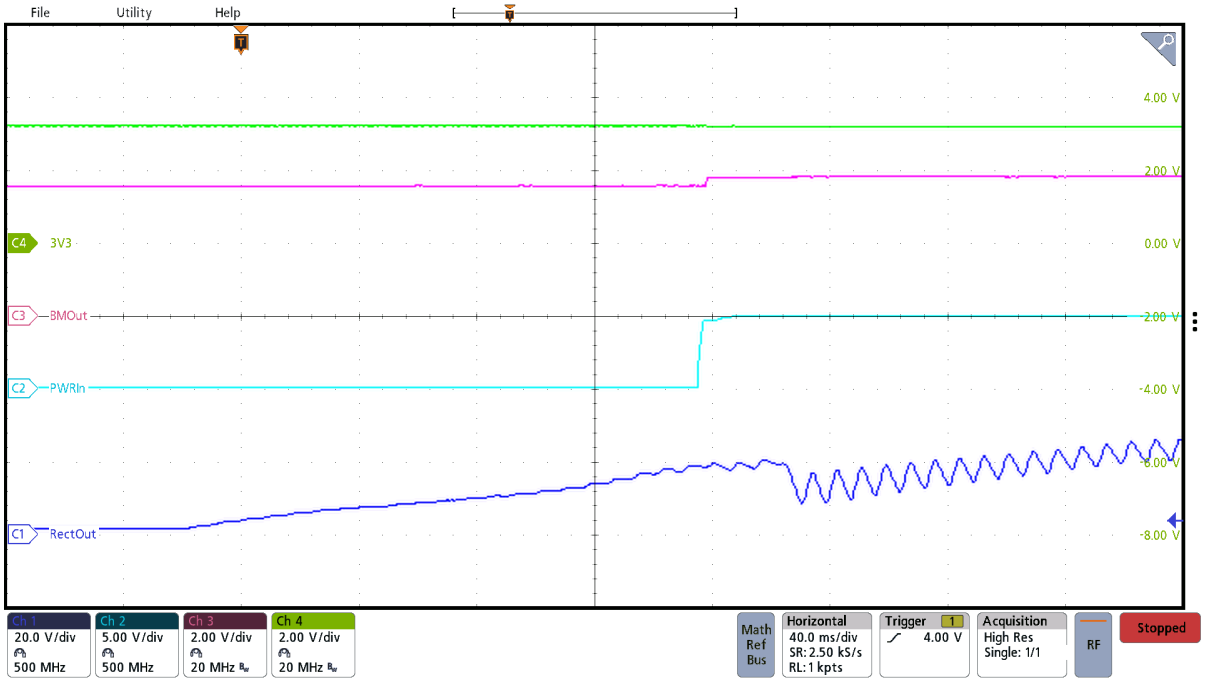

Figure 3-8. 20-VAC Start-Up

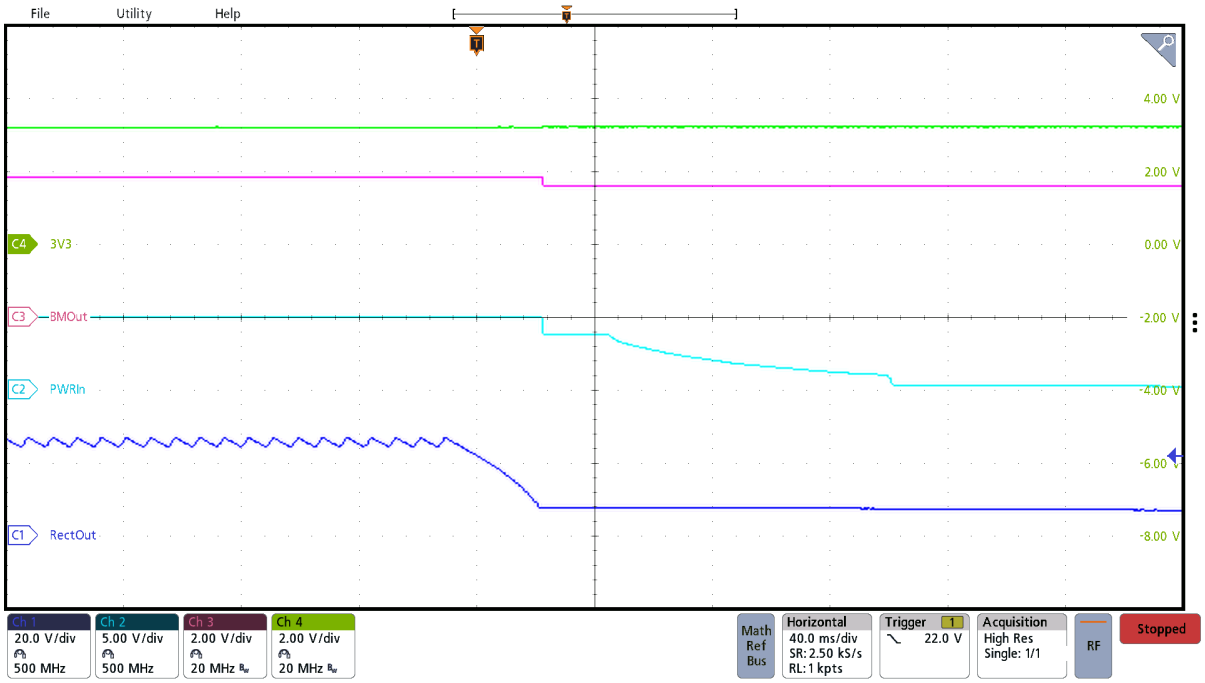

Figure 3-9. 20-VAC Shutdown

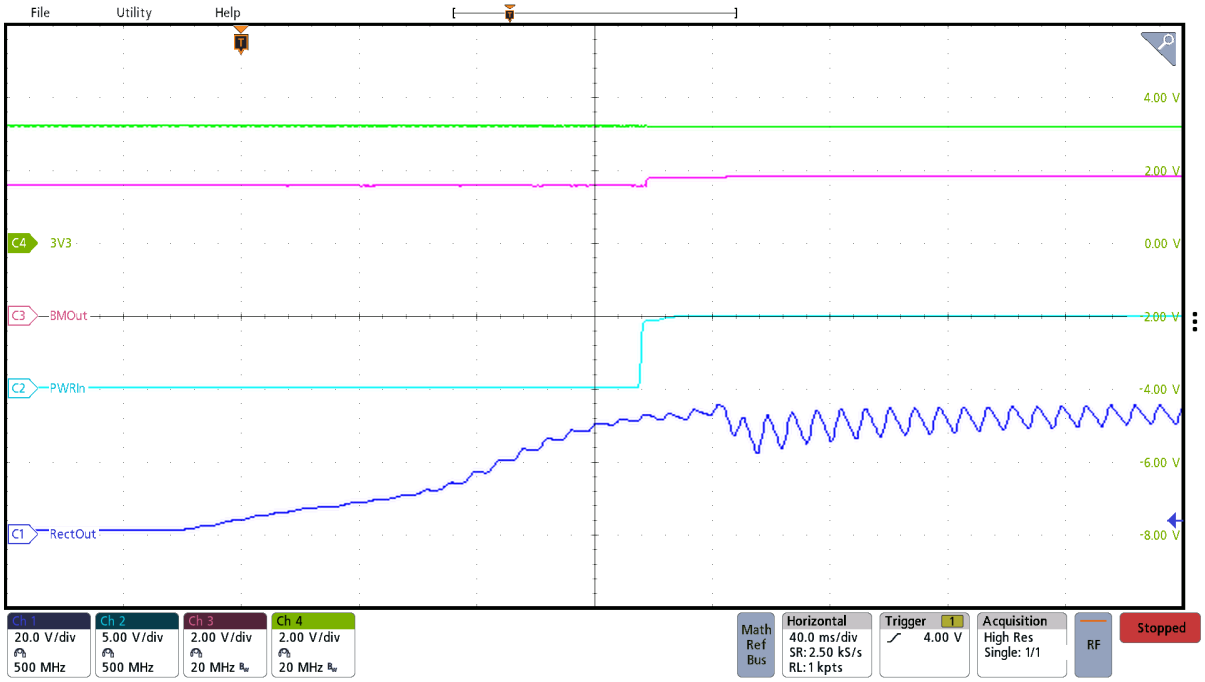

Figure 3-10. 30-VAC Start-Up

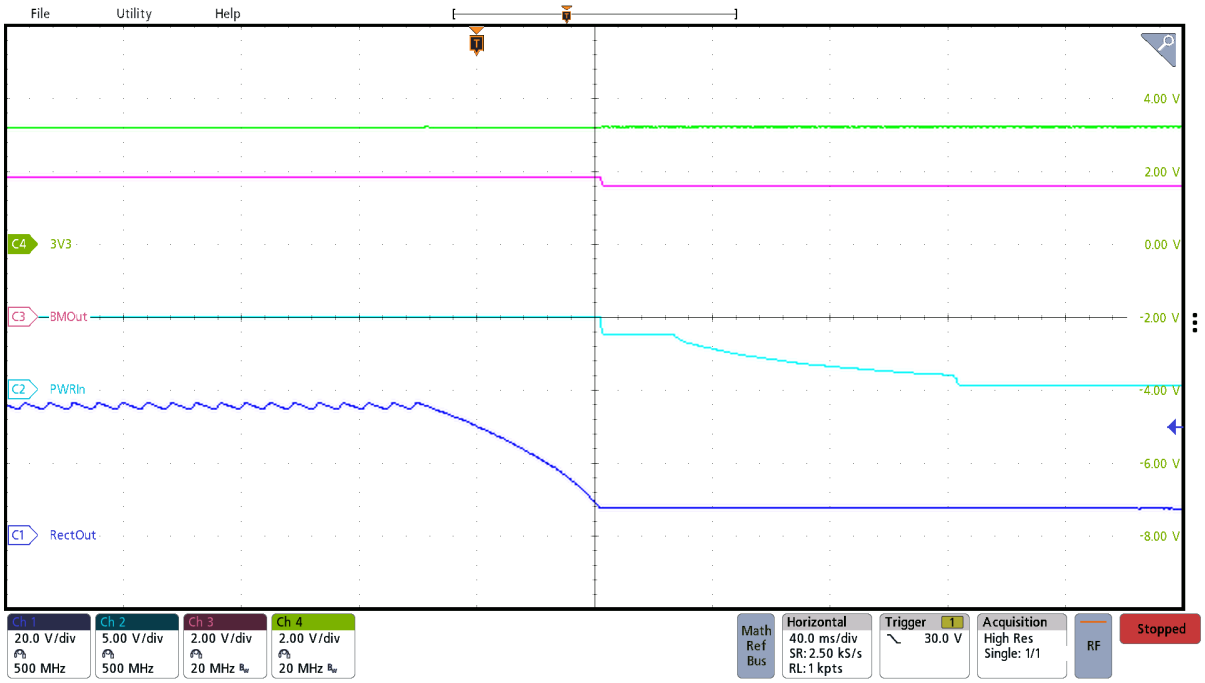

Figure 3-11. 30-VAC Shutdown

3.3.2 USB Start-Up and Shutdown

Figure 3-12 shows a 5.1-V USB cable being plugged into the system (A 3-ft USB A to USB micro-B cable was used for Figure 3-12 and Figure 3-13). The node USBin exhibits no overshoot, which is due, in part, to the snubber circuit detailed in Section 2.2.3.2. The PWRIn, which is the output of the ORing circuit, matches the response of the USBin. This test shows 4 ms passes before the battery management system regulates the output, BMOut, to 200 mV plus VBATT. As with the 24-VAC start-up, the battery was previously supplying the load when the USB was plugged in. Upon USB plug in, the battery management begins charging the battery with up to 300 mA. The 3V3 rail shows no significant transient response to the change in power sources. Figure 3-13 shows power transition back to the battery as the USB is unplugged. Approximately 20 ms passes before the

USBIn rail diminishes towards zero. A slight drop at BMOut is seen as the system switches to battery power and thus VBATT. The 3V3 rail remains very steady with no significant transient response during the transition.

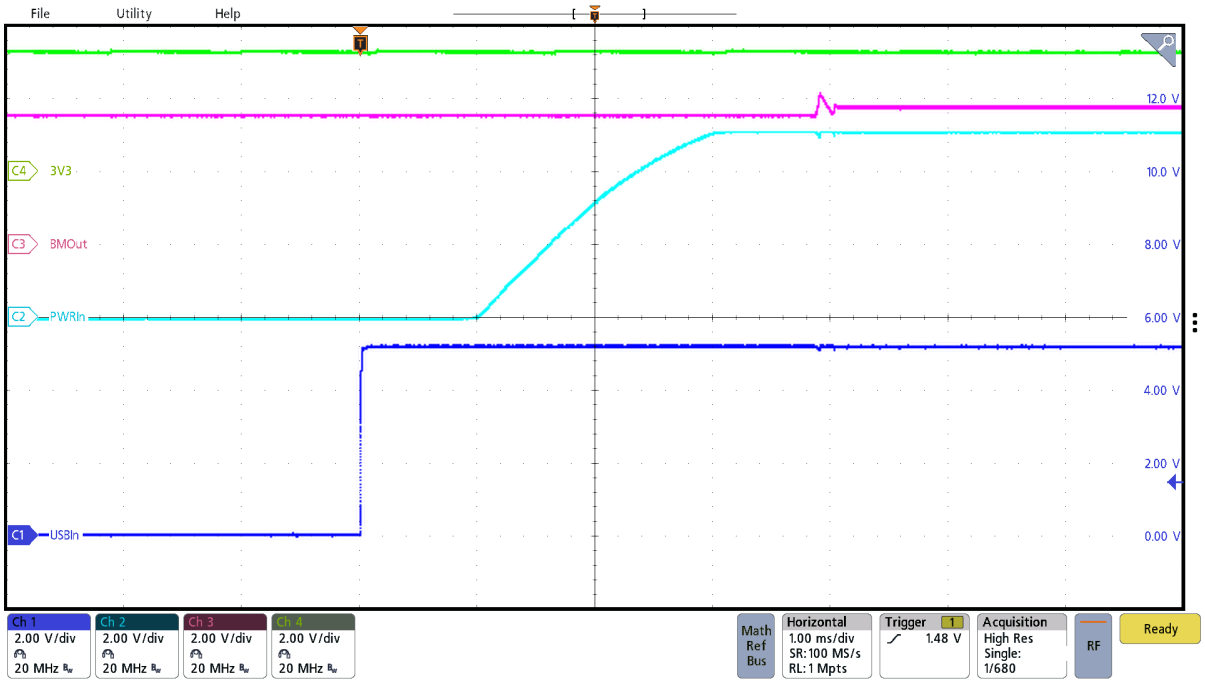

Figure 3-12. USB 5.1-V Start-Up

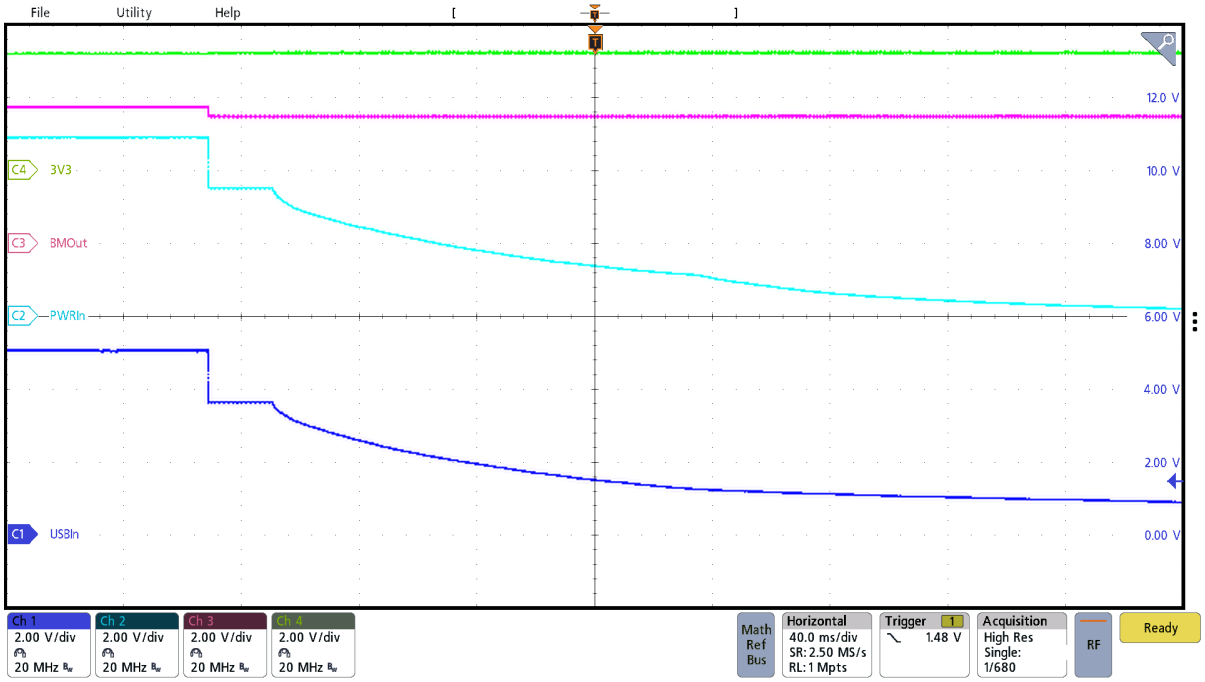

Figure 3-13. USB 5.1-V Shutdown

Figure 3-14 shows a start-up variation with USBin at 4.35 V, the minimum allowed per USB 2.0 specifications. The actual tests for Figure 3-14 and Figure 3-15 were performed with banana to grabber cables. These cables are not isolated and exhibit significantly more parasitic inductance than a typical USB cable. Even so, a very minimal overshoot of 150 mV is observed. The high-level voltage of the USB rail is reached approximately 2 µs after initial plug in. As observed in Figure 3-14, the delay time for the ORing circuit to pass the USBin to the PWRIn rail is approximately 100 µs. Figure 3-16 and Figure 3-17 show similar results.

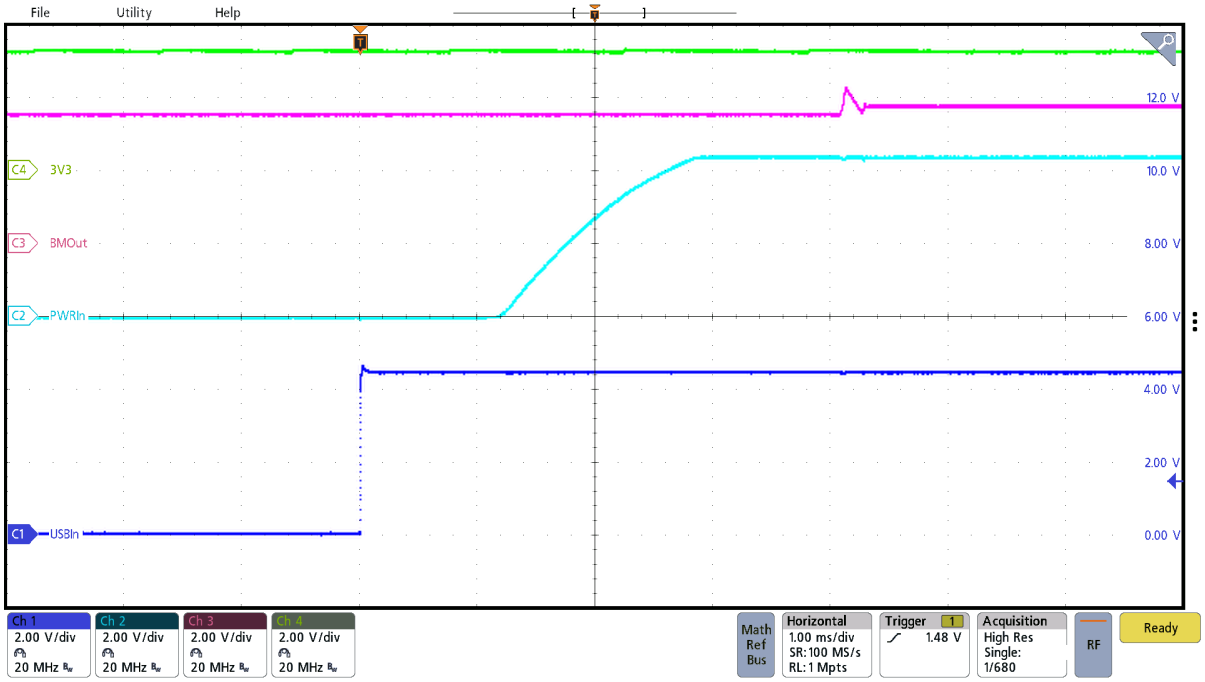

Figure 3-14. USB 4.35-V Start-Up

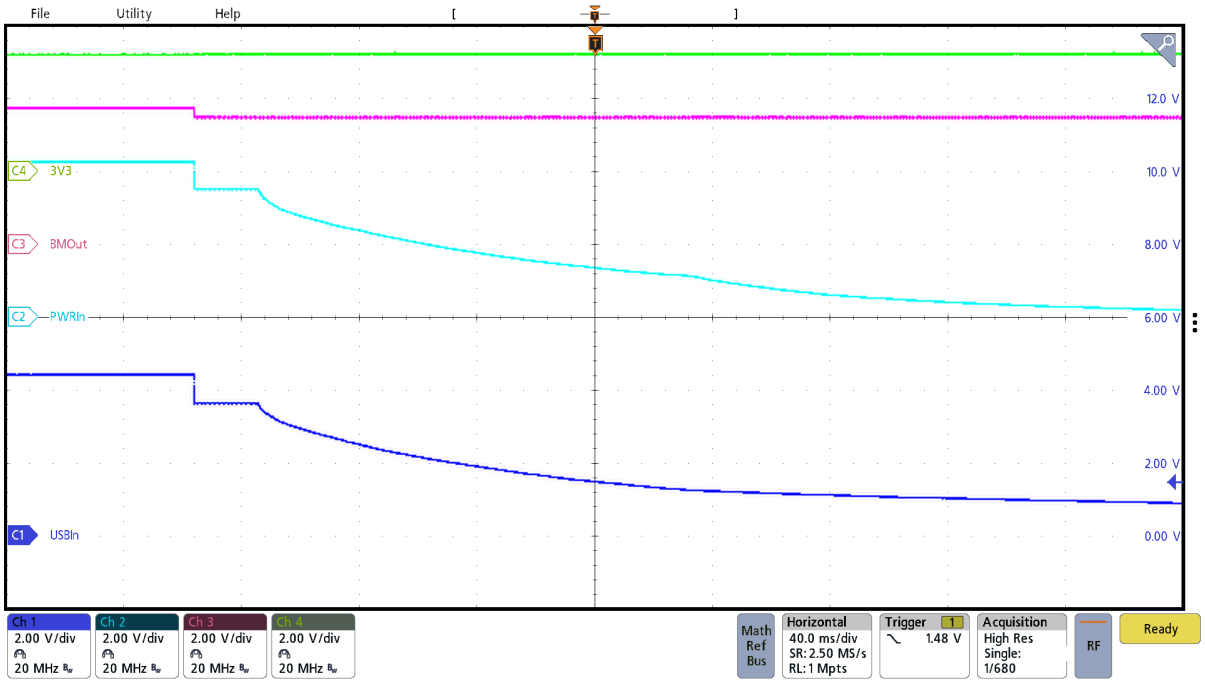

Figure 3-15. USB 4.35-V Shutdown

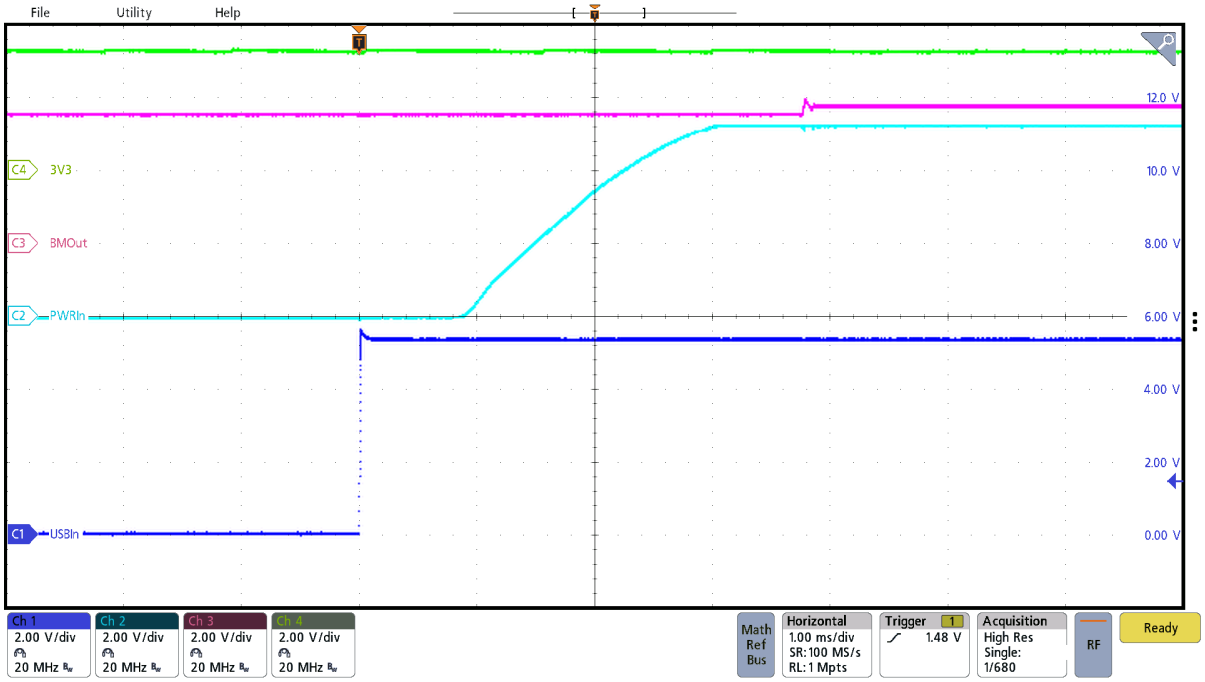

Figure 3-16. USB 5.25-V Start-Up

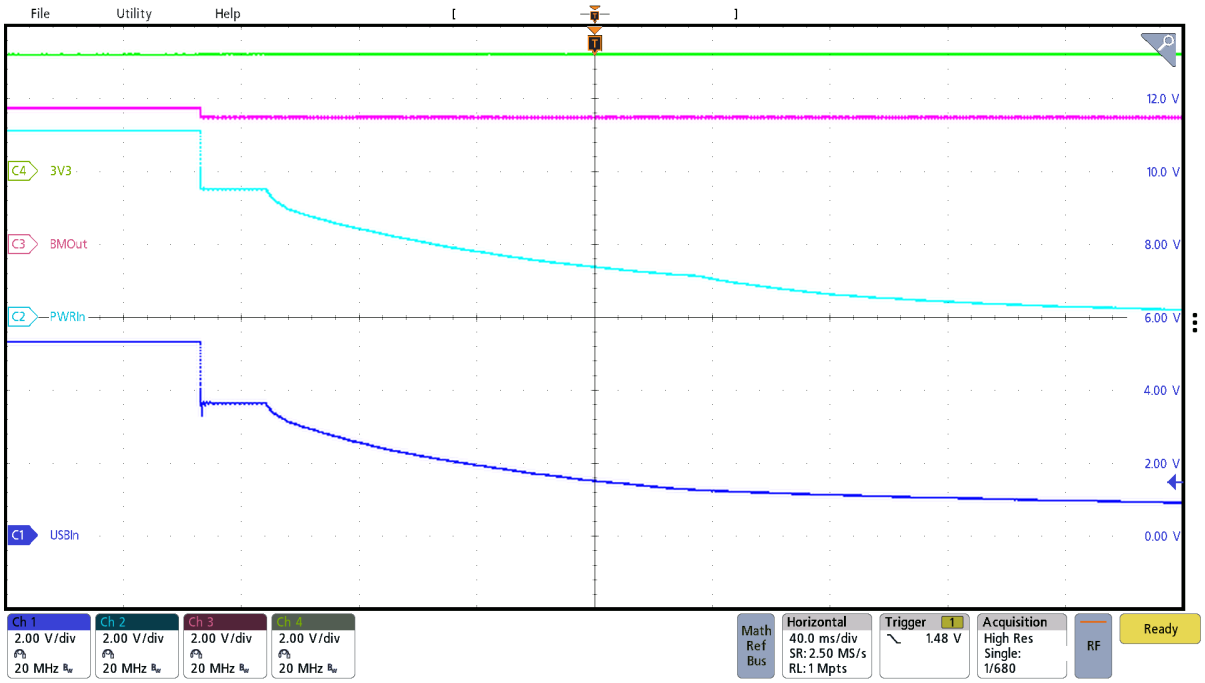

Figure 3-17. 5.25-V Shutdown

3.3.3 ORing

The ORing circuit as described in Section 2.2.4 is tested in this section. Figure 3-18 shows LMOut dominating USB upon plug in. Prior to LMOut powering up, USB is shown high and LMRC is high, forcing the USBin associated FETs on and LMOut FETs off. Once LMOut is powered up, the LMOnOff node begins to be pulled up, thus driving LMRC low, thereby turning the LM associated FETs on, and the USB associated FETs off. Figure 3-19 shows the opposite activity when LMOut shifts low. When the USB power is not present, the LM still passes through to output by pulling LMOnOff high as shown in Figure 3-20 and Figure 3-21.

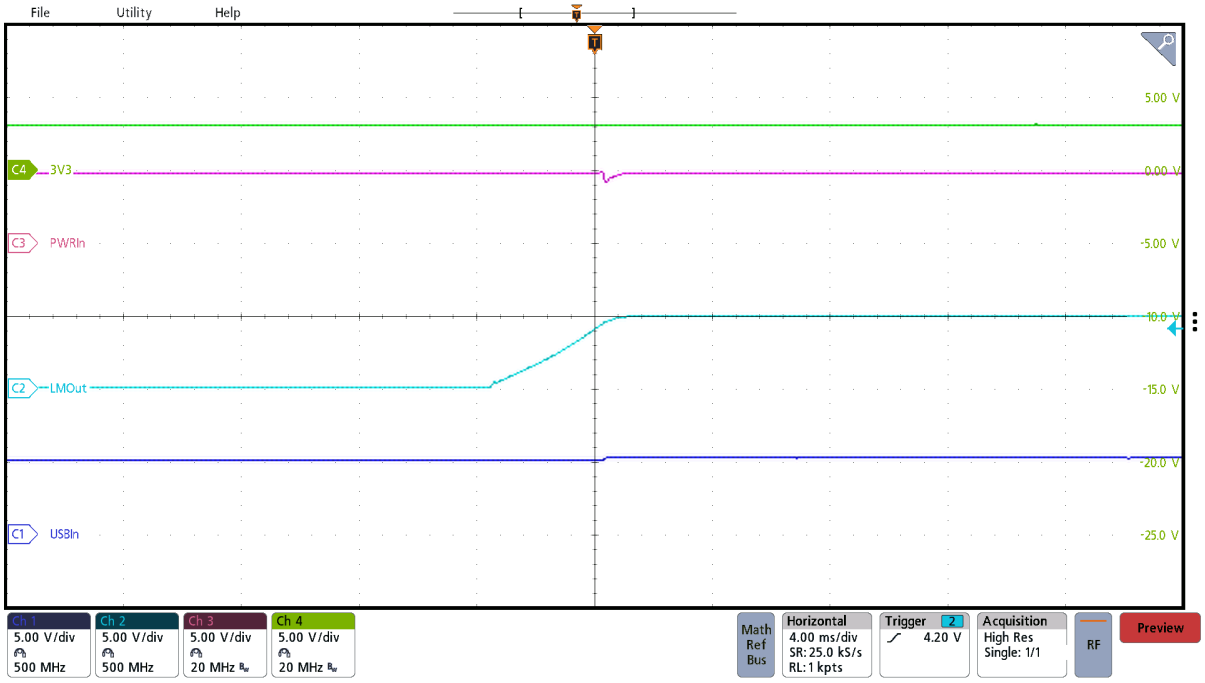

Figure 3-18. ORing Start-Up (LMOut Power Up: USB Source Present)

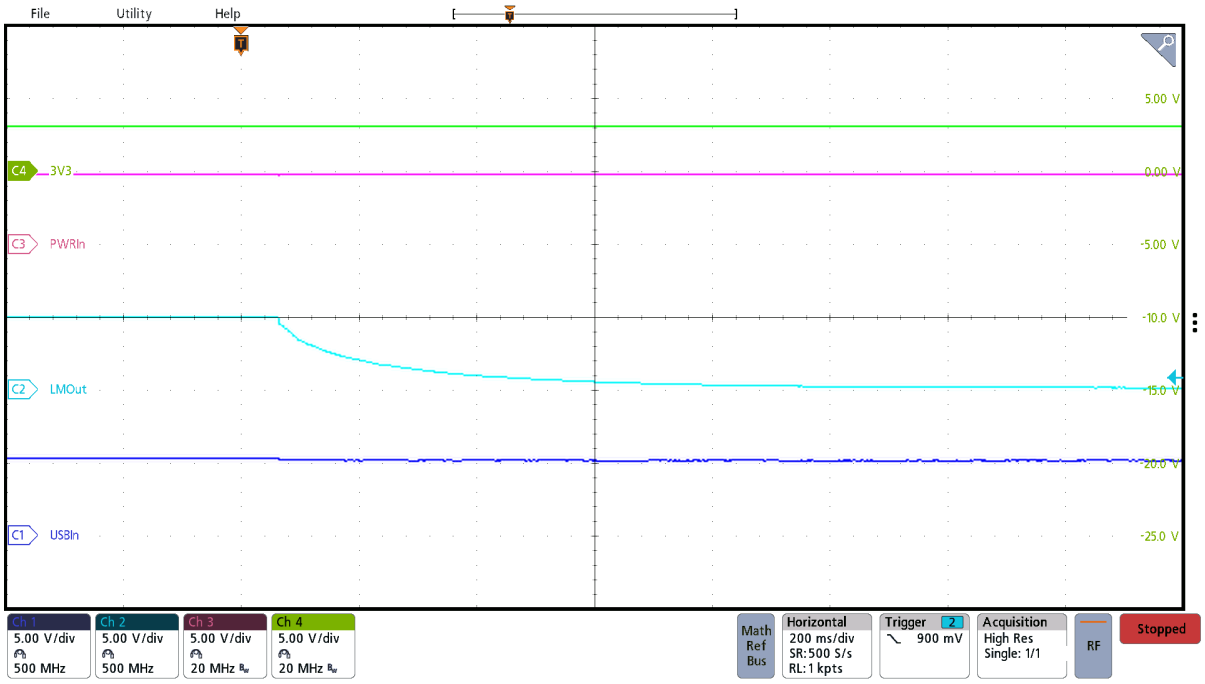

Figure 3-19. ORing Shutdown (LMOut Power Loss: USB Source Present)

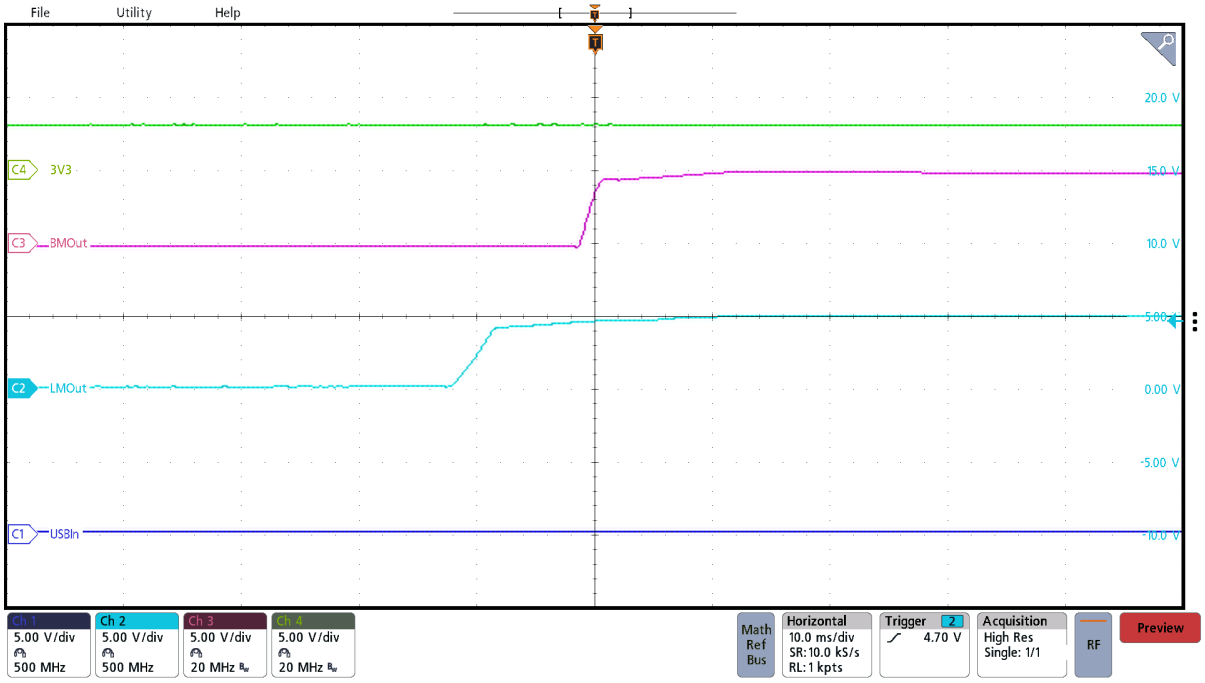

Figure 3-20. ORing Start-Up (LMOut Power Up: USB Source Absent)

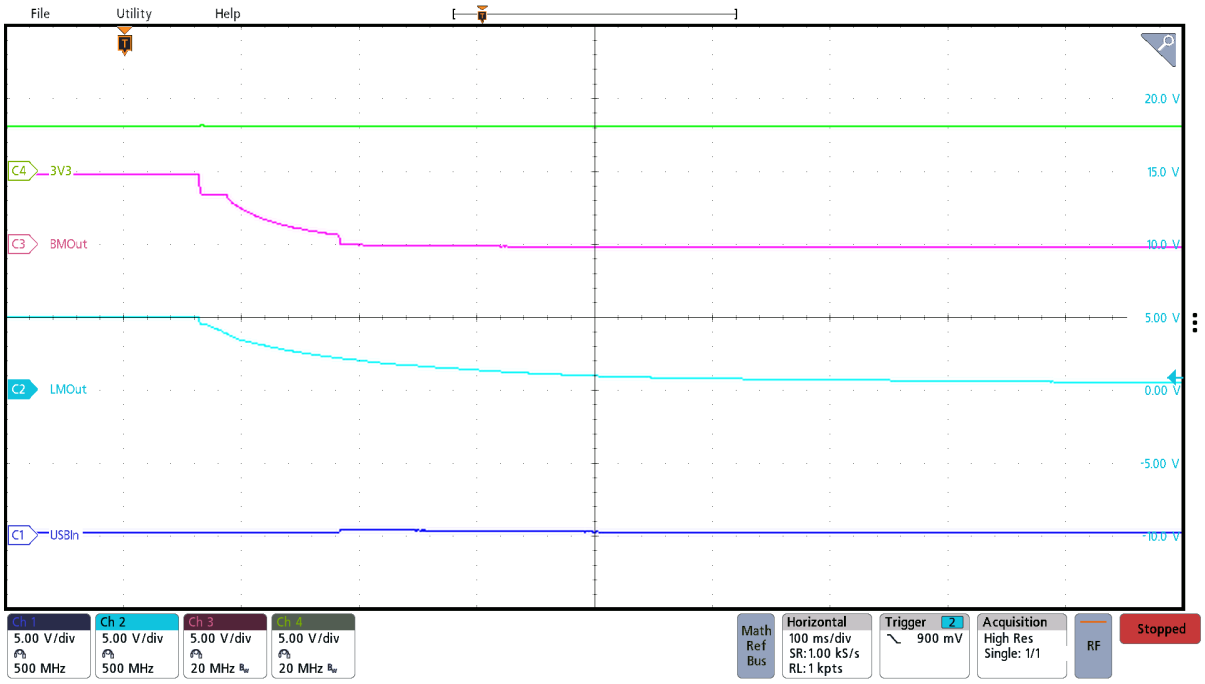

Figure 3-21. ORing Shutdown (LMOut Power Loss: USB Source Absent)

3.3.4 LMR36520

Figure 3-22 shows the transition of the LMR36520 from DCM to CCM operating modes as is evident by the differing ripple frequencies during no load and 480 mA. A transition from DCM to CCM causes the worst-case transient response. The transient response while operating only in CCM is significantly smaller as seen in Figure 3-23. Figure 3-24 provides the load current rise and associated transient response on a small-time scale to allow closer analysis.

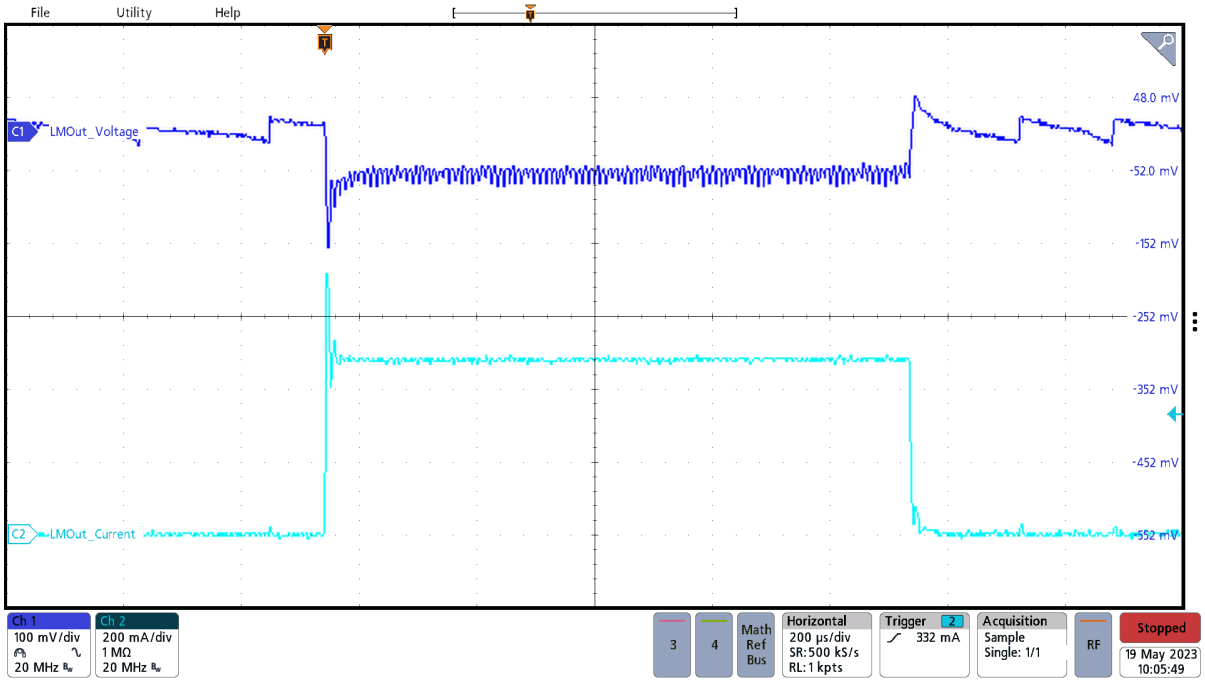

Figure 3-22. LMR36520 Transient Response (0 to 480 mA)

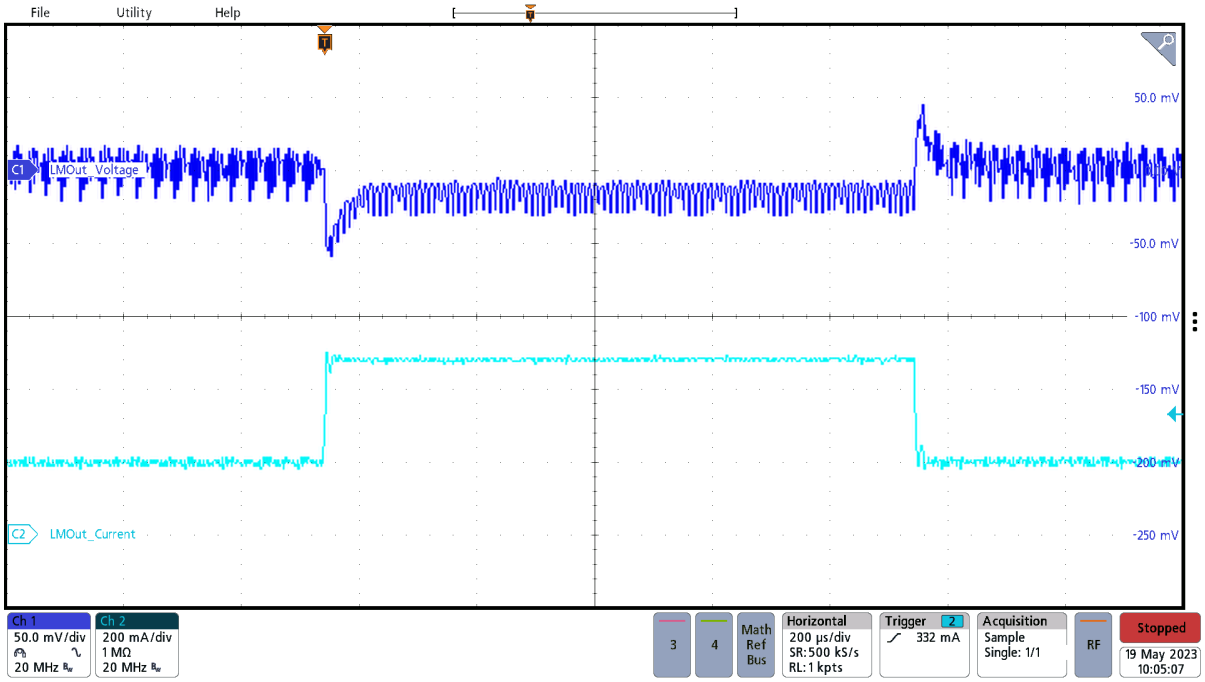

Figure 3-23. LMR36520 Transient Response (200 to 480mA)

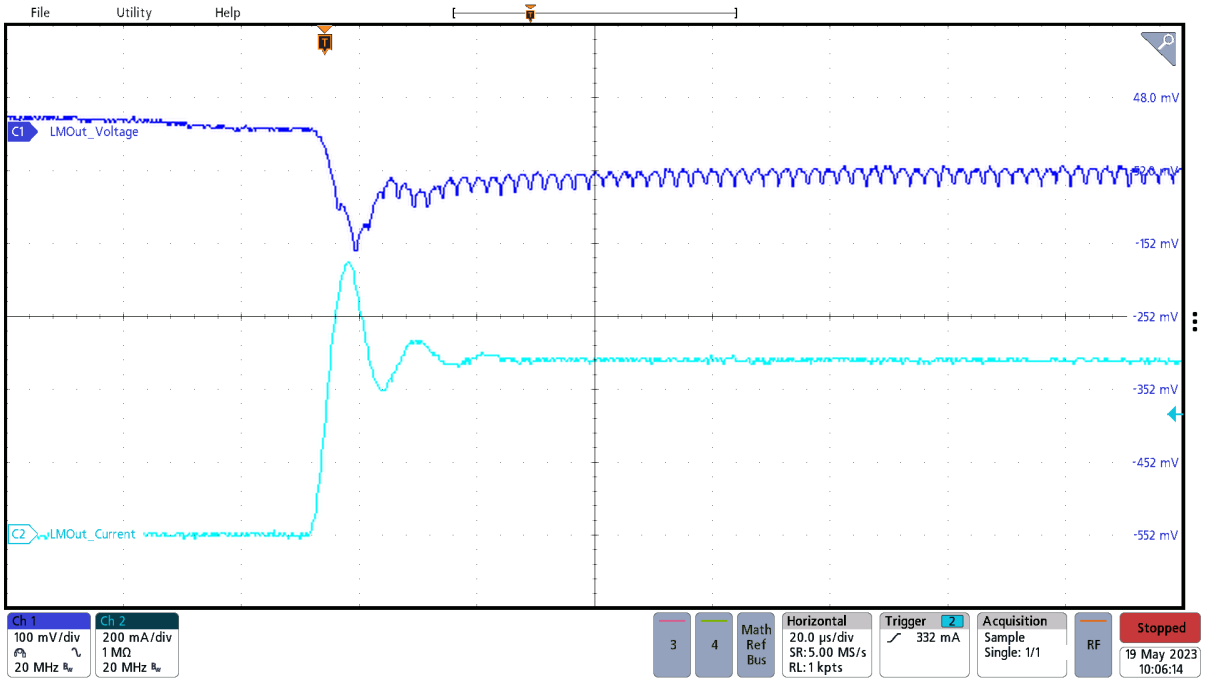

Figure 3-24. LMR36520 Transient Response Slew

3.3.5 TLV62568 Transient Response

The 3V3 rail is the primary power bus powering a system load and thus ripple and transient response on this rail must remain small. In this reference design, the TLV62080 operates very well, with a transient response of less than 6% for a 0-A to 1-A load step.

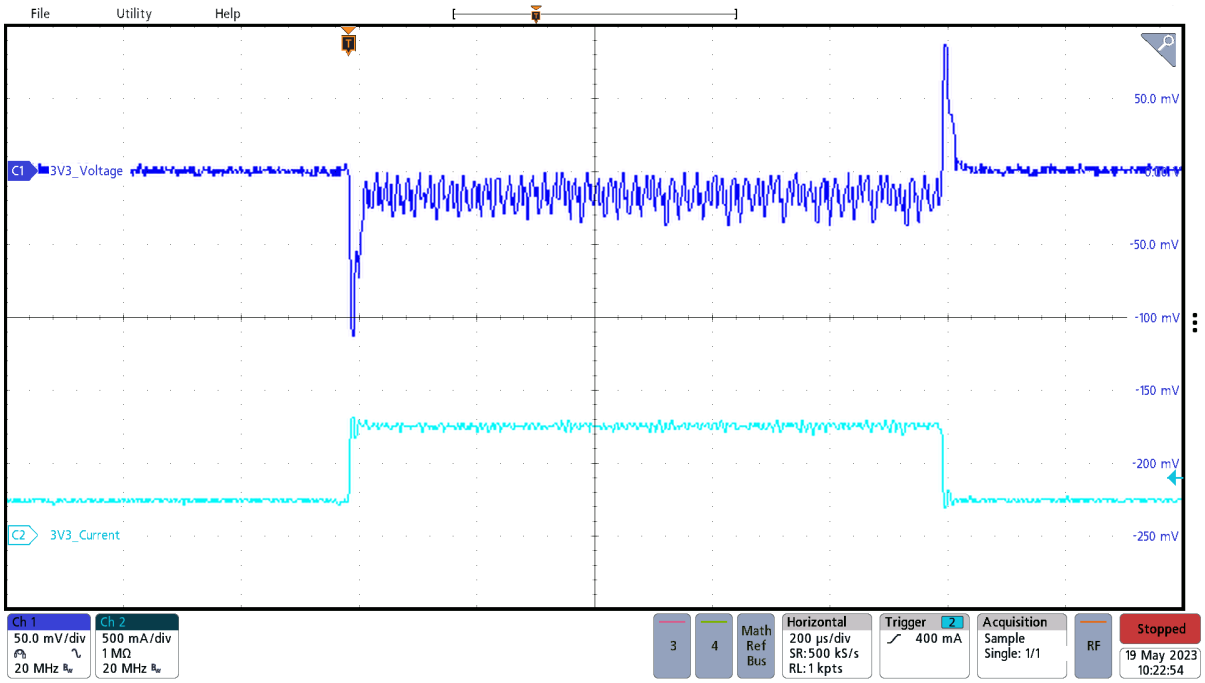

Figure 3-25. TLV62568 Transient Response (250 to 750 mA)

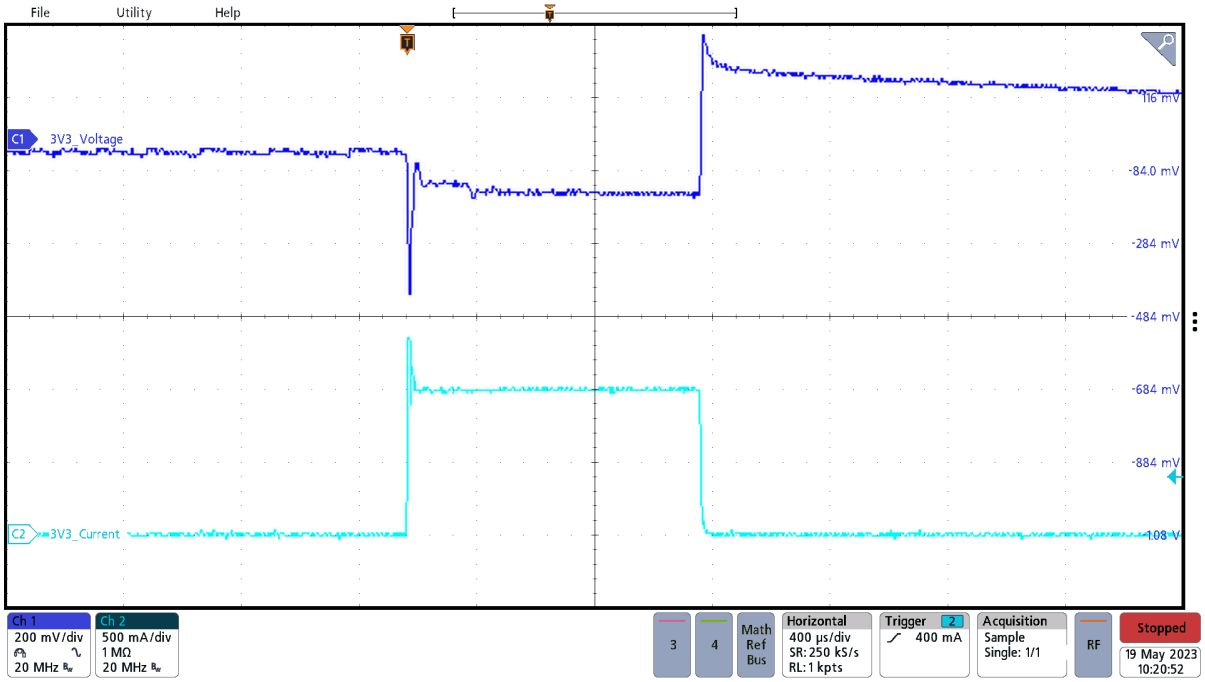

Figure 3-26. TLV62568 Transient Response (0 to 1 A)

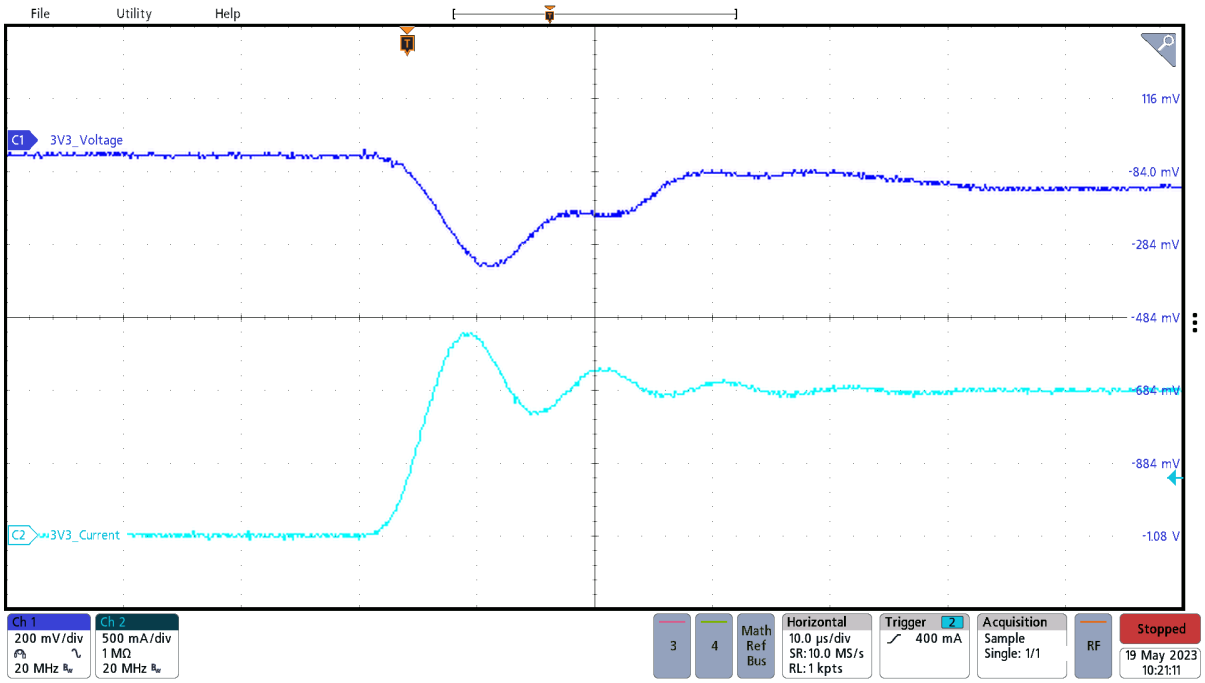

Figure 3-27. TLV62568 Transient Response Slew

3.3.6 BM24072 Transient Response

The battery management system transient response is more complicated than the LMR36520 and TLV62568 as the BM24072 must pull current from two sources, the battery and the PWRin node, when load currents exceed 500 mA. Figure 3-28 shows a 250-mA to 750-mA load step on the BM24072 output. As the load current becomes too high for the PWRin node to supply, the battery management system drops in voltage because it uses the battery as power assistance. BMOut returns to the initial voltage once the output current steps back down and the battery is no longer required to provide additional current. When the battery is the only source present, the transient response of the BM24072 exhibits only the voltage drop across the power line of the battery because current is pulled as shown in Figure 50 Figure 3-29.

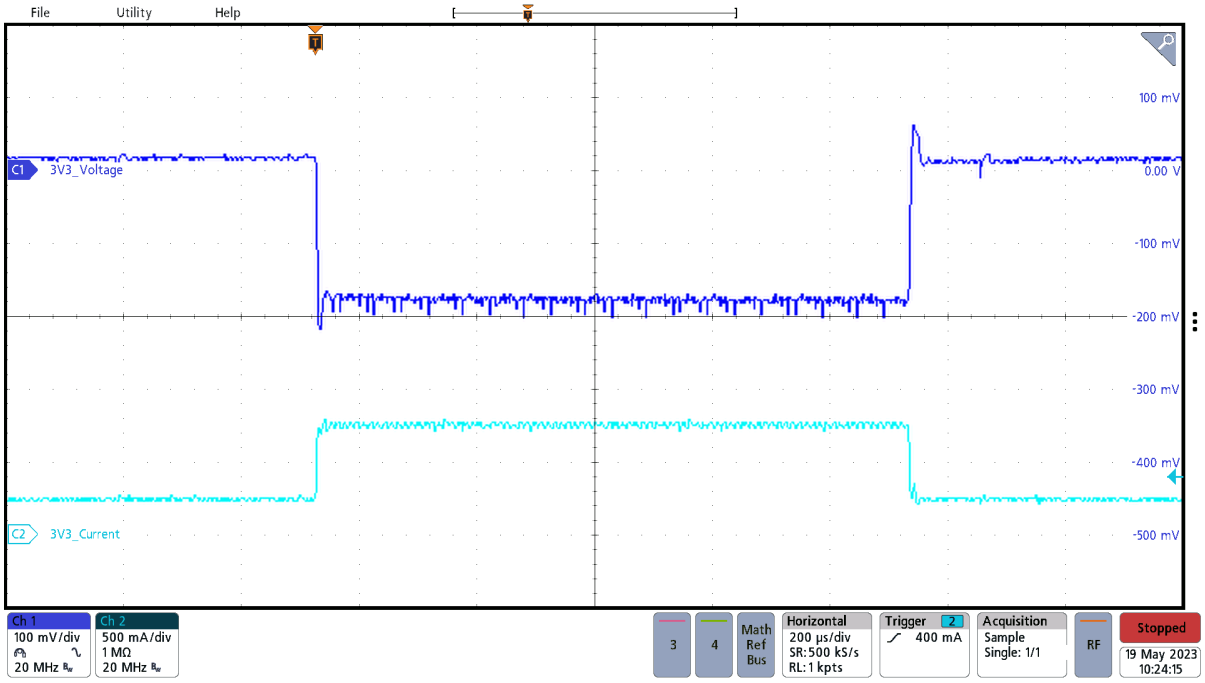

Figure 3-28. BM24072 Transient Response (250- To 750-mA; Battery and PWRin Source)

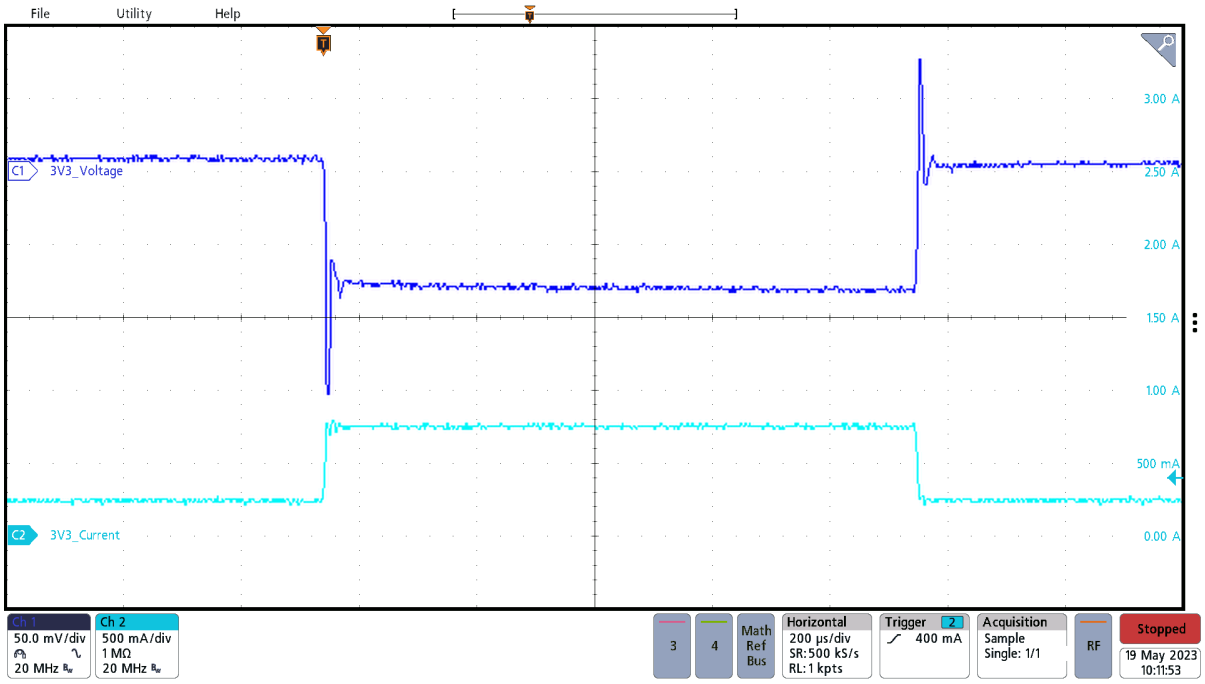

Figure 3-29. BM24072 Transient Response (250- To 750-mA; Battery Only)

3.3.7 TLV62568 (3V3 Power Rail)

Perhaps the most important power rail to monitor the ripple and noise is the TLV62568 3V3 because it is powering the system load. In this reference design, the TLV62568 exhibits very low amplitude ripple. At a 125-mA load test, shown in Figure 3-33, the ripple of the 3V3 rail is equal or less than the noise floor of the oscilloscope used for testing. Figure 3-34 shows low jitter on the switch node when using only one source. When using two sources during high current loads as shown in Figure 3-38, the battery in addition to the PWRin source, the SW node exhibits more jitter because the input voltage is constantly changing to balance battery and PWRin sources. Even while using dual sources and full load current the ripple of the 3V3 rail stays beneath 0.75%.

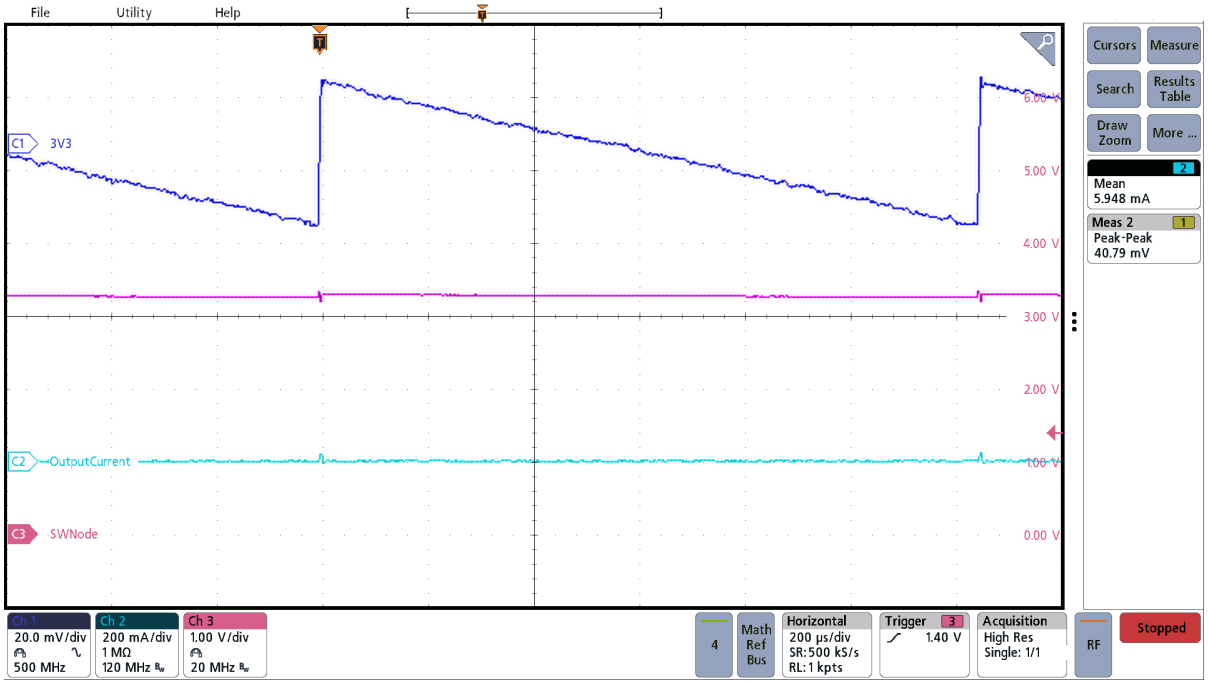

Figure 3-30. *3V3* Ripple (No Load; 24-VAC Source)

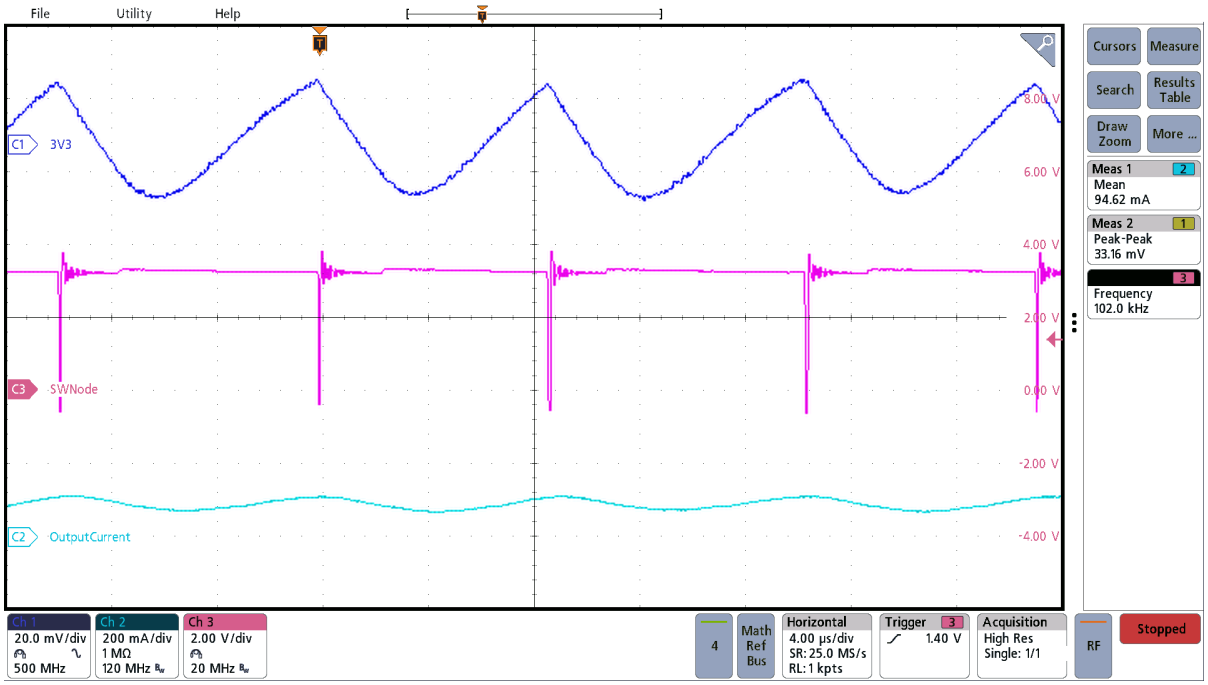

Figure 3-31. *3V3* Ripple (90-mA; 24-VAC Source)

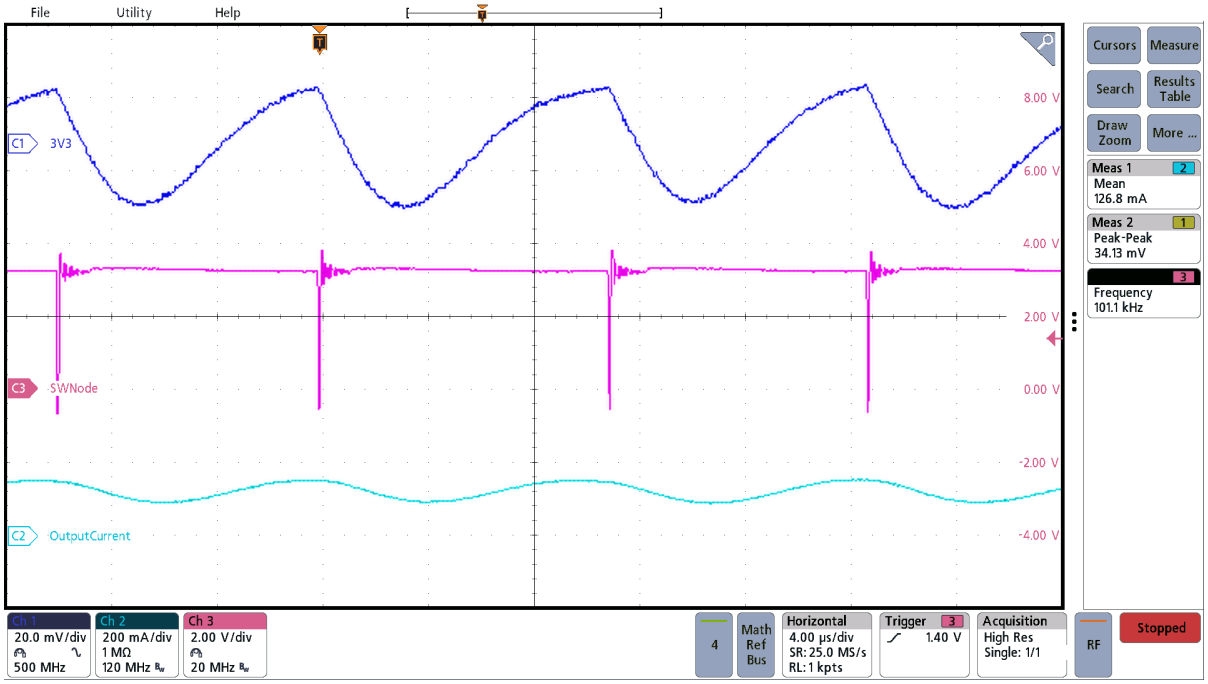

Figure 3-32. *3V3* Ripple (125-mA; 24-VAC Source)

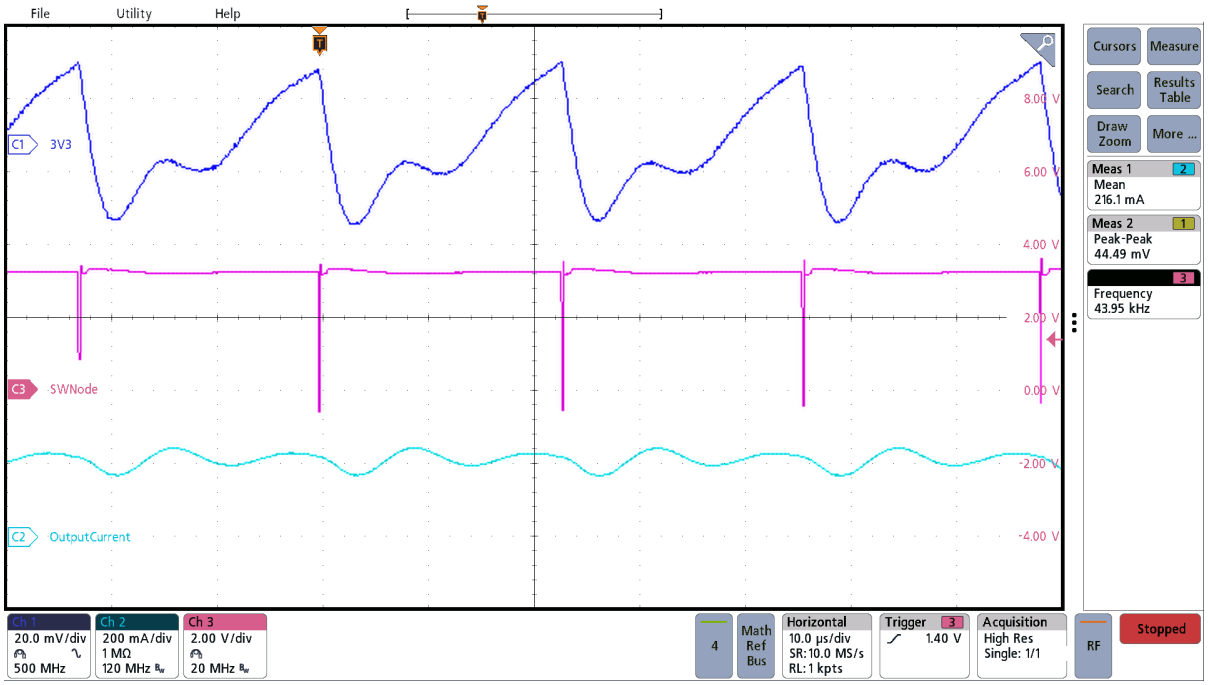

Figure 3-33. *3V3* Ripple (210-mA; 24-VAC Source)

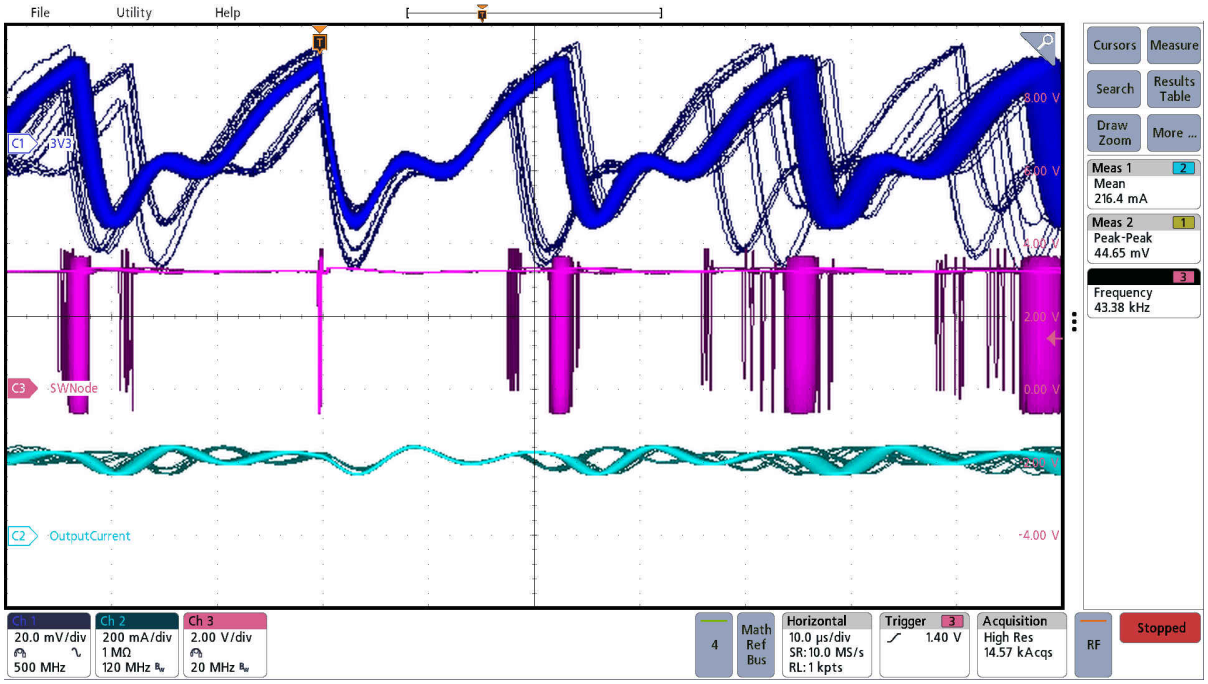

Figure 3-34. *3V3* Ripple Persist (210-mA; 24-VAC Source)

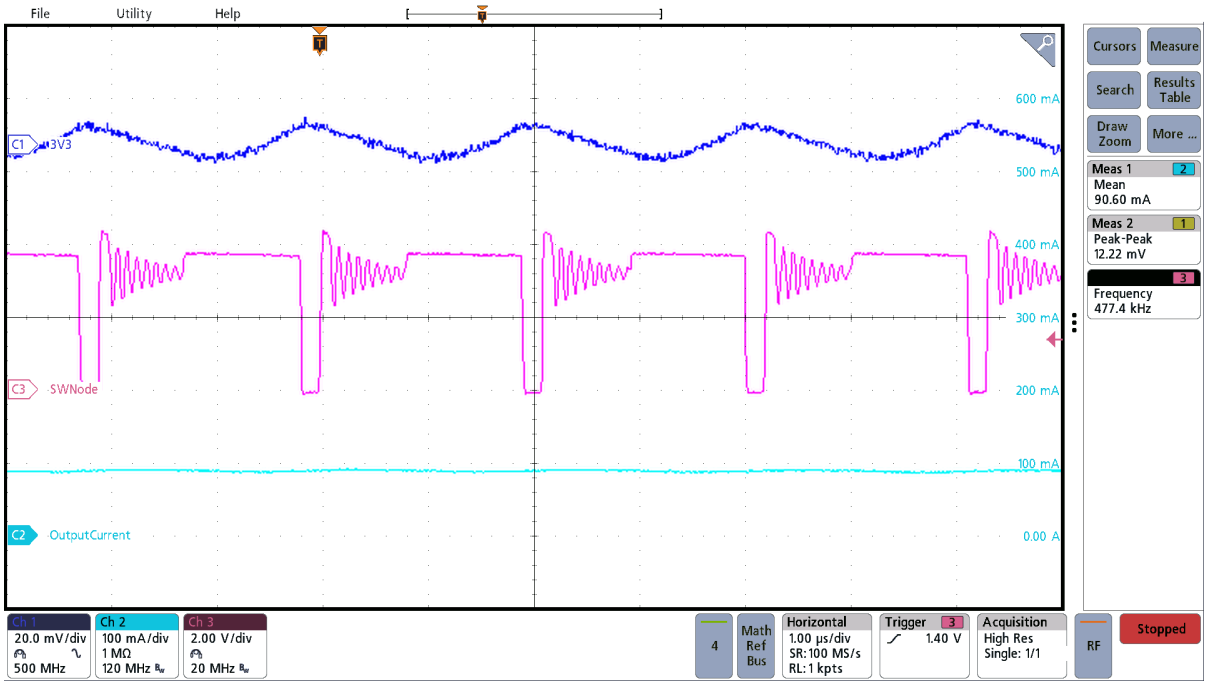

Figure 3-35. *3V3* Ripple (90-mA Load; 24-VAC Source Plus Battery)

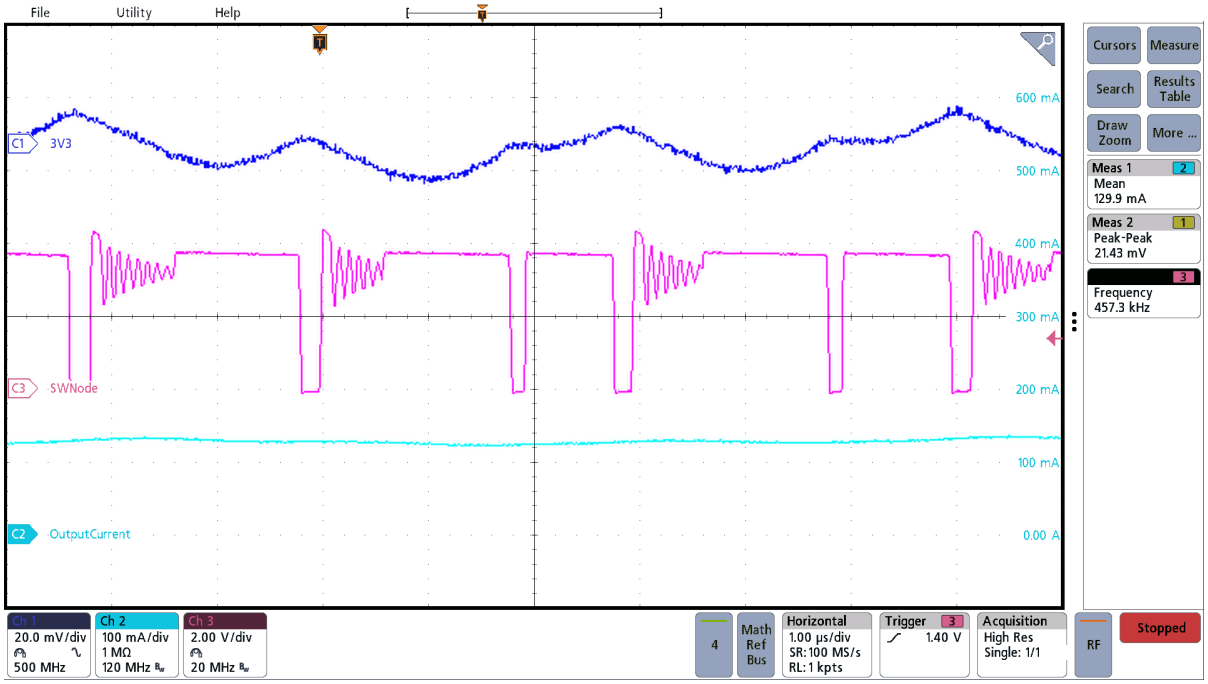

Figure 3-36. *3V3* Ripple (125-mA Load; 24-VAC Source Plus Battery)

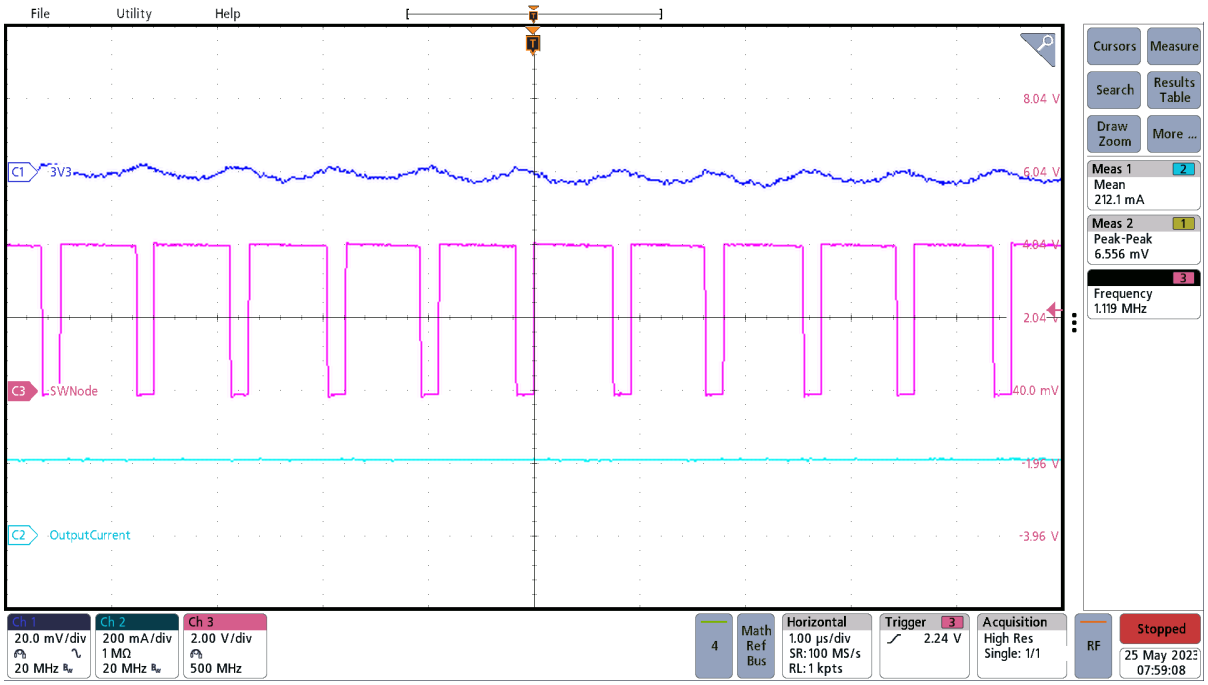

Figure 3-37. *3V3* Ripple (210-mA Load; 24-VAC Source Plus Battery)

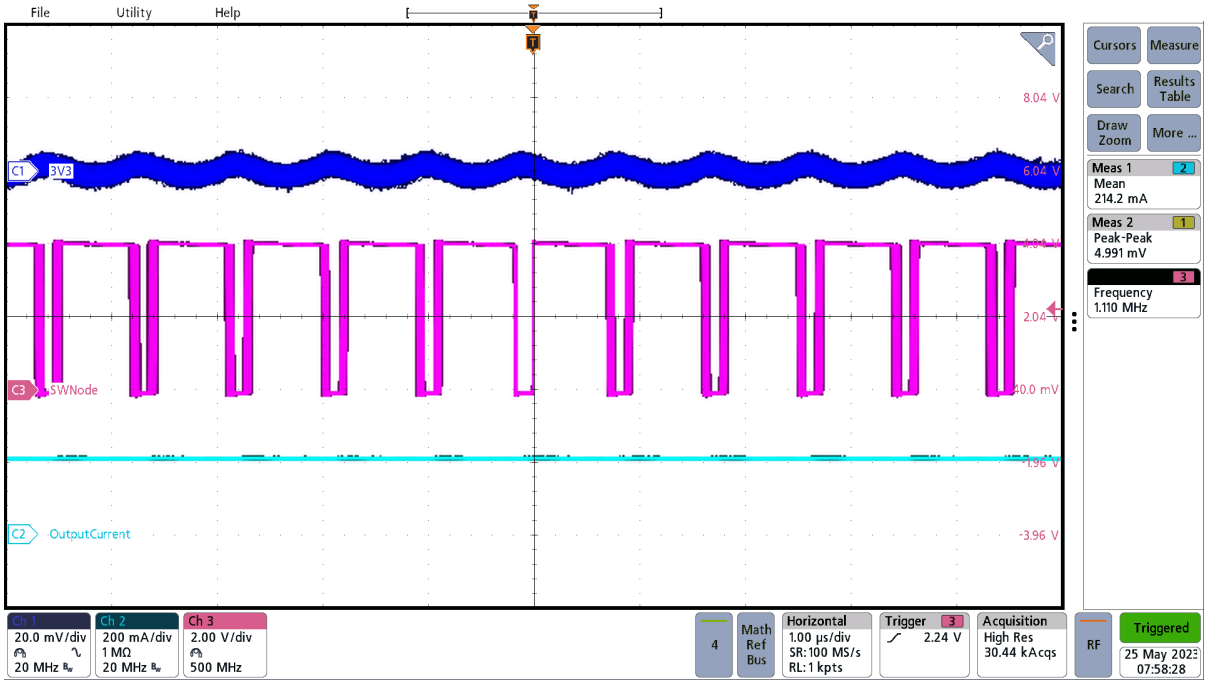

Figure 3-38. *3V3* Ripple Persist (210-mA Load; 24-VAC Source Plus Battery)

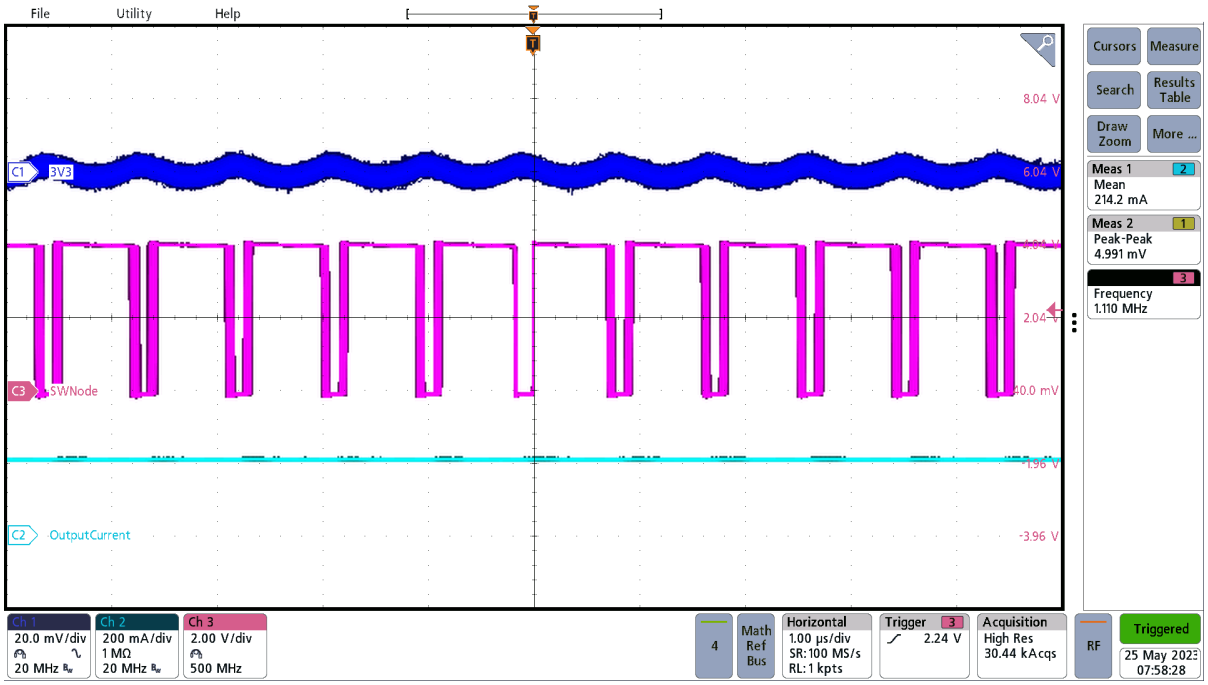

Figure 3-39. *3V3* Ripple Persist (1-A Load; 24-VAC Source Plus Battery)

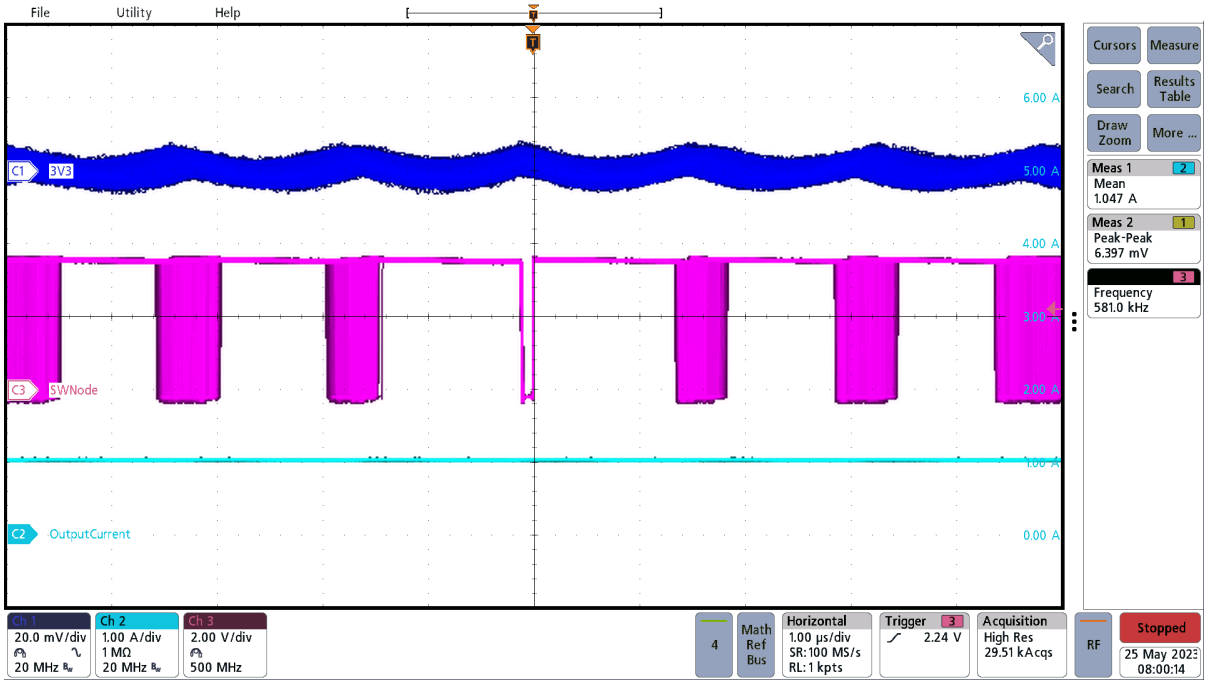

Figure 3-40. *3V3* Ripple Persist (1-A Load; Battery Only)

3.3.8 LMR36520 (LMOut Power Rail)

The LMR36520 produces a larger ripple when operating in DCM when compared to CCM. Regardless of the mode, the LMR36520 produces an output ripple of less than 1% across the entire load range. Jitter on the switch node as shown in Figure 3-41 is expected as the rectified 24 VAC exhibits significant ripple that the LMR36520 is constantly adjusting for. The amount of ripple exhibited on the rectified 24 VAC increases with higher load currents thereby increasing jitter on the LMR36520 switch node.

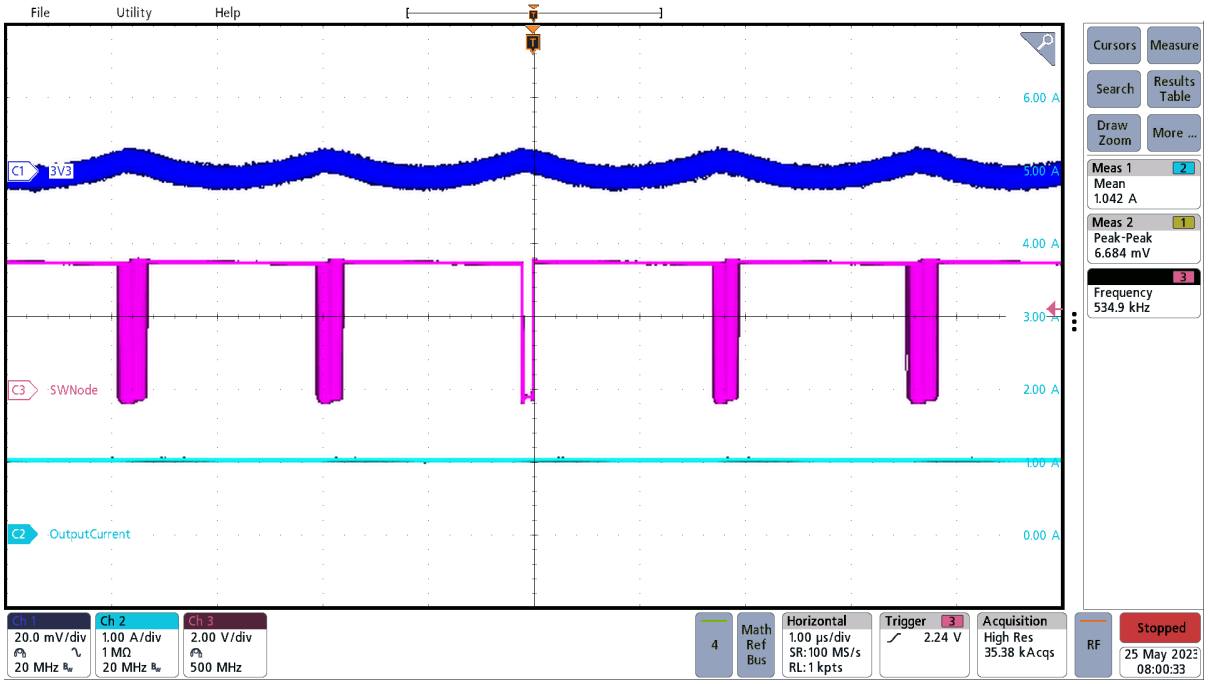

Figure 3-41. LMROut Ripple (No Load)

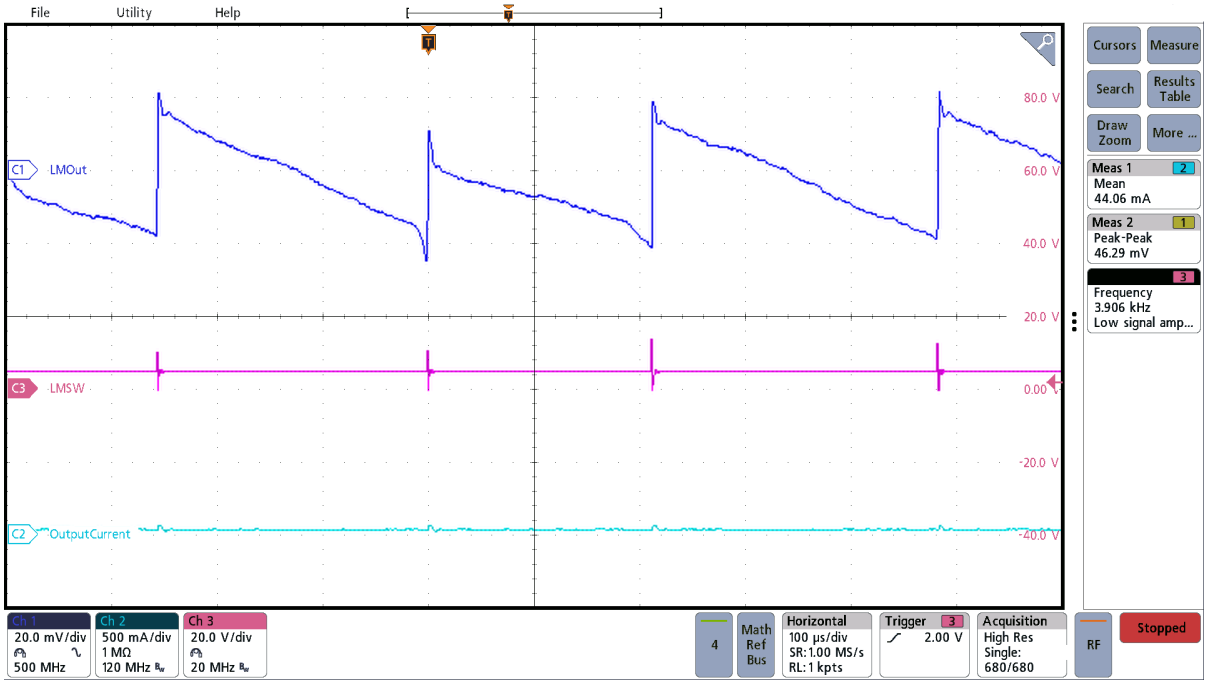

Figure 3-42. LMROut Ripple (150-mA Load)

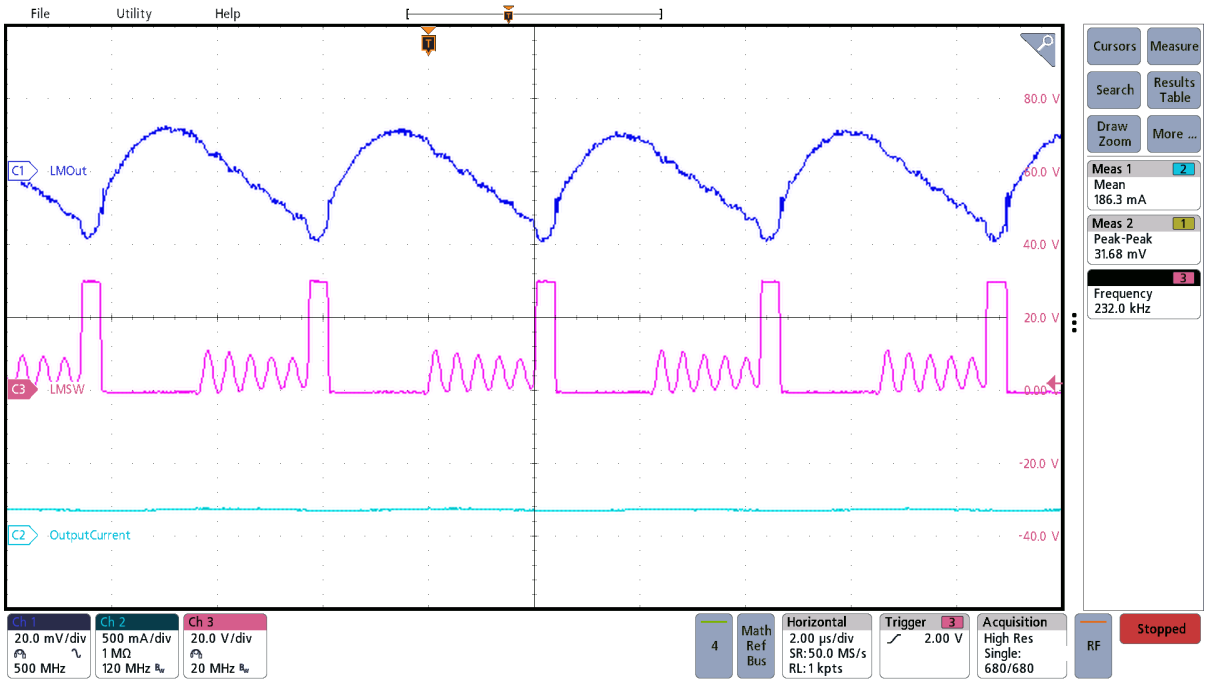

Figure 3-43. LMROut Ripple (300-mA Load)

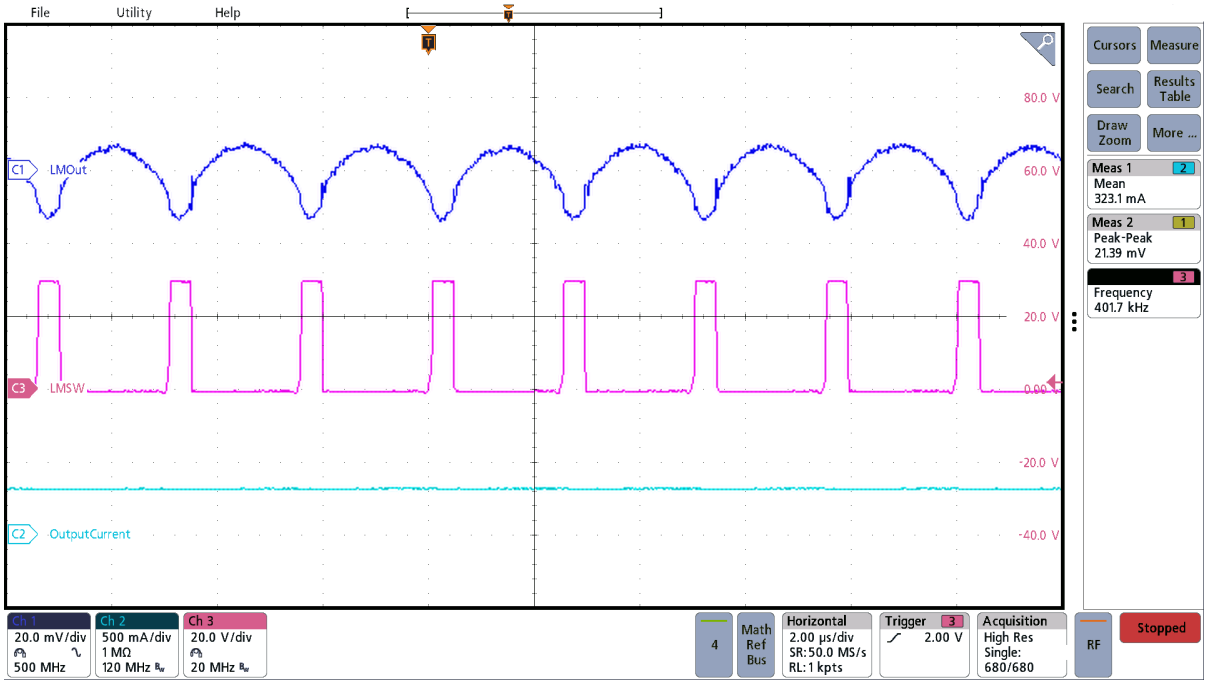

Figure 3-44. LMROut Ripple Persist (300-mA Load)

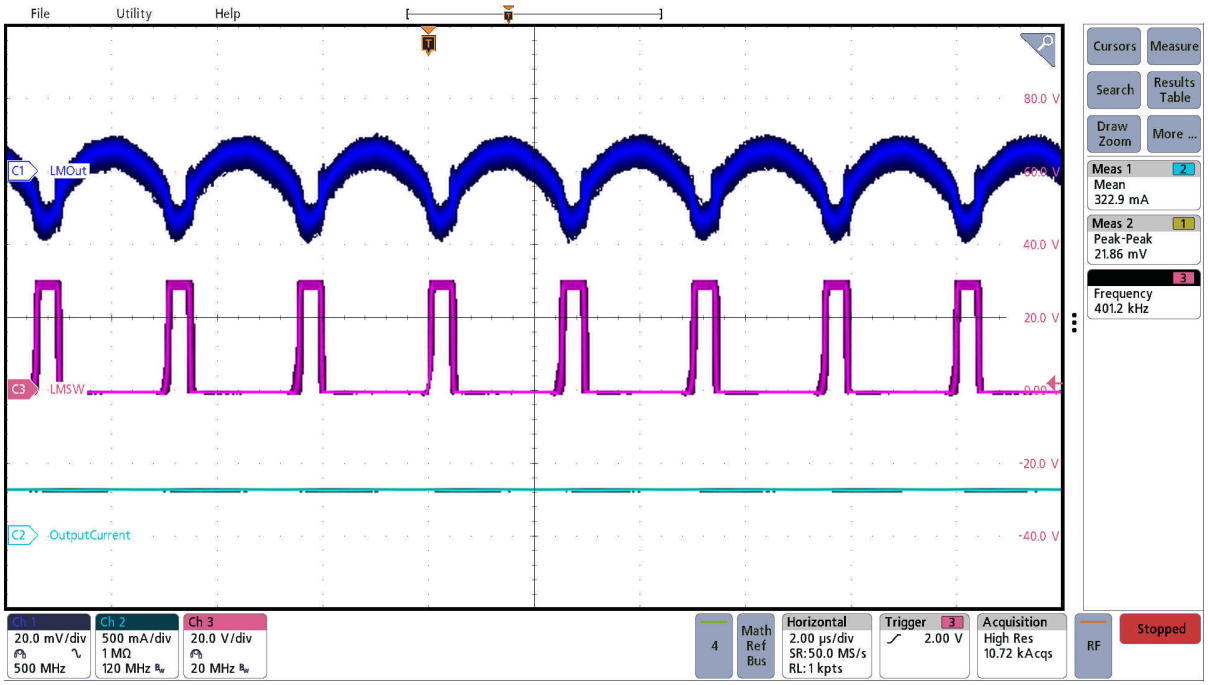

Figure 3-45. LMROut Ripple (490-mA Load)

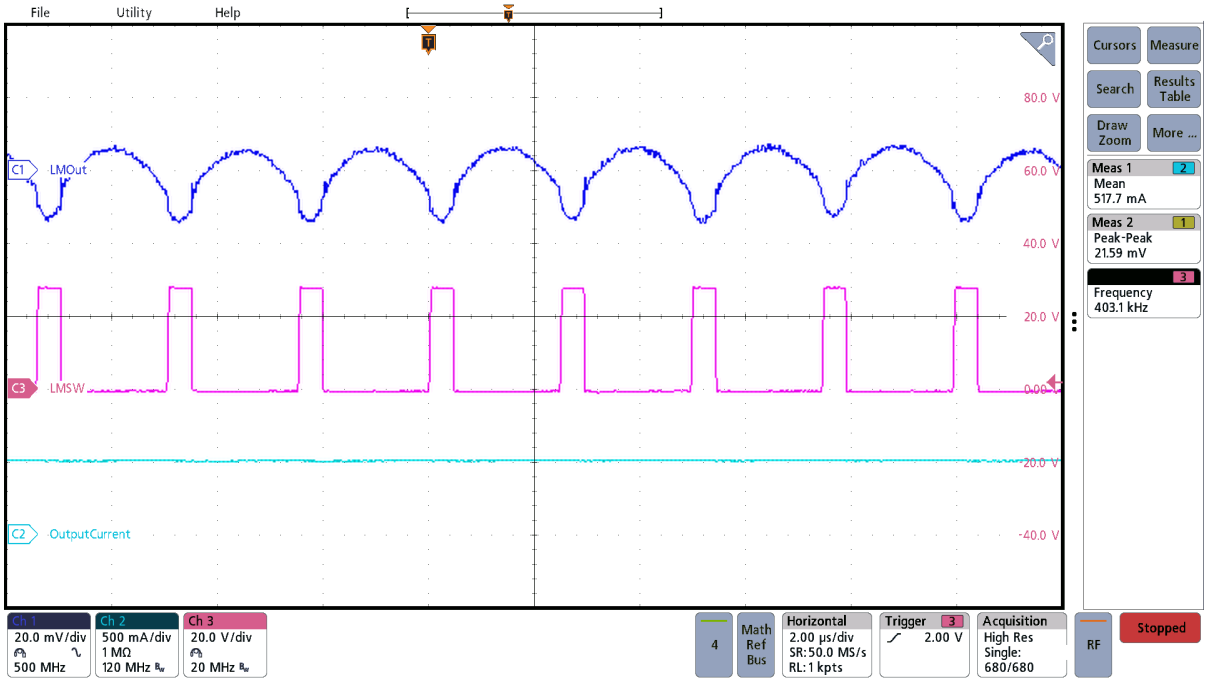

Figure 3-46. Needs Title

3.3.9 BM24072 (BMOut Power Rail)

The ripple on the BMOut power rail varies significantly between battery usage only versus a PWRin source with battery power assist. When using only the battery, the BM24072 connects the battery to the output by closing an internal FET. As a result, the noise during purely battery operation is equal or less than the noise floor of the oscilloscope used for measurement. Figure 65, Figure 66, and Figure 67 (Figure 3-47, Figure 3-48, and Figure 3-49) show an increased ripple when using a source other than the battery.

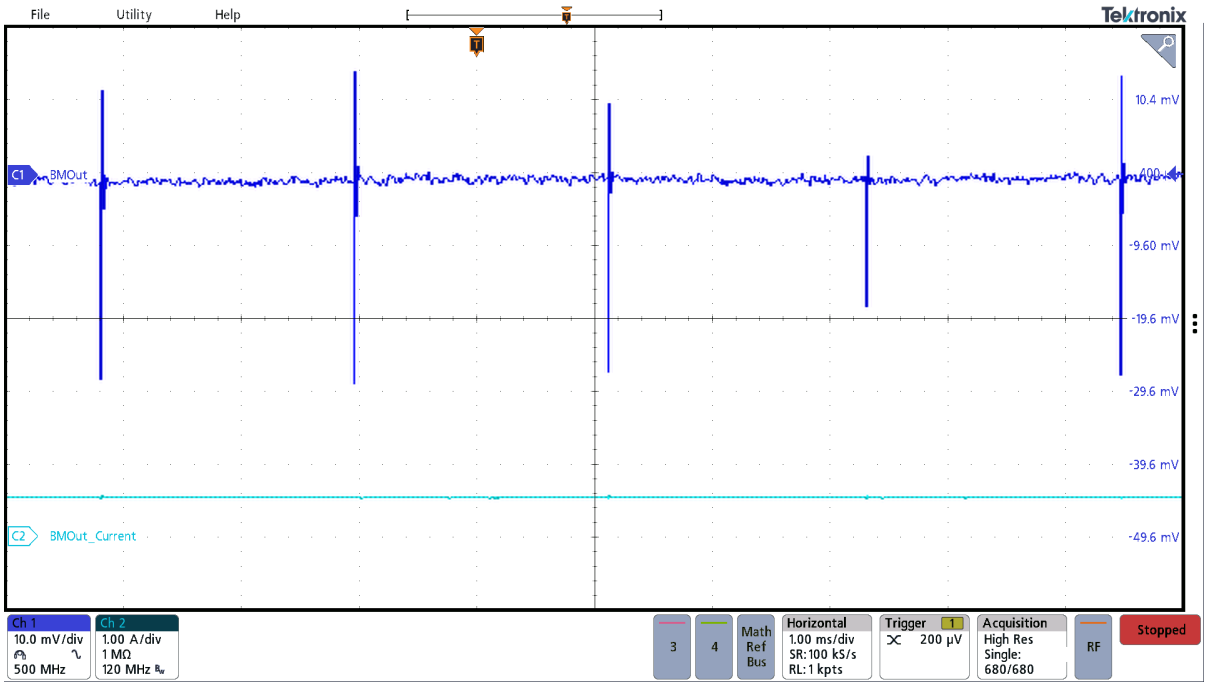

Figure 3-47. "BMOut" Ripple (0 A; Battery Source Only)

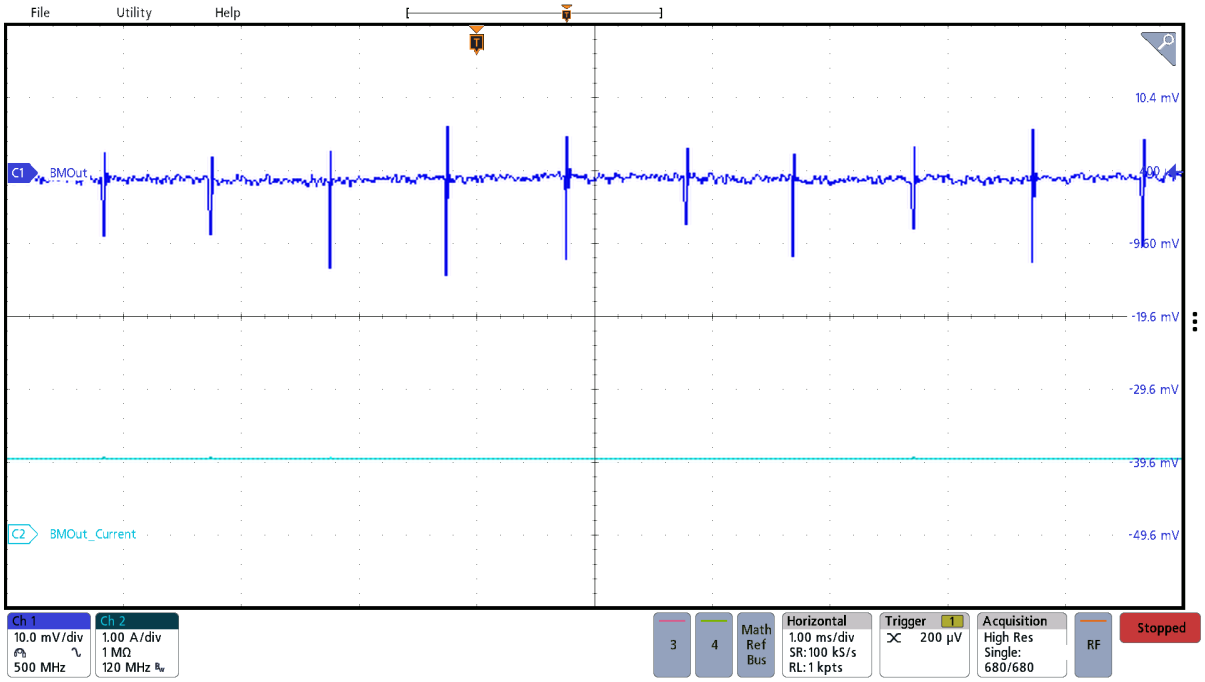

Figure 3-48. "BMOut" Ripple (1 A; Battery Source Only)

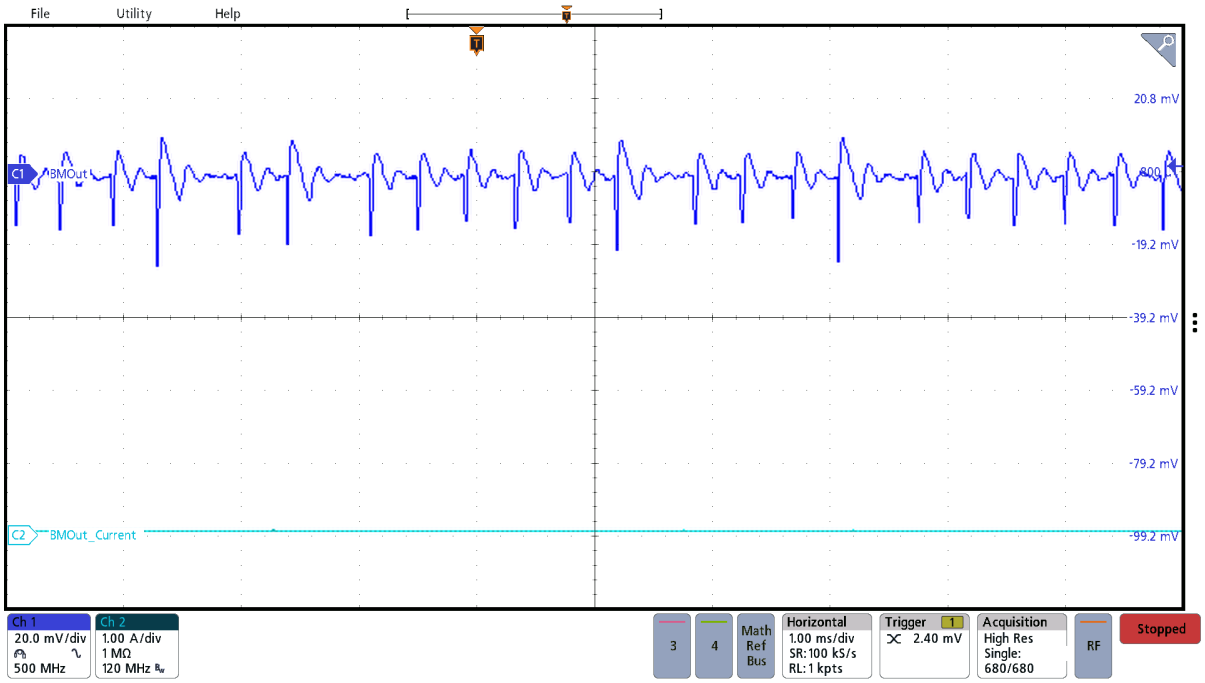

Figure 3-49. "BMOut" Ripple (1 mA; Battery and USB Sources)

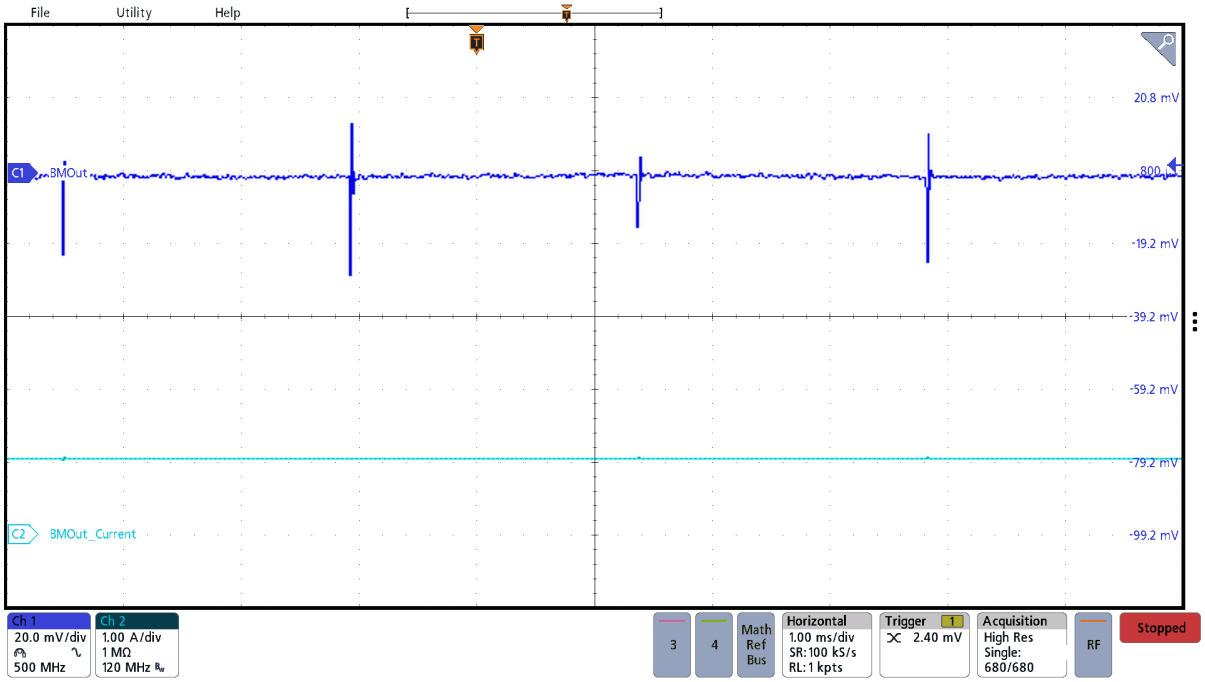

Figure 3-50. "BMOut" Ripple (1 A; Battery and USB Sources)

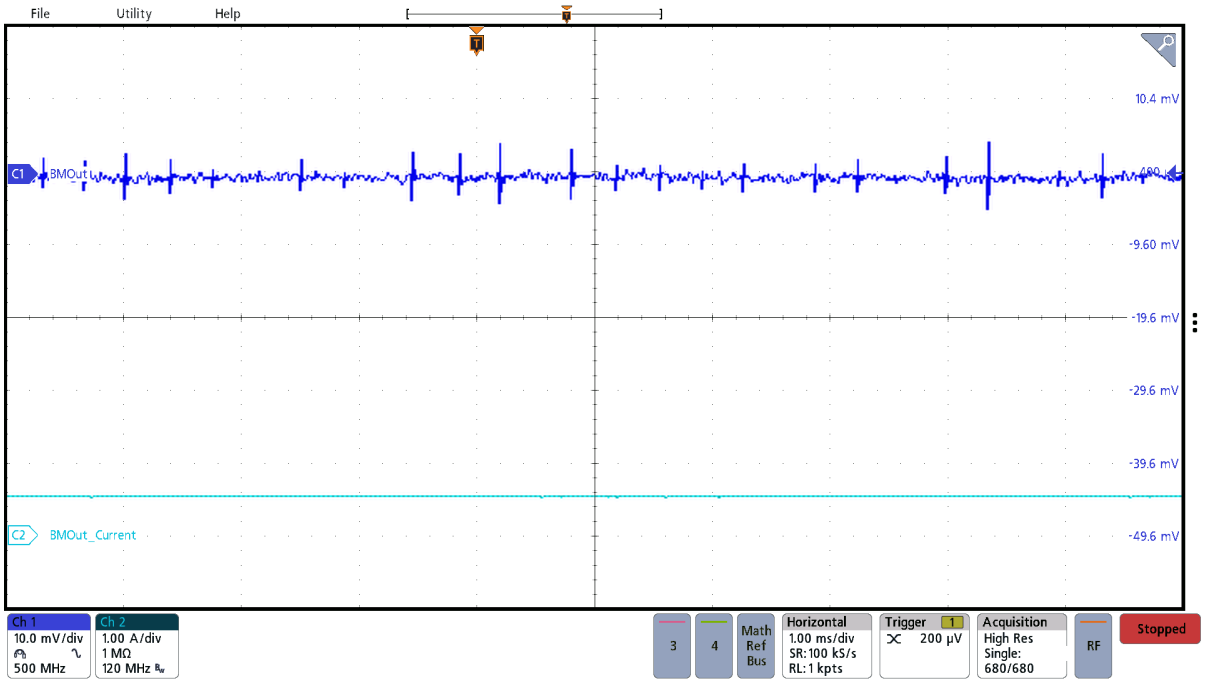

Figure 3-51. "BMOut" Ripple (500 mA; Battery and USB Sources)

3.3.10 Reference

3.3.10.1 TLV62568

Efficiency on the BATT to 3V3 path is perhaps the most crucial because high efficiency on this path allows longer battery life and a smaller battery. The TLV62568 device provides excellent efficiency, peaking at 96.6% efficiency at 150 mA at a nominal 3.7 battery voltage. The lower the battery voltage, the higher the efficiency of the BATT to 3V3 conversion. For this test, the input voltages were measured at C9 and the output voltages were measured at C10. The input current was fed at C9 and the output current to an electronic load was pulled from C10.

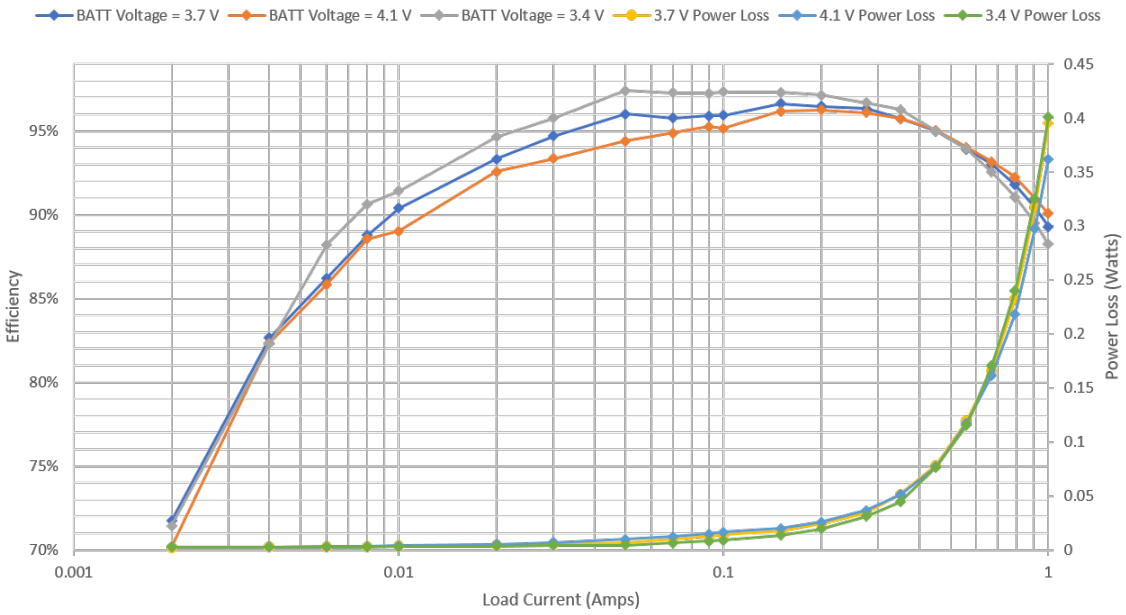

Figure 3-52. Battery to 3V3 Power Bus Efficiency and Power Loss

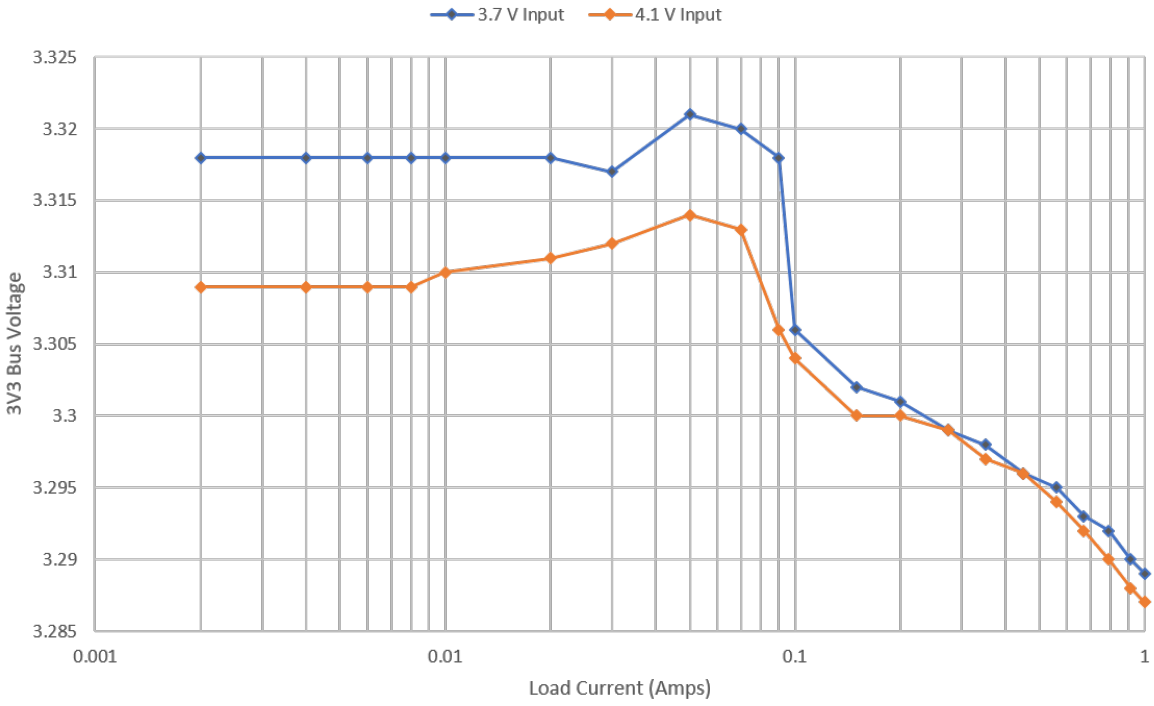

Figure 3-53. TLV62568 Load Regulation

3.3.10.2 LMR36520

The LMR36520 provides exceptional efficiency despite the large voltage difference between the input and output of the device. As with the BATT to 3V3 conversion, the efficiency of LMR36520 increases as the input voltage decreases. The input voltage was measured at node RectOut side of R9 and the output voltage was measured at C23. The input current was fed through node RectOut and the output current was drawn from LMOut side of C23 and C24.

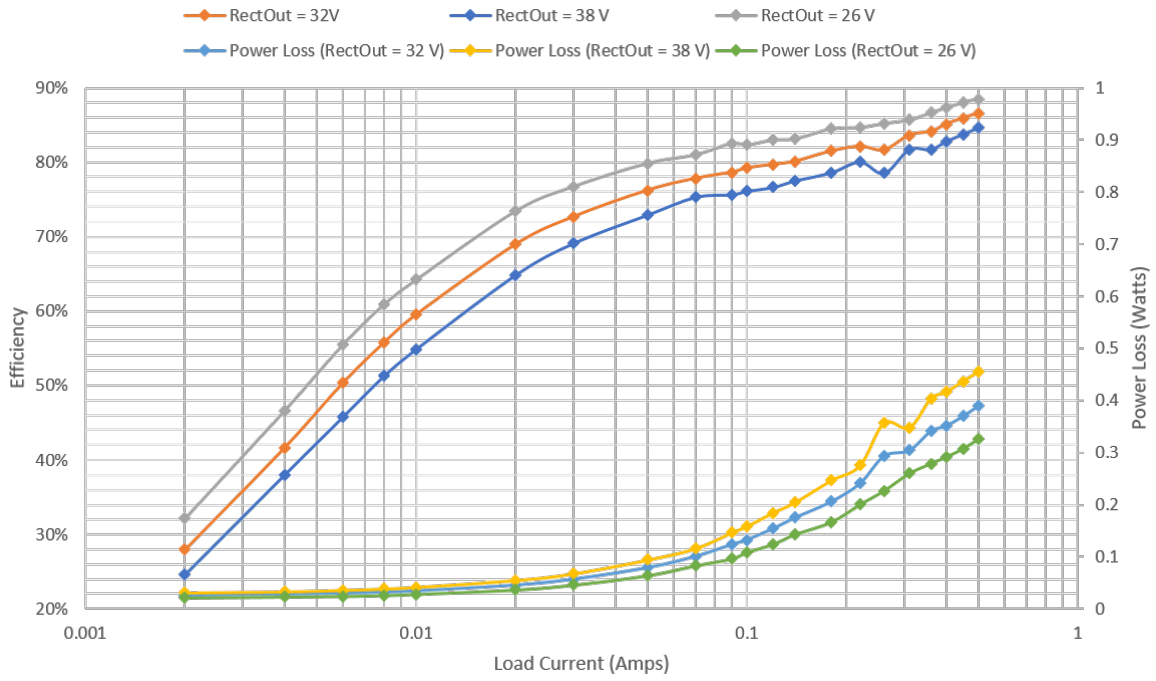

Figure 3-54. LMR36520 Efficiency and Power Loss

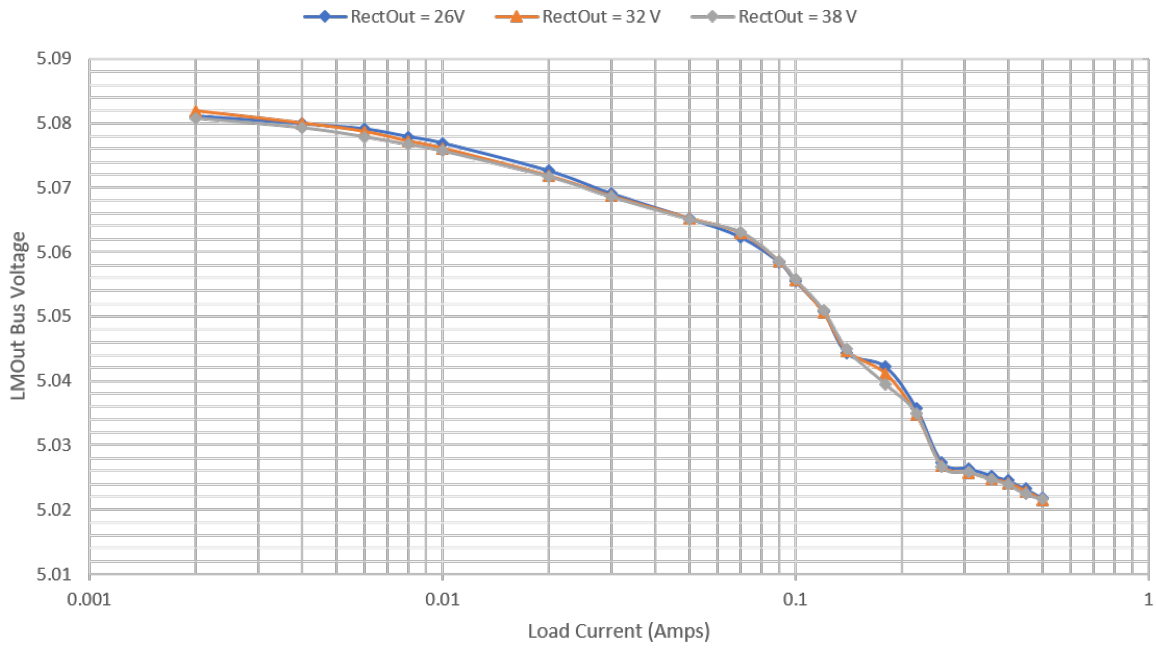

Figure 3-55. LMR36520 Load Regulation

4 Design and Documentation Support

4.1 Design Files

4.1.1 Schematics

To download the schematics, see the design files at TIDA-010932.

4.1.2 BOM

To download the bill of materials (BOM), see the design files at TIDA-010932.

4.2 Tools and Software

Tools

WEBENCH® Power Designer	Creates customized power supply circuits based on your requirements. The environment gives you end-to-end power supply design capabilities that save you time during all phases of the design process.

4.3 Documentation Support

1. Texas Instruments, *LMR36520 SIMPLE SWITCHER® 4.2-V to 65-V, 2-A Synchronous Step-down Converter* data sheet
2. Texas Instruments, *TPS2116 1.6 V to 5.5 V, 2.5-A Low I_Q Power Mux with Manual and Priority Switchover* data sheet
3. Texas Instruments, *TLV62568 1-A High Efficiency Synchronous Buck Converter in SOT Package* data sheet
4. Texas Instruments, *INAx180 Low- and High-Side Voltage Output, Current-Sense Amplifiers* data sheet
5. Texas Instruments, *TPS92360 38-V 1.2-A Single Channel LED Backlight Driver* data sheet
6. Texas Instruments, *TPS2640 42-V, 2-A eFuse with Integrated Reverse Input Polarity Protection* data sheet
7. Texas Instruments, *BQ2407x Standalone 1-Cell 1.5-A Linear Battery Chargers with Power Path* data sheet

4.4 Support Resources

TI E2E™ support forums are an engineer's go-to source for fast, verified answers and design help — straight from the experts. Search existing answers or ask your own question to get the quick design help you need.

Linked content is provided "AS IS" by the respective contributors. They do not constitute TI specifications and do not necessarily reflect TI's views; see TI's Terms of Use.

4.5 Trademarks

BoosterPack™, LaunchPad™, TI E2E™ are trademarks of Texas Instruments.
WEBENCH® is a registered trademark of Texas Instruments.
All trademarks are the property of their respective owners.

5 About the Author

BRIAN DEMPSEY is a systems designer at Texas Instruments, where he is responsible for developing reference design solutions for the industrial segment. Brian brings to this role his extensive experience in HVAC systems, along with his experience with mixed signal systems. Brian earned his bachelor of science in electrical engineering (BSEE) from Texas A&M University in College Station, TX.

JOHN ALBRECHT is an Analog Field Applications Engineer, where he is responsible for working on design solutions and answering customer technical questions. John earned his bachelors of science in electrical engineering (BSEE) from The University of Akron in Akron, Ohio.

IMPORTANT NOTICE AND DISCLAIMER

TI PROVIDES TECHNICAL AND RELIABILITY DATA (INCLUDING DATA SHEETS), DESIGN RESOURCES (INCLUDING REFERENCE DESIGNS), APPLICATION OR OTHER DESIGN ADVICE, WEB TOOLS, SAFETY INFORMATION, AND OTHER RESOURCES “AS IS” AND WITH ALL FAULTS, AND DISCLAIMS ALL WARRANTIES, EXPRESS AND IMPLIED, INCLUDING WITHOUT LIMITATION ANY IMPLIED WARRANTIES OF MERCHANTABILITY, FITNESS FOR A PARTICULAR PURPOSE OR NON-INFRINGEMENT OF THIRD PARTY INTELLECTUAL PROPERTY RIGHTS.

These resources are intended for skilled developers designing with TI products. You are solely responsible for (1) selecting the appropriate TI products for your application, (2) designing, validating and testing your application, and (3) ensuring your application meets applicable standards, and any other safety, security, regulatory or other requirements.

These resources are subject to change without notice. TI grants you permission to use these resources only for development of an application that uses the TI products described in the resource. Other reproduction and display of these resources is prohibited. No license is granted to any other TI intellectual property right or to any third party intellectual property right. TI disclaims responsibility for, and you will fully indemnify TI and its representatives against, any claims, damages, costs, losses, and liabilities arising out of your use of these resources.

TI’s products are provided subject to TI’s Terms of Sale or other applicable terms available either on ti.com or provided in conjunction with such TI products. TI’s provision of these resources does not expand or otherwise alter TI’s applicable warranties or warranty disclaimers for TI products.

TI objects to and rejects any additional or different terms you may have proposed.

Mailing Address: Texas Instruments, Post Office Box 655303, Dallas, Texas 75265